

Proceedings of the 16th International Symposium on Polar Sciences

Polar Exploration with ARAON(아라온)

**June 10 - 12, 2009
Korea Polar Research Institute
Incheon, Korea**

**Sung-Hyun Park and Tae Siek Rhee
*Editors***

**Organized by
Korea Polar Research Institute**



Symposium Program

June 10, 2009

08:30 - 09:30 **Registration**

Opening Ceremony & Welcoming Address

Chair: Tae Siek Rhee

09:30 - 09:50 Hong Kum Lee (Director-General of Korea Polar Research Institute)

Session 1: Climate Change and Polar Ocean System

Chair: Hyoung Chul Shin & Sang Heon Lee

09:50 - 10:00 Hyoung Chul Shin KOPRI's Ocean and Climate Research Plan in the Southern Ocean

10:00 - 10:30 **Keynote Speech:** E. Fahrbach Decadal Fluctuations of the Water Mass Properties in Atlantic Sector of the Southern Ocean

10:30 - 10:50 T. Trull The Influence of Natural Iron Inputs on Southern Ocean Productivity and Carbon Sequestration

10:50 - 11:10 S. F. Ackley Antarctic Sea Ice Processes and Climate; What We Have Learned and What We Need to Know Further

11:10 - 11:30 A. Stoessel The Role of Sea Ice Measurements in Climate Modeling

11:30 - 11:50 J. A. Dowdeswell Glaciers, Ice sheets and the Marine Record: Evidence from Submarine Landforms

Group Photo

12:00 - 13:00

Lunch

13:00 - 13:10 Sang Heon Lee KOPRI Research Program in the Arctic Ocean

13:10 - 13:30 T. Whitledge Biological Production in the Western Arctic and Possible Future Research Directions

13:30 - 13:50 K. Shimada Mechanism of Catastrophic Climate Changes in the Arctic Ocean

Session 2: Tectonics and Hydrothermal Vent

Chair: Sung-Hyun Park & Minkyu Park

14:00 - 14:20 Minkyu Park & Sung-Hyun Park Introduction of KOPRI Polar Ridge and Hydrothermal Vent Plan

14:20 - 14:50 **Keynote Speech:** J. Lin Major Opportunities for International Multi-disciplinary Research and Exploration of the Global Mid-ocean Ridge System

14:50 - 15:10 Sang-Mook Lee Comparisons between Back Arc Basin and Mid Ocean Ridges

15:10 - 15:30 A. Briais The Pacific-Antarctic Ridge: Geophysical and Geochemical Results from the French Expeditions Obtained with R/V L'Atalante (1996 and 2002)

15:30 - 15:50 K. W. W. Sims Application of U- and Th Decay Series Disequilibria to Dating Submarine Basalts

15:50 - 16:10		<i>Coffee Break</i>
16:10 - 16:40	Special Lecture: D.R. Yoerger	Autonomous Discovery, Mapping, And Sampling Of Deep Sea Hydrothermal Vents
16:40 - 17:00	S. E. Beaulieu	Larval Supply, Colonization, and Faunal Community Development at Hydrothermal Vents on the East Pacific Rise
17:00 - 17:20	R. P. Dziak	Tectono-magmatic Activity and Ice Dynamics in the Bransfield Strait Back-arc Basin, Antarctica
17:20 - 17:40	F. J. Davey	Cenozoic Tectonics of the Western Ross Sea region
18:00 - 20:00		<i>Banquet</i>

Workshop Program on Geology & Geophysics

June 11, 2009

Session 1: Ice-Shelf, Sedimentation & Paleoclimate

Chair: Ho Il Yoon & Jaeil Lee

09:30 - 09:45	E. W. Domack	LARsen Ice Shelf System (LARISSA): A Multi-disciplinary Earth Systems Approach to Antarctic Environmental Change
09:45 - 10:00	Jaehyung Yu	Study of Dry and Melt Snow Zones of Lambert Glacier – Amery Ice Shelf, Antarctica Using ETM + Data
10:00 - 10:15	B. Coakley	Unfinished Business; Capturing the Value of Extended Continental Shelf Data Sets to Understand the History of the Arctic Ocean.
10:15 - 10:30	E. V. Ivanova	The Barents Sea Paleoenvironments over the Last 15ka

10:30 - 10:50

Coffee Break

Session 2: Geology & Geophysics in Antarctica

Chair: Jong-Kuk Hong

10:50 - 11:05	Y. Nogi	Japanese Marine Geophysical and Geological Research Activities in the Antarctic Ocean
11:05 - 11:20	M. Kanao	Broadband Seismic Deployments in East Antarctica: IPY Contribution to Understand Earth Deep Interior
11:20 - 11:35	G. Toyokuni	Accurate and Efficient Computation of Global Seismic Wavefield for Investigation of the Deep Earth, from Antarctica
11:35 - 11:50	Won-Sang Lee	Hydroacoustic Monitoring in the Scotia sea, Antarctica

11:50 - 13:00

Lunch

Session 3: Tectonics and Magmatism at Polar Ridges

Chair: Sung-Hyun Park & J. Lin

13:00 - 13:15	J. Chen	Recent Progress in Mid-ocean Ridge Research in China
13:15 - 13:30	Sukyong Yun	Southeast Indian Ocean-Ridge Earthquake Sequences from Cross-Correlation Analysis of Hydroacoustic Data
13:30 - 13:45	K. W. W. Sims	Generation of ²³¹ Pa, ²²⁶ Ra, ²³⁸ U, and ²³⁰ Th Excesses in Arctic Mid-ocean Ridge Basalts from the Kolbeinsey, Mohns, Knipovich, and Gakkel Ridges
13:45 - 14:00	Yoon-Mi Kim	Gravity Anomaly Comparison of Subduction Zones in the Western Pacific
14:00 - 14:15	T. Himeno	Analysis of the Seismicity in the Antarctic Plate by the Statistical Method
14:15 - 14:30	A. Briais	The Tectonic Evolution of the Pacific Antarctic Ridge, Recent Changes in Plate Motion, Intraplate Tectonics and Axial Morphology
14:30 - 18:00		Posters and Group Discussion

Dongbok Shin	Hydrothermal Alteration and Isotopic Variations of Igneous Rocks in Barton Peninsula, King George Island, Antarctica
S. E. Beaulieu	Photographic Identification Guide to Larvae at Hydrothermal Vents
E. T. Baker	Exploration Strategies for Polar Environments: High-Resolution Mapping of Hydrothermal Discharge Using an Autonomous Underwater Vehicle
I. Ilhan	Preliminary Interpretation of Multi-channel Seismic Data from the Ross Sea
J. H. Haxel	Regional Comparisons of Deep-ocean Sound from the Bransfield Strait and Scotia Sea
A. Briaies	Evidence for off-axis seamounts on the flanks of the Southeast Indian Ridge, 128°E-150°E. Implications for mantle dynamics east of the Australia-Antarctic Discordance

14:45 - 15:00	K. Shimada	A Perspective on Future Observational Research to Understand the Fate of Arctic Ocean and Global Climate
15:00 - 15:15	B. J. (Phil) Hwang	Sea Ice Variability in the Chukchi Borderland of the Arctic Ocean
15:15 - 15:30	J. Wilkinson	Sea Ice Mass Balance
15:30 - 15:50	<i>Coffee Break</i>	
15:50 - 16:05	Jeomshik Hwang	Particulate Organic Carbon Cycle in the Deep Canada Basin
16:05 - 16:20	I. Tolosa	The MALINA Project: Carbon Cycling and Retrospective Paleoclimatic Approach in the Mackenzie Bay, Arctic Ocean
16:20 - 16:35	J. He	The Picoplankton in the Arctic Ocean in Summer 2008
16:35 - 16:50	T. Whitledge	New U.S. Ice-capable Research Vessel - New Opportunities for Collaboration
16:50 - 17:05	P. McRoy	Arctic Collaboration with International Arctic Research Center in Alaska
17:05 - 17:20	Sang Heon Lee	Korean Long-term Observation in the Western Arctic Ecosystem
17:20 - 17:30	<i>Coffee Break</i>	
17:30 - 18:30	<i>Discussion</i>	
<i>Poster Session: Climate Change and Polar Ocean System</i>		<i>Chair: Tae Siek Rhee</i>
	Tae-Seok Ahn	Bacteria from Sediment of Lake Baikal can be used as Evidence of Paleoclimate Change
	M. Ikehara	Paleoproductivity Variations Off Lützw-Holm Bay in the Indian Sector of the Southern Ocean during the Past 650 kyrs
	Hyounghmin Joo	Distributions of Phytoplankton Communities at Different Regions in the Arctic Ocean
	Yongwon Kim	Regulating Factors on Continuous Winter CO ₂ Flux in Black Spruce Forest Soils, Interior Alaska
	Miok Park	Fluorescence Characteristics of CDOM in Different Water Masses of Scotia Sea, Antarctica
	Tae Siek Rhee	Observation of Trace Gases in the Air and Surface Water along Atlantic Meridional Transect
	Mi Sun Yun	Carbon and Nitrogen Uptake Rates of Phytoplankton in the Chukchi Sea and Central Arctic Ocean

The 16th International Symposium on Polar Sciences
June 10-12, 2009, Incheon, Korea

TABLE OF CONTENTS

KEYNOTE SPEECH

Decadal Fluctuations of the Water Mass Properties in Atlantic Sector of the Southern Ocean17

E. Fahrbach O. Boebel, M. Hoppema, O. Klatt, G. Rohardt and A. Wisotzki*

Major Opportunities for International Multi-disciplinary Research and Exploration of the Global Mid-ocean Ridge System.....22

*J. Lin**

SESSION I : CLIMATE CHANGE AND POLAR OCEAN SYSTEM

The Influence of Natural Iron Inputs on Southern Ocean Productivity and Carbon Sequestration27

*T. Trull**

The Influence of Natural Iron Inputs on Southern Ocean Productivity and Carbon Sequestration.....28

*S. F. Ackley **

The Role of Sea Ice Measurements in Climate Modeling30

*A. Stoessel**

Glaciers, Ice sheets and the Marine Record: Evidence from Submarine Landforms35

*J. A. Dowdeswell**

Biological Production in the Western Arctic and Possible Future Research Directions.....38

T. Whitley and Sang Heon Lee*

Mechanism of catastrophic climate changes in the Arctic Ocean42

*K. Shimada**

SESSION II : TECTONICS AND HYDROTHERMAL VENT

Comparisons between Back Arc Basin and Mid Ocean Ridges.....50

*Sang-Mook Lee**

The Pacific-Antarctic Ridge: Geophysical and Geochemical Results from the French Expeditions Obtained with R/V L'Atalante (1996 and 2002).....	51
<i>L. Geli, H. Ondréas, L. Dosso, F. Klingelhofer, A. Briaïs*, D. Aslanian and the Pacantartic 1&2 Groups</i>	
Application of U- and Th Decay Series Disequilibria to Dating Submarine Basalts	52
<i>K. W. W. Sims* C. Waters, J. Standish</i>	
Autonomous Discovery, Mapping, and Sampling of Deep Sea Hydrothermal Vents	57
<i>D. R. Yoerger*</i>	
Larval Supply, Colonization, and Faunal Community Development at Hydrothermal Vents on the East Pacific Rise.....	58
<i>S. Beaulieu*, L. Mullineaux, and D. Adams</i>	
Tectono-magmatic Activity and Ice Dynamics in the Bransfield Strait Back-arc Basin, Antarctica.....	62
<i>R. P. Dziak*, Minkyu Park, Won Sang Lee, H. Matsumoto, D.R. Bohnenstiehl, J. H. Haxel</i>	
Cenozoic Tectonics of the Western Ross Sea region	72
<i>F. J. Davey*</i>	

The 16th International Symposium on Polar Sciences
June 10-12, 2009, Incheon, Korea

WORKSHOP PROGRAM ON GEOLOGY & GEOPHYSICS

SESSION 1: ICE-SHELF, SEDIMENTATION & PALEOCLIMATE

LARsen Ice Shelf System (LARISSA): A Multi-disciplinary Earth Systems Approach to Antarctic Environmental Change80
E. W. Domack and LARISSA team*

Study of Dry and Melt Snow Zones of Lambert Glacier – Amery Ice Shelf, Antarctica Using ETM + Data82
Jaehyung Yu, Samuel Cantu, Joonghyeok Heo, Hongxing Liu*

Unfinished Business; Capturing the Value of Extended Continental Shelf Data Sets to Understand the History of the Arctic Ocean..... 83
B. Coakley, L. Mayer, K. Brumley, M. Jakobsson, B. Baker*

The Barents Sea Paleoenvironments over the Last 15ka85
E.V. Ivanova, I. Murdmaa, N. Chistyakova, B. Risebrobakken and G. Alekhina*

SESSION 2: GEOLOGY & GEOPHYSICS IN ANTARCTICA

Japanese Marine Geophysical and Geological Research Activities in the Antarctic Ocean..... 92
Y. Nogi, H. Miura, M. Ikehara, N. Seama*

Broadband Seismic Deployments in East Antarctica: IPY Contribution to Understand Earth Deep Interior93
M. Kanao, D. Wiens, S. Tanaka, A. Nyblade, and S. Tsuboi*

Investigation of the Deep Earth, from Antarctica98
G. Toyokuni, H. Takenaka, M. Kanao*

Hydroacoustic Monitoring in the Scotia sea, Antarctica99
Won-Sang Lee, Minkyu Park, R. P. Dziak, Haru Matsumoto, D. R. Bohnenstiehl, J. H. Haxel, Sukyoung Yun*

SESSION 3: TECTONICS AND MAGMATISM AT POLAR RIDGES

Recent Progress in Mid-ocean Ridge Research in China102
J. Chen and J.B. Li*

Southeast Indian Ocean-Ridge earthquake sequences from cross-correlation analysis of hydroacoustic data105
Sukyoung Yun, Sidao Ni, Minkyu Park and Won Sang Lee*

Generation of ^{231}Pa , ^{226}Ra , ^{238}U , and ^{230}Th Excesses in Arctic Mid-ocean Ridge Basalts from the Kolbeinsey, Mohns, Knipovich, and Gakkel Ridges	106
<i>L. J. Elkins, K.W.W. Sims*, J. Prytulak, J. Blichert-Toft, J. Blusztajn, S. Fretzdorff, K. Haase, T. Elliott, S. Humphris, J.-G. Schilling</i>	
Gravity Anomaly Comparison of Subduction Zones in the Western Pacific ...	107
<i>Yoon-Mi Kim* and Sang-Mook Lee</i>	
Analysis of the Seismicity in the Antarctic Plate by the Statistical Method	108
<i>T. Himeno*, M. Kanao</i>	
The Tectonic Evolution of the Pacific Antarctic Ridge, Recent Changes in Plate Motion, Intraplate Tectonics and Axial Morphology.....	109
<i>L. Géli, H. Ondréas, L. Dosso, F. Klingelhofer, A. Briais*, D. Aslanian and the Pacantartic 1&2 Groups</i>	

The 16th International Symposium on Polar Sciences
June 10-12, 2009, Incheon, Korea

WORKSHOP PROGRAM ON CLIMATE CHANGE AND POLAR OCEAN SYSTEM

SESSION 1: THE SOUTHERN OCEAN

Polarstern: Operation of An Icebreaking Multi-purpose Research Vessel in the Arctic and Antarctic	112
<i>E. Fahrbach*</i>	
Variability of the Surface Transport at the Drake Passage.....	113
<i>Jae Hak Lee*</i>	
Antarctic Sea Ice in the International Polar Year: Results from the SIMBA and SIPEX Expeditions	114
<i>S. F. Ackley*</i>	
Sea Ice Observations and Modeling	115
<i>Achim Stössel*</i>	
Establishing a Southern Ocean Time Series Program for Biogeochemistry and Carbon Cycling.....	117
<i>T. Trull*</i>	
Long-term Variation of Oceanic CO ₂ and Possible Acidification in the Indian Sector of the Southern Ocean	118
<i>G. Hashida*, T. Yamanouchi, S. Nakaoka, S. Aoki, T. Nakazawa</i>	
Phytoplankton Community Structure and Photosynthetic Physiology within a Natural Iron Gradient in the Southern Drake Passage.....	119
<i>H. Wang*, B. G. Mitchell</i>	
Optical Discrimination of Phytoplankton Groups to Derive dimethylsulfoniopropionate (DMSP) Concentration in the Southern Ocean	120
<i>T. Hirawake*, N. Kagawa, N. Kondo, N. Kasamatsu, S. Saitoh</i>	
Development of a New Ship-board Sky-radiometer for Remote-sensing of Column Aerosol Optical Properties over the Ocean from Japanese New Antarctic R/V Shirase.....	121
<i>M. Shiobara*, and the POM-01 MK III Skyradiometer Development Team</i>	
Finding from Atlantic Meridonal Transect Program and its Implication to Pacific Meridional Transect Program	124
<i>Young-Nam Kim*</i>	

Seasonality of phytoplankton abundance in the southwest Atlantic sector of the Southern Ocean.....125
Jisoo Park, Im-Sang Oh, Hyun-Cheol Kim, Hyoung-Chul Shin, and Sinjae Yoo*

Sea Ice, Biogeochemistry, and Ecosystem in the Most Rapidly Warming part of the Southern Ocean135
*Hyoung Chul Shin**

SESSION 2: THE ARCTIC OCEAN

Marine Geological and Geophysical Science in a Rapidly Changing Arctic... 139
*J. A. Dowdeswell**

A Perspective on Future Observational Research to Understand the Fate of Arctic Ocean and Global Climate.....140
*K. Shimada**

Sea Ice Variability in the Chukchi Borderland of the Arctic Ocean144
B. J. (Phil) Hwang and J. Wilkinson*

Sea Ice Mass Balance..... 148
J. Wilkinson, P. Hwang and T. Maksym*

Particulate Organic Carbon Cycle in the Deep Canada Basin.....149
*Jeomshik Hwang**

The MALINA Project: Carbon Cycling and Retrospective Paleoclimatic Approach in the Mackenzie Bay, Arctic Ocean150
I. Tolosa, J.C. Miquel, J. R. Oh, M. Babin*

The Picoplankton in the Arctic Ocean in Summer 2008.....154
*J. He**

New U.S. Ice-capable Research Vessel - New Opportunities for Collaboration155
*T. Whitley**

Collaboration Opportunities with the International Arctic Research Center (IARC).....156
*P. McRoy**

Korean Long-term Observation in the Western Arctic Ecosystem.....157
*Sang Heon Lee**

The 16th International Symposium on Polar Sciences
June 10-12, 2009, Incheon, Korea

POSTER SESSION

SESSION 1: GEOLOGY&GEOPHYSIS

- Hydrothermal alteration and isotopic variations of igneous rocks in Barton Peninsula, King George Island, Antarctica163
Dongbok Shin, Jong-Ik Lee, Jeong Hwang, and Soon-Do Hur*
- Photographic identification guide to larvae at hydrothermal vents.....165
S. W. Mills, S. E. Beaulieu, and L. S. Mullineaux*
- Exploration strategies for polar environments: High-resolution mapping of hydrothermal discharge using an Autonomous Underwater Vehicle.....166
E. T. Baker, S. L. Walker, C. E. de Ronde, J. A. Resing, R. E. Embley, D. Yoerger*
- Preliminary interpretation of multi-channel seismic data from the Ross Sea ..168
I. Ilhan, Gwang H. Lee, Deniz Cukur, Jong K. Hong, Young K. Jin*
- Regional Comparisons of Deep-Ocean Sound from the Bransfield Strait and Scotia Sea.....169
J. H. Haxel, R. P. Dziak, M. Park, H. Matsumoto, W. S. Lee, T. K. Lau, and M. Fowler*
- Evidence for off-axis seamounts on the flanks of the Southeast Indian Ridge, 128°E-150°E. Implications for mantle dynamics east of the Australia-Antarctic Discordance.....170
A. Briais, O. Gomez and R. Lataste*

SESSION 2: CLIMATATE CHANGE AND POLAR OCEAN SYSTEM

- Bacteria from Sediment of Lake Baikal can be used as Evidence of Paleoclimate Change.....173
Tae-Seok Ahn, J.Y Kim, Y.J. Jung, V. Parfenova, N. Belkova*
- Paleoproductivity Variations Off Lützow-Holm Bay in the Indian Sector of the Southern Ocean during the Past 650 kyrs.....174
M. Ikehara, B. K. Khim, S. Okamoto, M. Kobayashi, K. Katsuki, Y. Sukanuma, M. Yamane, Y. Yokoyama Y.H. Kim*
- Distributions of Phytoplankton Communities at Different Regions in the Arctic Ocean.....175
Hyoung Min Joo, Sang Heon Lee, Kyung Ho Chung, Sung-Ho Kang, Yu Na Shin, Sung Soo Hong, Oh Youn Kwon, Jin Hwan Lee*

Regulating Factors on Continuous Winter CO ₂ Flux in Black Spruce Forest Soils, Interior Alaska.....	176
<i>Yongwon Kim* Y. Kodama M. Ishikawa</i>	
Fluorescence Characteristics of CDOM in Different Water Masses of Scotia Sea, Antarctica	181
<i>Miok Park*, S. W Kang and B. G. Mitchell</i>	
Observation of Trace Gases in the Air and Surface Water along Atlantic Meridional Transect.....	182
<i>Tae Siek Rhee*, A. J. Kettle, and M. O. Andreae</i>	
Carbon and Nitrogen Uptake Rates of Phytoplankton in the Chukchi Sea and Central Arctic Ocean.....	183
<i>Sang Heon Lee, Hyung-Min Joo, Mi Sun Yun*, Kyung Ho Chung</i>	

KEYNOTE SPEECH

DECADAL FLUCTUATION OF THE WATER MASS PROPERTIES IN ATLANTIC SECTOR OF THE SOUTHERN OCEAN

Eberhard Fahrbach¹, Olaf Boebel¹, Mario Hoppema¹, Olaf Klatt¹, Gerd Rohardt¹ and
Andreas Wisotzki¹

¹Alfred-Wegener-Institut für Polar- und Meeresforschung in der Helmholtz-
Gemeinschaft, Bremerhaven, Germany
Eberhard.Fahrbach@awi.de

INTRODUCTION

The Southern Ocean contributes through atmosphere-ice-ocean interaction processes to the variability of the global climate system (Rintoul et al, 2001). Atmosphere-ice-ocean interactions, occurring in the open ocean and on the shelves, lead to water mass conversions. Whereas the shelf processes affect a reservoir limited through the shallow water depth (Baines and Condie, 1998) and the cross frontal transports at the shelf edges, open ocean processes can affect deeper layers directly if the stability of the water column is weak. A major contribution to the global deep and bottom water formation occurs in the Weddell Sea (Carmack, 1977, Rintoul, 1998). It is controlled by the transport of source waters into the Weddell Sea, transformation processes within the Weddell Sea, and the transport of modified water out of the Weddell Sea (Gill, 1973).

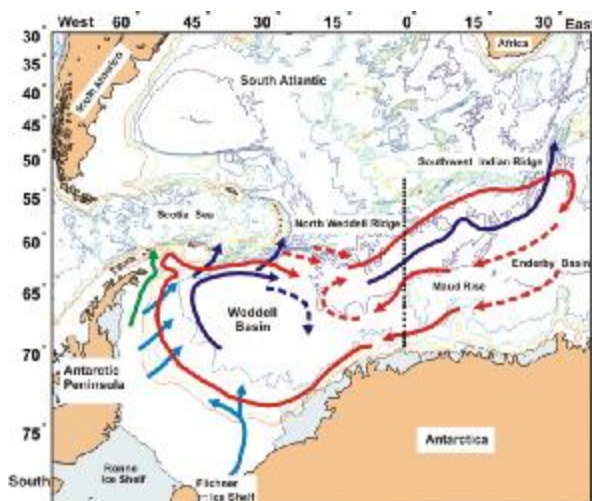


Figure 1 Schematic representations of the Weddell gyre circulation and the location of the transect displayed in figure 2 (dotted line). Red arrows indicate inflow and circulation of Warm Deep Water, light blue arrows sinking water masses at the continental slope. Dark blue arrows stand for deep and bottom water circulation and water masses leaving the basin. The green arrow indicates shelf

water leaving the western Weddell Sea.

In the Weddell Sea, Circumpolar Deep Water enters from the north and circulates as Warm Deep Water in intermediate layers within the large-scale cyclonic gyre (Figure 1). Heat and salt are transported from that water mass into the surface layer by means of upwelling and entrainment. The vertical transport of heat and salt compensates the heat loss and the fresh water gain at the sea surface. The delicate balance of buoyancy loss and gain controls the stability of the water column. The vertical transport can be significantly affected by vertical flow and enhanced mixing in the vicinity of topographical features like Maud Rise. Even relatively small-scale topographical structures may have a significant effect on the water flow and mixing due to the generally weak stratification in polar oceans.

Under conditions of a relatively stable water column, shallow open ocean convection represents a preconditioning for the shelf processes through heat extraction and salt redistribution of the source waters which are involved in frontal processes over the continental slope. In the case of relatively unstable conditions, open ocean convection can reach deeper layers and contribute directly to the deep water formation. Unstable conditions enhance the heat transport from the ocean towards the surface to an extent that large areas of the winter sea ice are melted and an open-ocean polynya is formed which then allows large heat losses of the ocean increasing the water mass conversion.

Recent observations indicate that the water mass properties of the Warm Deep Water are subject to significant variations. After an initial warming and salinity increase observed during the nineties a cooling followed during the last years (Robertson et al, 2002, Fahrbach et al, 2004). The variations are most likely due to changes in the inflow from the circumpolar water belt, in combination with changes in the ice-ocean-atmosphere interaction in the Weddell Sea induced by changes in the atmospheric forcing conditions. The time variability of the Antarctic Circumpolar Wave (White and Peterson, 1996), the Southern Annular Mode (Thompson and Solomon, 2002) or the Antarctic Dipole (Yuan, 2004) might affect the Weddell Sea and generate the observed variations. Whereas the properties of the Weddell Sea Deep Water have remained essentially constant, the Weddell Sea Bottom Water has been subject to significant changes as well. Since the Warm Deep Water is the source water of bottom water, the variations of the two water masses are likely to be related through the formation process.

THE DATA

Data from ship-borne surveys over more than twenty years in the Atlantic sector of the Southern Ocean are used to construct time series of water mass properties from 1984 to 2008 (Fahrbach et al, 2007). The most recent data set was obtained during a cruise of RV *Polarstern* in the context of the IPY Climate of Antarctica and the Southern Ocean (CASO) project.

In order to reduce the effect of small or mesoscale features on the detection of low period changes of water mass properties, cross-basin averages of temperature and salinity were calculated. Changes of the mean temperature of a water mass are a measure of changes in the heat content. Since the shift of the Weddell Front would affect the mean properties significantly, the calculations were limited to the area south of 56°S to exclude the front (Figure 2). In addition to the hydrographic transects which were repeated in intervals of 2 to 3 years, moored instruments were deployed which provided quasi-continuous time series. Our time series data allow to draw the conclusion that the longer-term changes detected from the repeat sections are not the

result of aliased higher frequency signals in spite that variations of seasonal to interannual time scales are clearly visible in the quasi-continuous records.

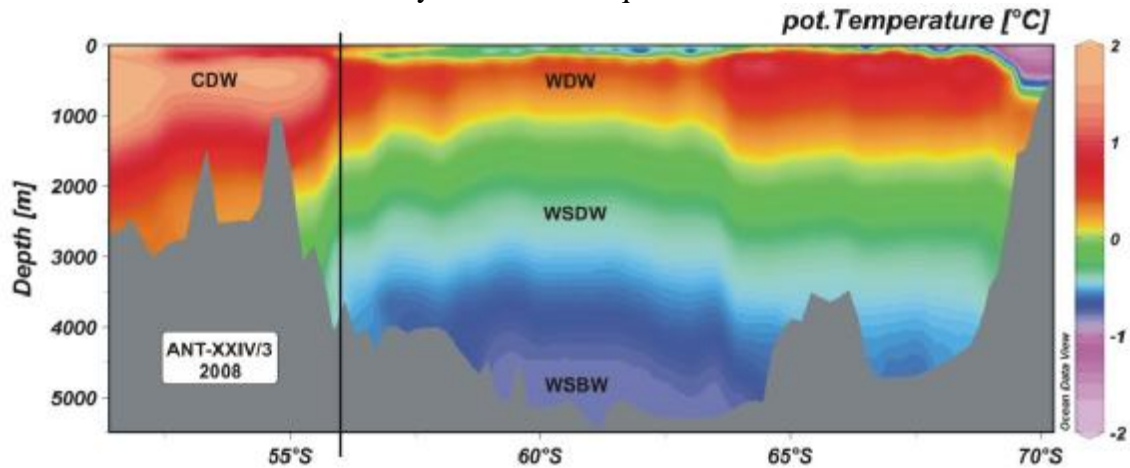


Figure 2 Vertical transect of potential temperature from the Southwest Indian Ridge (left) to the Antarctic continent (right) displaying the isotherms ascending to the South in the Antarctic Circumpolar Current and the doming related to the Weddell gyre as measured during *Polarstern* cruise ANT XXII/3 in 2005. The major water masses are the Circumpolar Deep Water (CDW), the Warm Deep water (WDW), the Weddell Sea Deep Water (WSDW) and the Weddell Sea Bottom Water (WSBW). The black vertical line indicates the northern limit for the calculation of the average properties of the water masses. The location of the transect is displayed in figure 1.

THE VARIATIONS OF THE WATER MASS PROPERTIES

The most prominent patterns are variations of temperature and salinity of the Warm Deep Water and the Weddell Sea Bottom Water (Figure 3). In the bottom water of the Weddell Sea proper a temperature increase by 0.12°C was observed over 16 years from 1989 to 2005. At the Prime Meridian warming occurred in the Warm Deep Water from 1984 to 1996 followed by cooling. The warming trend in the bottom water is detected here as well and started in 1992. It is coinciding with the increase of salinity. This is in stark contrast to the situation in the Northwestern Weddell Sea where Weddell Sea Bottom Water is cooling and getting fresher since the early nineties (Heywood et al., in prep).

The variations in the near-surface layers are more difficult to quantify because of the intensive annual cycle. Therefore the properties of the Winter Water were derived using combined winter data from profiling floats and the CTD transects: Properties measured at the CTD sections were corrected for the seasonal variation derived from float data thus resolving the annual cycle. The main result is that the salinity of the Winter Water was subject to significant increase until 2004, potentially reducing the stability of the upper water column, but since then it is decreasing again. Consequently, the stability of the water column increased again and a renewed occurrence of a large polynya becomes less likely.

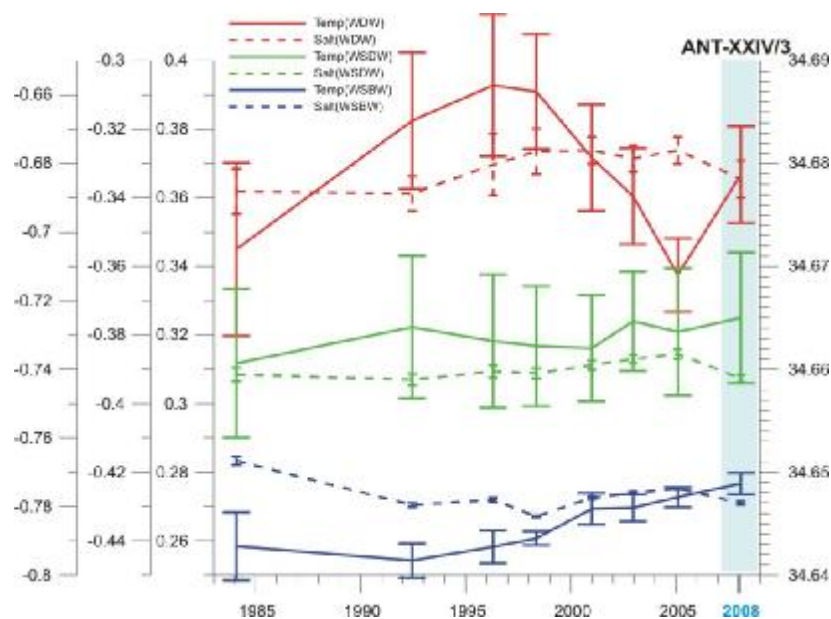


Figure 3 Variations of the watermass properties in the Weddell gyre from 1984 to 2008 observed on the meridional transect displayed in figure 1 and shown on the transect in figure 2. The red line stands for the Warm Deep Water, green for the Weddell Sea Deep Water and dark blue for Weddell Sea Bottom Water. The full lines stand for potential temperature the broken lines for salinity.

DISCUSSION AND CONCLUSIONS

Pronounced variations on a multi-annual time scale occur in the water mass properties of the Warm Deep Water, the Weddell Sea Bottom Water, the Winter Water and the winter sea ice thickness. The Warm Deep Water temperature increased until the mid 1990s, decreased until 2005 and is warming again since then. Whereas the temperature of the Weddell Sea Bottom Water is still increasing on the Greenwich meridian, it cools in the Weddell Sea proper since the early 2000s. The salinity of the Winter Water decreased with increasing Warm Deep Water temperature and is increasing from the mid 1990s to the mid 2000s and decreasing since. Since the Warm-Deep-Water core was shrinking and the Winter-Water layer deepening, input of salt from Warm Deep Water is a likely cause increasing salinity in Winter Water and a loss of stability of the upper layers. However, winter sea ice thickness was increasing until early 2000s and decreasing since, suggesting that heat transport from the Warm Deep Water is not directly controlled by the density difference if the stability of the water column is above a certain threshold. The long-term change of the water mass properties corresponds to an increase of the meridional air pressure difference on the Greenwich meridian from the early 90s to the early 2000s and a later decrease. However the active mechanism is still under investigation.

REFERENCES

Baines P. G. and S Condie, Observations and modelling of Antarctic downslope flows: A review. In: Jacobs SS, Weiss RF (eds) Ocean, ice, and atmosphere: Interactions at the Antarctic continental margin, Antarctic Research Series 75, American Geophysical Union, pp 29-49.1998.

- Carmack E. C., Water characteristics of the Southern Ocean south of the Polar Front. In: Angel M (ed) *A Voyage of Discovery, George Deacon 70th Anniversary Volume*, Pergamon Press, pp 15-41, 1977.
- Fahrbach, E., G. Rohardt and R. Sieger, 25 Years of Polarstern Hydrography (1982-2007), WDC-MARE Reports 5, 94 pp, 2007.
- Fahrbach, E., M. Hoppema, G. Rohardt, M. M. Schröder and A. Wisotzki, Decadal-scale variations of water mass properties in the deep Weddell Sea. *Ocean Dynamics*, 54, 77-91, 2004.
- Gill A. E., Circulation and bottom water production in the Weddell Sea. *Deep-Sea Res* 20: 111-140, 1973.
- Heywood, K.J., Thompson, A .F., Fahrbach, E., Mackensen, A., and Aoki, S., Cooling and Freshening of the Weddell Sea Outflow, in prep.
- Rintoul S.R, On the origin and influence of Adélie Land Bottom Water. In: Jacobs SS, Weiss RF (eds) *Ocean, ice, and atmosphere: Interactions at the Antarctic continental margin*, *Antarctic Research Series 75*, American Geophysical Union, pp 151-171, 1998.
- Rintoul S. R., C. W. Hughes and D. Olbers, The Antarctic Circumpolar Current system. In: Siedler G., J. Church, J. Gould (Eds.) *Ocean circulation and climate: Observing and modelling the global ocean*, Academic Press, pp 271-302, 2001.
- Robertson R., Visbeck M., Gordon A.L., Fahrbach E. (2002) Long-term temperature trends in the deep waters of the Weddell Sea. *Deep-Sea Res II* 49: 4791-4806.
- Thompson, D. W. J., and S. Solomon, Interpretation of Recent Southern Hemisphere Climate Change. *Science*, 296, 895-899, 2002.
- White W. B. & R. G. Peterson, An Antarctic circumpolar wave in surface pressure, wind, temperature and sea-ice extent. *Nature* 380: 699-702, 1996.
- Yuan, Y., ENSO-related impacts on Antarctic sea ice: a synthesis of phenomenon and mechanisms. *Antarctic Science*, 16 (4), 415 – 426, 2004

**MAJOR OPPORTUNITIES FOR INTERNATIONAL MULTI-DISCIPLINARY
RESEARCH AND EXPLORATION OF THE GLOBAL MID-OCEAN
RIDGE SYSTEM**

Jian Lin

Department of Geology & Geophysics, Woods Hole Oceanographic Institution,
Woods Hole, MA 02543 USA
jlin@whoi.edu

The 60,000-km-long mid-ocean ridge volcanic mountain range is the longest geological feature on Earth and the solar system. It plays an essential role in the renewal of the surface of our planet, recycling of oceanic lithosphere, and release of heat and chemicals from Earth's interior to oceans. Geological processes at ocean ridges determine the shape of ocean basins and the geochemical compositions of oceanic crust and lithosphere. About 75% of Earth's total heat flux occurs through oceanic crust, much of it at ocean ridges through complex hydrothermal interactions between the lithosphere and oceans. Since deep-sea hydrothermal vents were first discovered at the Galapagos Spreading Center in 1977 by submersible *Alvin*, active hydrothermal vents have now been found along ocean ridges beneath all major oceans, although a significant length of the ridge system, especially those in high-latitude regions, is still little explored. Hydrothermal vents are areas of focused and rapid outflow of seawater through permeable oceanic crust, heated by high-temperature magma sources beneath ocean ridges. At typical depths of 2,000-4,000 m beneath the ocean surface, sunlight is not available for life through photosynthesis. However, life is thriving at hydrothermal vents and is supported instead by chemosynthesis, in which the interaction of seawater with chemical elements emitted from hydrothermal vents and with seafloor rocks plays an essential role. Thus studying deep-sea chemosynthetic processes and their complex interactions with ocean ridge hydrothermal and volcanic systems has direct implications on understanding the origin of life on Earth and other planetary bodies. Furthermore, metal-rich hydrothermal sulfide deposits offer prospect of potential industrial deep-sea mining at a time of rising demands for industrial use of metals by growing economies.

International cooperation is essential in ocean ridge research. It is recognized that most ocean ridges are located in international waters, the scientific objectives and interests of researchers transcend national boundaries, and the scope of ocean ridge science is so large that it can never be covered fully by the resources of any single nation. InterRidge < www.interridge.org > is an international program to coordinate and promote international, multi-disciplinary research of the global ocean ridges, reaching more than 2,500 individual researchers and science managers in 60 countries and regions. InterRidge working groups promote and coordinate international collaboration on active research areas of global interest, currently focusing on eight themes: 1) Long-range exploration of ridges by autonomous underwater vehicles; 2) seafloor mineralization processes; 3) biogeochemical interactions at deep-sea vents; 4)

hydrothermal vent ecology; 5) mantle imaging; 6) real-time ridge monitoring and observatories; 7) deep Earth sampling; and 8) ultra-slow spreading ridges. During this presentation, the author will discuss the recent international advances in research of the deep-sea processes at mid-ocean ridges. The presentation will highlight increasing contributions by Asian countries to deep-sea research and exploration and will discuss exciting new opportunities for Korean science community to lead the multi-disciplinary investigation and exploration of the geological, hydrothermal, and biological processes of the Pacific-Antarctic Ridge and other polar ridge regions through strong international collaborations.

SESSION I

CLIMATE CHANGE AND POLAR OCEAN SYSTEM

THE INFLUENCE OF NATURAL IRON INPUTS ON SOUTHERN OCEAN PRODUCTIVITY AND CARBON SEQUESTRATION

Tom Trull

Institute of Antarctic and Southern Ocean Studies, University of Tasmania, Australia
Tom.Trull@utas.edu.au

Artificial iron experiments have confirmed the role of iron as the limiting nutrient controlling Southern Ocean phytoplankton growth. But these experiments have struggled to determine the links between increased growth rates and transfer of the fixed carbon to the deep sea by sinking particles, and these links may be relevant only to short-term, small-scale iron supply. Study of regions where persistent elevated iron supply occurs naturally offer additional insights into ecosystem control of carbon cycling, although the magnitude of iron supply is less well constrained. Results from KEOPS project over the Kerguelen plateau suggest that carbon sequestration is approximately doubled by the enhanced iron supply, but the efficiency of the sequestration (in terms of C removed per unit iron added) remains under debate, as the mechanisms and magnitude of iron supply over the full seasonal cycle are not yet known. The 1000 km scale of the phytoplankton bloom that forms in the Antarctic Circumpolar Current downstream of the plateau suggest that iron is only relatively slowly removed from surface waters. Modelling of the phytoplankton production suggests that responses to changing iron supply in a changing climate will depend very much on the details of the interactions between the supply mechanisms and the surface ocean stratification, as well as details of higher-trophic level responses to changing production and changing climate.

ANTARCTIC SEA ICE PROCESSES AND CLIMATE; WHAT WE HAVE LEARNED AND WHAT WE NEED TO KNOW FURTHER

Stephen Ackley

S.F. Ackley, Geol. Sciences Dept., Univ of Texas at San Antonio, San Antonio TX
78249 USA

Stephen.ackley@utsa.edu

Antarctic sea ice in its formation, metamorphosis and decay exhibits unique characteristics. At present many of these processes are not represented well in current modeling efforts, and we review here those features that are both characteristic of the ice cover and yet provide difficulties in representation in large-scale coupled models. Better understanding of the spatio-temporal distribution and variability of Antarctic sea ice in its extent, thickness and properties and the relationship of the observed variability to atmospheric and oceanic forcing and changes are necessary. Arctic sea ice has been extensively affected by global warming and has shown a significant shrinking in extent and thickness. However, the trend of Antarctic sea ice extent remains ambiguous, with a general small overall increase in circumpolar extent (~1%/decade), as measured over the last thirty years with passive microwave satellite technology. In detail, however, large interannual variability(~5%) is observed in Antarctic sea ice extent and seemingly paradoxical behavior, where winter ice maximums(minimums) are sometimes followed by summer extent minimums(maximums) are observed. Interpretation from limited data and use of proxies (whaling catch) have led to some controversy about pre-satellite era ice extents, particularly if summer data is used to extrapolate to winter behavior where data is lacking for this era. As well, the observed slight overall increase in sea ice extent has large regional variability, with huge losses in sea ice in the Antarctic Peninsula region, compensated by relatively similar increases in the adjacent Ross Sea Sector. Therefore while the overall behavior of the sea ice would leave the impression of a slight cooling in the circumpolar sea ice zone, instead the Antarctic Peninsula is undergoing a warming trend over the recent decades commensurate with the Arctic region warming, with millennial-scale changes in the retreat of ice shelves, and dramatic changes in both the marine and terrestrial ecology.

Ice thickness is the principal quantitative measure of ocean-air exchanges and better datasets will therefore be the gold standard for validation of air-ice-ocean coupled models, and thereby increase confidence in our capability for understanding sea ice and its climate connection as well as the prediction of future sea ice and climate changes. There is however, no systematic and reliable data available on Antarctic sea ice thickness and snow cover on sea ice (IPCC-C4, 2007) that can show long-term trends, if any exist. In the Arctic, submarine transects with Upward Looking Sonar have allowed the secular change in ice thickness distribution to be determined, but the Antarctic sea ice zone has no similar data set. Instead, ship-based observations are used to describe regional and seasonal changes in the thickness distribution and characteristic

of sea ice and snow cover thickness around Antarctica. The data set is comprised of more than 25,000 observations collected over more than two decades of activity and has been compiled as part of the Scientific Committee on Antarctic Research (SCAR) Antarctic Sea Ice Processes and Climate (ASPeCt) program. The results show the seasonal progression of the ice thickness distribution for six regions around the continent together with statistics on the mean thickness, surface ridging, snow cover and local variability for each region and season. Since it is not possible to estimate the long-term (inter-annual or decadal) variability for the sea ice thickness field from the ASPeCt data set, it represents the mean thickness climatology, rather than the conditions at any specific location or time within a region. The long-term mean and standard deviation of total Antarctic sea ice thickness is 0.87 ± 0.91 m. This value is 40% higher than the level ice thickness mean (0.62 m) which we interpret as the significant influence of deformation processes on the thickness distribution of Antarctic sea ice. We also note here that the standard deviation of the total thickness is greater than the mean, indicating the highly variable nature of the ice thickness field in Antarctica, both seasonally and regionally. Characterizations of the ice thickness in Antarctic sea ice by a single mean thickness therefore misrepresents the significant variability in thickness and therefore in growth, decay and metamorphic processes that are necessary to accurately represent the evolution of the ice cover on an annual basis. These variable processes are however, reflected well in the regional ice thickness distributions that are now available from the analysis of the ASPeCt data archive.

In terms of “What we need to know further about Antarctic Sea Ice”, we pose three questions that remain under study and are relevant to the determination of the two-way effects of sea ice on the climate and ocean and the effects on marine ecosystems in the Antarctic. Preliminary results, where available, on these questions will be discussed.

What are the heat and salt fluxes associated with sea ice, impacting climate and deepwater formation?

What are the physical-biogeochemical interactions in sea ice and connections with the carbon cycle, sulfur cycle, krill and top predators life cycles?

How can we use ship-based measurements to validate remote sensing of sea ice?

THE ROLE OF SEA ICE MEASUREMENT IN CLIMATE MODELING

Achim Stössel

Department of Oceanography, Texas A&M University, College Station, USA
astoessel@ocean.tamu.edu

INTRODUCTION

Meteorological, oceanographic, as well as sea ice measurements from research icebreakers play a vital role in the validation of climate models. Besides directly from research vessels/icebreakers (Fig.1), sea-ice thickness is measured with upward-looking sonar, and sea-ice concentration is derived using various satellite sensors. With this invaluable data source we were able to observe that over the last 50 years Arctic sea ice decreased, while Antarctic sea ice generally remained unchanged.

LINK TO CLIMATE MODELING

Both outcomes are consistent with IPCC type of climate scenario integrations with coupled atmosphere – sea-ice – ocean general circulation models (GCMs). While perhaps suitable for projections over a time period of 100 years, we argue that these types of climate models do not (yet) constitute reliable tools for projections over periods marked by substantial change of the deep ocean. This is due to the properties and the circulation of the deep ocean being mainly determined by polar processes, which are poorly resolved in climate models. As an example, Southern Ocean sea ice and convection play a crucial role in the formation of Antarctic Bottom Water. Being the dominant contributor to the world ocean's water volume below 2500 m depth (Orsi et al., 2001), its distribution, properties, and abundance determine to a large extent the global meridional overturning circulation, and thus the meridional heat transport.

RESULTS

In terms of climate modeling, this talk will address the representation of Southern Ocean sea ice (Fig.2) and convection in a global ocean GCM of the kind typically used in climate models, together with its long-term deep-ocean equilibrium response. The talk will conclude with a verification of the simulated Antarctic winter ice-thickness distribution based on data gathered exclusively from research icebreakers (Worby et al., 2008), and derived from satellite remote sensing (Zwally et al., 2008). Both data sources confirm the crucial role that ice dynamics play for a realistic representation of the sea-ice thickness distribution in a sea-ice – ocean GCM. This has been figured almost 20 years ago (e.g., Stössel et al., 1990), during the time when the first fully coupled GCMs emerged (e.g., Cubasch et al., 1992), based on point measurements of ice thickness (e.g., Wadhams et al., 1987). Bitz et al. (2005) and Stössel (2008), on the other hand, recently demonstrated the crucial role of upper-ocean temperature in determining the quality of a Southern Ocean sea-ice simulation. By enhancing the resolution of the sea-ice component (about 20 km) versus that of the ocean component (Stössel et al., 2007), and by constraining the upper-ocean temperature by satellite-derived sea-ice concentration, Stössel (2008) was able to arrive at a much more realistic sea-ice simulation, as well as long-term global deep-ocean properties. Fig.3 shows a typical simulated winter ice-thickness distribution using the same approach, but with the ocean component also run at 20 km resolution, albeit only in a regional Southern Ocean configuration.

CONCLUSIONS

Based on 20 years of experience in trying to simulate Southern Ocean sea ice in the framework of a global ocean GCM, I come to the conclusion that an unrealistic sea-ice simulation is generally not the result of a poor sea-ice model, but rather the result of a poor representation of its adjacent components, i.e. either the atmosphere (in particular winds) or the ocean (in particular oceanic heat flux), or both. By deteriorating the sea-ice simulation, a poor atmospheric and oceanic (near) surface representation will, most importantly, also deteriorate the surface buoyancy fluxes, which in turn will affect the rate of deep- and bottom-water formation, and thus the long-term global ocean properties and circulation. We thus might think about improving the high-latitude atmosphere and ocean (near) surface conditions in global models designed for long-term integrations by employing/assimilating data gathered through satellite remote sensing and from research icebreakers. Of particular importance in this regard is the resolution and quality of data along the Antarctic coastline. Since satellite passive-microwave retrievals are not very reliable along complex coastlines, besides coastal stations, we will need to rely primarily on research icebreakers.



Fig.1: Sea ice measurements from the German research vessel Valdivia during BEPERS-88 (Bothnian Experiment in Preparation for ERS-1), Sea of Bothnia, Baltic Sea, March 1988.

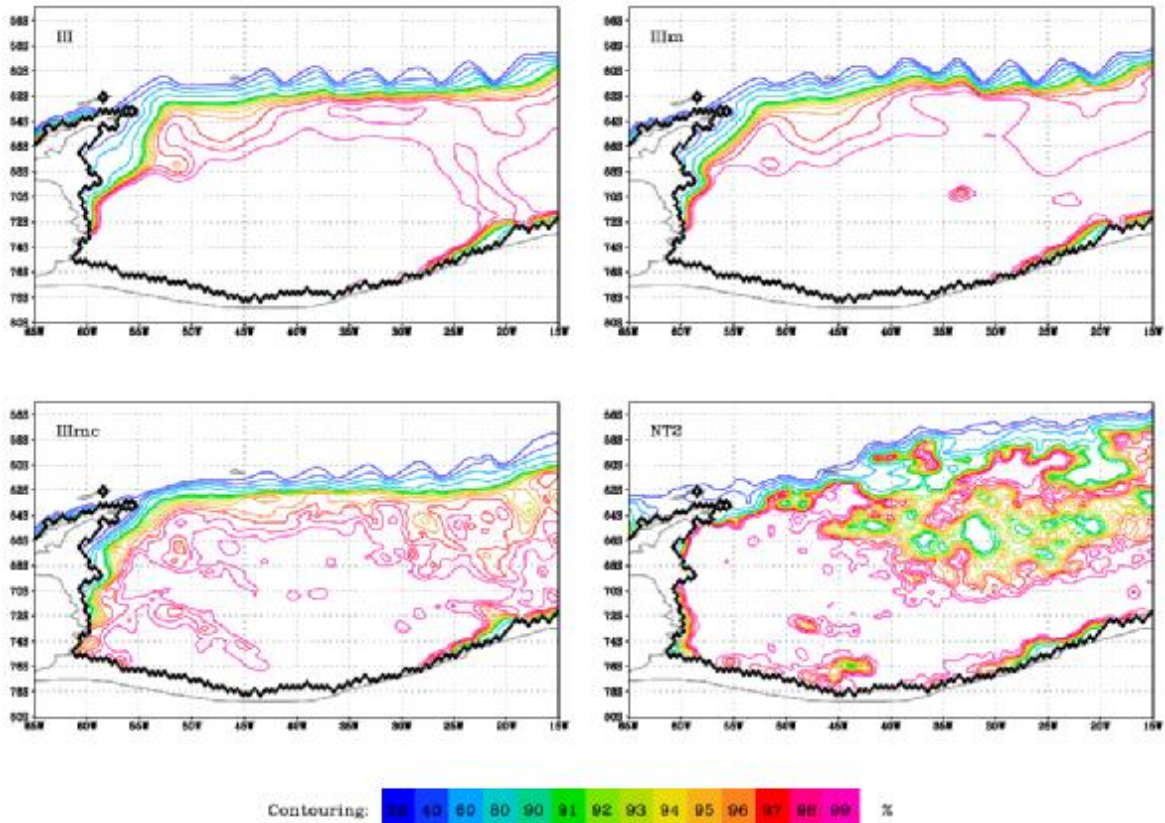


Fig.2: Mid-September snapshots of ice concentration in the Weddell Sea as simulated in reference case (III), with idealized ice-shelf melting (III_m), with additional idealized tidal currents (III_mc), and as derived from satellite passive microwave data using the NASA Team 2 (NT2) algorithm (Markus and Cavalieri, 2000). From Stössel et al. (2007).

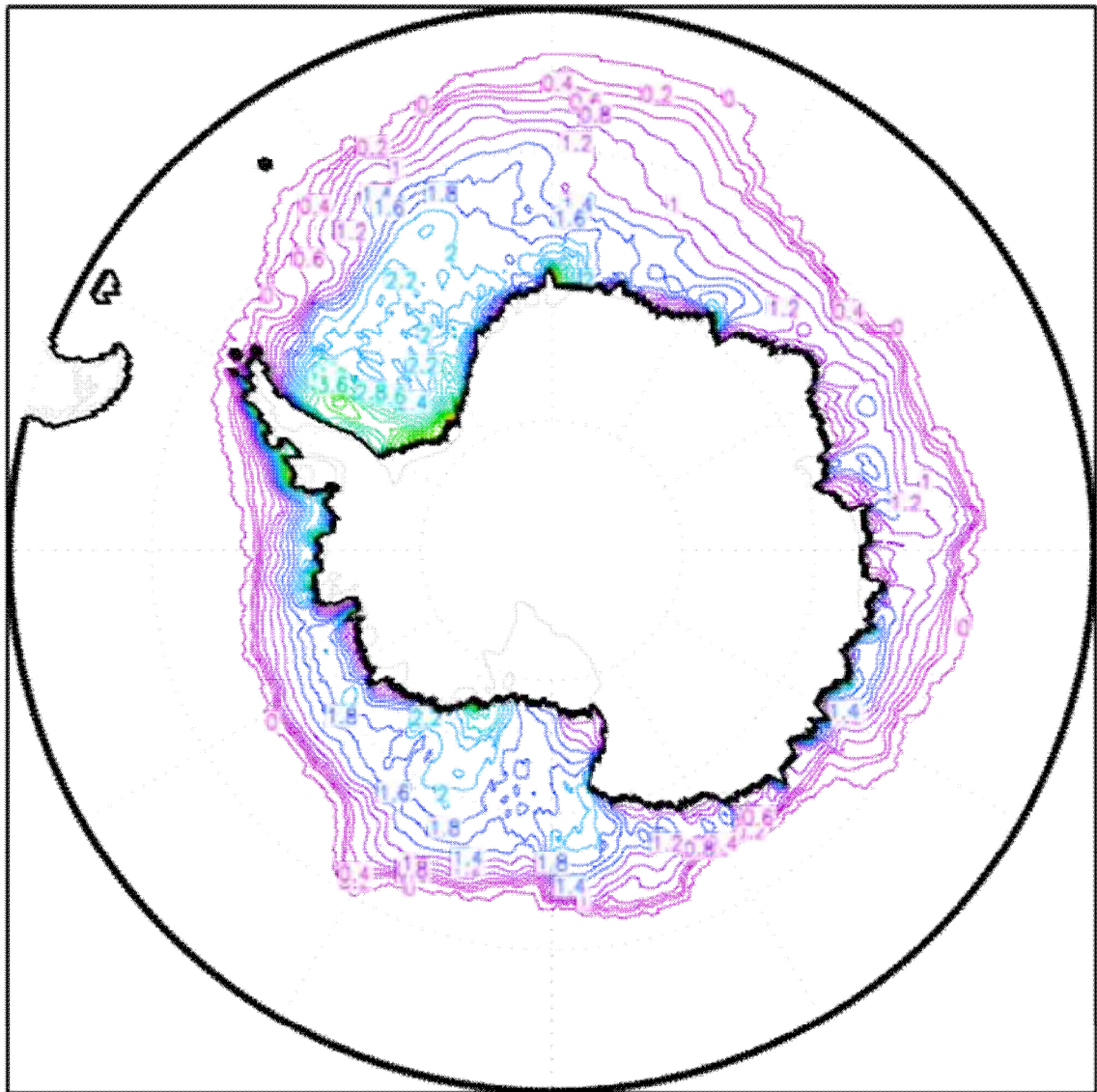


Fig.3: Snapshot of winter sea-ice thickness distribution as simulated with a 20 km resolution sea-ice – ocean GCM in which the upper-ocean temperature has been constrained by satellite-derived sea-ice concentration following Stössel (2008). Isoline increment is 0.2 m.

REFERENCE

- Bitz, C.M., Holland, M.M., Hunke, E.C., and Moritz, R.E. 2005. Maintenance of the sea ice edge. *J.Climate* 18, 2903-2921.
- Cubasch, U., Hasselmann, K., Höck, H., Maier-Reimer, E., Mikolajewicz, U., Santer, B.D., and Sausen, R. 1992. Time-dependent greenhouse warming computations with a coupled ocean – atmosphere model. *Clim.Dyn.*8, 55-69.
- Markus, T. and Cavalieri, D.J. 2000. An enhancement of the NASA Team sea ice algorithm. *IEEE Trans.Geosc.and Remote Sens.* 38, 1387-1398.
- Orsi, A.H., Jacobs, S.S., Gordon, A.L., and Visbeck, M. 2001. Cooling and ventilating the abyssal ocean. *Geophys.Res.Let.*28, 2923-2926.
- Stössel, A., Lemke, P., and Owens, W.B. 1990. Coupled sea ice – mixed layer simulations for the Southern Ocean. *J.Geophys.Res.*95, 9539-9555.
- Stössel, A., Stössel, M.M., and Kim, J.T. 2007. High-resolution sea ice in long-term global ocean GCM integrations. *Ocean Modelling* 16, 206-223.
- Stössel, A. 2008. Employing satellite-derived sea ice concentration to constrain upper-ocean temperature in a global ocean GCM. *J.Climate* 21, 4498-4513.
- Thompsson, T., and Leppäranta, M. (eds.) 1988. BEPERS-88, Experiment plan. *Winter Navigation Research Board, Swedish Administration of Shipping and Navigation, Finnish Board of Navigation*, Research Report No.46.
- Wadhams, P., Lange, M.A., and Ackley, S.F. 1987. The ice thickness distribution across the Atlantic sector of the Antarctic ocean in midwinter. *J.Geophys.Res.*92, 14,535-14,552.
- Worby, A.P., Geiger, C.A., Paget, M.J., Van Woert, M.L., Ackley, S.F., and DeLiberty, T.L. 2008. Thickness distribution of Antarctic sea ice. *J.Geophys.Res.*113, C05S92, doi: 10.1029/2007JC004254.
- Zwally, H.J., Yi, D., Kwok, R., and Zhao, Y. 2008. ICESat measurements of sea ice thickness in the Weddell Sea. *J.Geophys.Res.*113, C02S15, doi: 10.1029/2007JC004284.

GLACIERS, ICE SHEETS AND THE MARINE RECORD: EVIDENCE FROM SUBMARINE LANDFORMS

Julian A. Dowdeswell¹

¹Scott Polar Research Institute, University of Cambridge, Cambridge CB2 1ER, UK
jd16@cam.ac.uk

INTRODUCTION

Ice sheets cover about 16 million km² of the Earth's surface today. During the last glacial maximum, about 20,000 years ago, ice covered about double this area, contributed to mainly by the growth of the North American and Eurasian ice sheets and the advance of the Antarctic and Greenland ice sheets across the adjacent continental shelves (Clark and Mix, 2002). Significant portions of the margins of these contemporary and past ice sheets terminate in marine waters. From this ice-ocean interface, icebergs, meltwater and the sediments they transport, are released into the oceans. About 10% of modern oceans are affected directly by glacier-derived sediments and sedimentation, and this area approximately doubled at the last glacial maximum.

The continental margins of high- and mid-latitudes, that is the continental shelves, slopes and deep-sea basins beyond, therefore contain a record of both present and past glacial-marine processes and products. We describe marine-geophysical and -geological data from Arctic margins, including slope, shelf and fjord settings. In particular, we present swath-bathymetric and sub-bottom profiler data showing well-preserved submarine landforms indicative of the past flow of Arctic glaciers and ice sheets.

METHODS

Both geophysical and geological datasets are presented. These include sediment cores, swath-bathymetry and three-dimensional (3D) seismic imagery with horizontal resolution of 3-50 m in grid-cell size. Most swath-bathymetric data have been acquired using Kongsberg Simrad multibeam systems, including EM120 and EM3000, for deep and shallow water work, respectively. Several sub-bottom profilers have also been used to acquire acoustic-stratigraphic data.

The preserved beds of former ice sheets, revealed on polar shelves and in fjords by ice retreat, can be imaged relatively straightforwardly due to: a) access to shelves using icebreaking ships; and b) the relative ease of geophysical work through water. In addition, there has been little modification of many submarine landforms since deposition and little sedimentation since deglaciation. By contrast, investigating modern ice-sheet beds beneath kilometres of ice is very expensive and difficult.

Three main topics relating to submarine landforms and past ice-sheet form and flow will be discussed.

RECONSTRUCTING PAST ICE-SHEET FLOW

Evidence from terrestrial sediments and landforms has long been used to reconstruct the configuration of past ice sheets. As more geophysical and geological data have become available from polar waters, imagery of well-preserved submarine landforms is adding important new insights on the flow patterns of former marine-based ice sheets (e.g. Ottesen et al., 2005). In Arctic Eurasia, the dimensions of ice at the Last Glacial Maximum (LGM) and the timing of deglaciation have been reconstructed using evidence on postglacial-emergence and dated lithostratigraphies from terrestrial sections and marine cores, together with numerical ice-sheet modelling. However, the detailed pattern of Late Weichselian ice flow in the northern Barents Sea, and the extent of major ice-sheet drainage basins flowing northwards into the Arctic Ocean, has remained illusive. This is due mainly to a lack of observations from the seas east of Svalbard and in the Russian Arctic. Changing sea-ice conditions allowed acquisition of swath-bathymetric imagery of well-preserved subglacial landforms characterizing Late Weichselian ice-flow directions over about 150,000 km² of the NW Barents Sea (Dowdeswell et al, Submitted). Interpretation of streamlined submarine landforms produced beneath former ice sheets shows that an ice dome was located on easternmost Spitsbergen or southern Hinlopen Strait, controlling the regional flow pattern. Ice flowed eastward around Kong Karls Land into Franz Victoria Trough and north through Hinlopen Strait. An ice dome west of Kong Karls Land is required to explain the observed ice-flow pattern, but does not preclude an additional ice dome to the south-east. Discrepancies with earlier ice-sheet reconstructions reflect the lack of previous sea-floor observations, with evidence limited to past ice loading and deglacial rebound.

BASAL PROCESSES: MELTWATER FLOW AND BED DEFORMATION

Satellite data show that large volumes of water can flow between Antarctic subglacial lakes. Flow acceleration on the Greenland Ice Sheet is also linked with surface meltwater lubricating parts of the bed. However, we still know little about ice-sheet basal hydrological partly because it is obscured today by ice several kilometers thick. By contrast, former ice-sheet beds are well-preserved on high-latitude continental shelves, from which ice retreated <15,000 years ago. We present images of submarine landforms, produced by subglacial meltwater when ice last advanced across polar continental shelves. The landforms, which cover hundreds of square kilometers, indicate water flow in both channels and as a form of sheet flow beneath former ice sheets in the Norwegian Arctic, providing an analogue for elements of the basal hydrology of modern polar ice sheets. Sediment-filled former channels from Arctic shelves show surface-meltwater penetration to the bed, similar to modern Greenland.

Fast-flowing ice streams and outlet glaciers currently account for up to 90% of the discharge from the Antarctic and Greenland ice sheets. Although the deformation of subglacial material has been proposed as the mechanism for this rapid motion, such sediment is usually hidden under several kilometers of ice. Marine-geophysical records have allowed reconstruction of the three-dimensional thickness of the sedimentary bed beneath a large Antarctic palaeo-ice stream (Dowdeswell et al., 2004). Fast flow is indicated by streamlined sea-floor lineations which form the surface of a layer of low shear-strength unsorted sediment, averaging 4.6 m thick. Rapid motion of the paleo-ice stream was a result of subglacial deformation within this layer.

ICE-SHEET RETREAT: A TEST OF ICE-SHEET NUMERICAL MODELS

The rate of ice-sheet retreat across Arctic and Antarctic continental shelves during deglaciation, and the possibility of ice-stream collapse and associated sea-level rise, has been much debated. We show that the rapidity of ice retreat can be inferred from diagnostic assemblages of submarine landforms, produced at ice-stream beds and preserved in the geological record (Dowdeswell et al., 2008). These landforms, exposed by ice retreat across high-latitude shelves, demonstrate that deglaciation occurs in three ways: rapidly, by floatation and breakup; episodically, between grounding events; or by slow retreat of grounded ice. Submarine landform assemblages imply, through the common presence of grounding zone wedges overprinting mega-scale glacial lineations in many Arctic and Antarctic cross-shelf troughs, that ice retreat is more often episodic than catastrophic through the length of an ice stream. These spatially extensive geological observations provide a robust test of the ability of numerical models to predict the varied response of ice-sheet drainage basins to environmental changes.

REFERENCES

- Clark, P.U. and Mix, A.C., 2002. Ice sheets and sea level of the Last Glacial Maximum. *Quaternary Science Reviews*, 21, 1-7.
- Dowdeswell, J.A., Ó Cofaigh, C. and Pudsey, C.J., 2004. Thickness and extent of the subglacial till layer beneath an Antarctic paleo-ice stream. *Geology*, 32, 13-16.
- Dowdeswell, J.A., Ottesen, D., Evans, J., Ó Cofaigh, C. and Anderson, J.B., 2008. Submarine glacial landforms and rates of ice-stream collapse. *Geology*, 36, 819-822.
- Dowdeswell, J.A., Hogan, K.A., Evans, J., Noormets, R., Ó Cofaigh, C. and Ottesen, D. Past ice-sheet flow east of Svalbard inferred from streamlined subglacial landforms. Submitted to *Geology*.
- Ottesen, D., Dowdeswell, J.A. and Rise, L., 2005. Submarine landforms and the reconstruction of fast-flowing ice streams within a large Quaternary ice sheet: the 2,500 km-long Norwegian-Svalbard margin (57° to 80°N). *Geological Society of America, Bulletin*, 117, 1033-1050.

BIOLOGICAL PRODUCTION IN THE WESTERN ARCTIC AND POSSIBLE FUTURE RESEARCH DIRECTIONS

T.E. Whitley¹ and S.H. Lee²

¹Institute of Marine Science, University of Alaska Fairbanks, Fairbanks, AK 99775,
U.S.A.

terry@ims.uaf.edu

²Korea Polar Research Institute, Incheon, R.O.K.

Since the most rapid changes in ice-cover has occurred in the western Arctic there is a critical need to have better measurements of the physical and biological processes that contribute to the biological productivity in that region in order to understand and hopefully predict their biological effects. The removal of seasonal and permanent ice cover can alter several important processes such as the depth of mixing, stratification, light penetration, nutrient supply, temperature-related processes and possibly photochemical reactions.

The lack of ice-capable research vessels contributed greatly to the delay in carrying out scientific research in both the seasonal and “permanent” ice covered regions of the Arctic Ocean. But in the past decade an increased attention to the western Arctic has occurred with programs of Canada, China, Japan, Korea, Russia and United States that studied the physical and biological processes occurring there. A considerable amount of new understanding has been achieved in circulation patterns and water mass structure over the western Arctic shelves during summer/fall seasons but additional details are still missing with regard to many of the boundaries with the Arctic Basin especially during winter through early summer seasons. Likewise, nutrient-plankton studies related to biomass and fluxes have been accomplished for the summer and autumn seasons in the shelf regions but only a few studies have occurred in the basin and its boundaries.

The ice-free waters in the Chukchi and Beaufort Seas have been the most studied regions for the distribution and fluxes of nutrients, pigments, phytoplankton species, primary productivity and zooplankton grazers. An example of typical late summer nutrient (Figure 1) and primary production (Figure 2) measurements are shown for the Chukchi Sea in 2004. The range of nutrient concentrations may vary by as much as 100-fold from the nutrient depleted Alaska Coastal Water to the relatively enriched Anadyr Water in the western Chukchi Sea. Phytoplankton biomass as estimated by chlorophyll-a content has often been observed to have a similarly large horizontal gradient. The wide range of summer nutrient and primary production values is speculated to continue during other seasons while sufficient sunlight is available but very few measurements have been collected outside of the summer ice-minimum period when the physical and nutrient environments are relatively stable. The interannual

variations of the conditions leading to nutrient concentrations, chlorophyll biomass and primary production are not predictable at the present time.

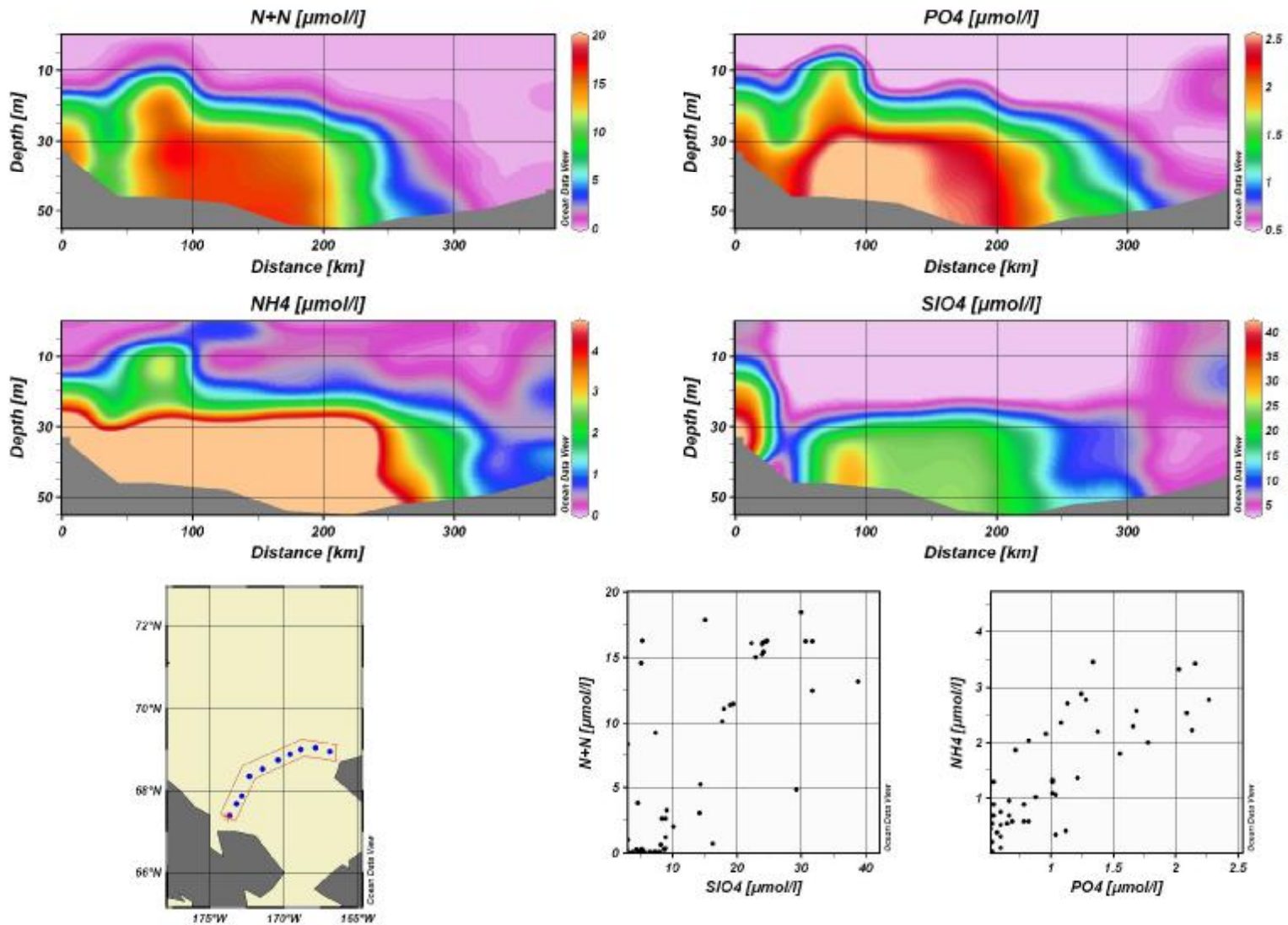


Figure 1. Nitrate plus nitrite (N+N), phosphate (PO₄), Ammonium (NH₄) and Silicate (SiO₄) in a transect across the Chukchi Sea during September 2004. Units are : mole/liter.

- Carbon uptake rates in Bering

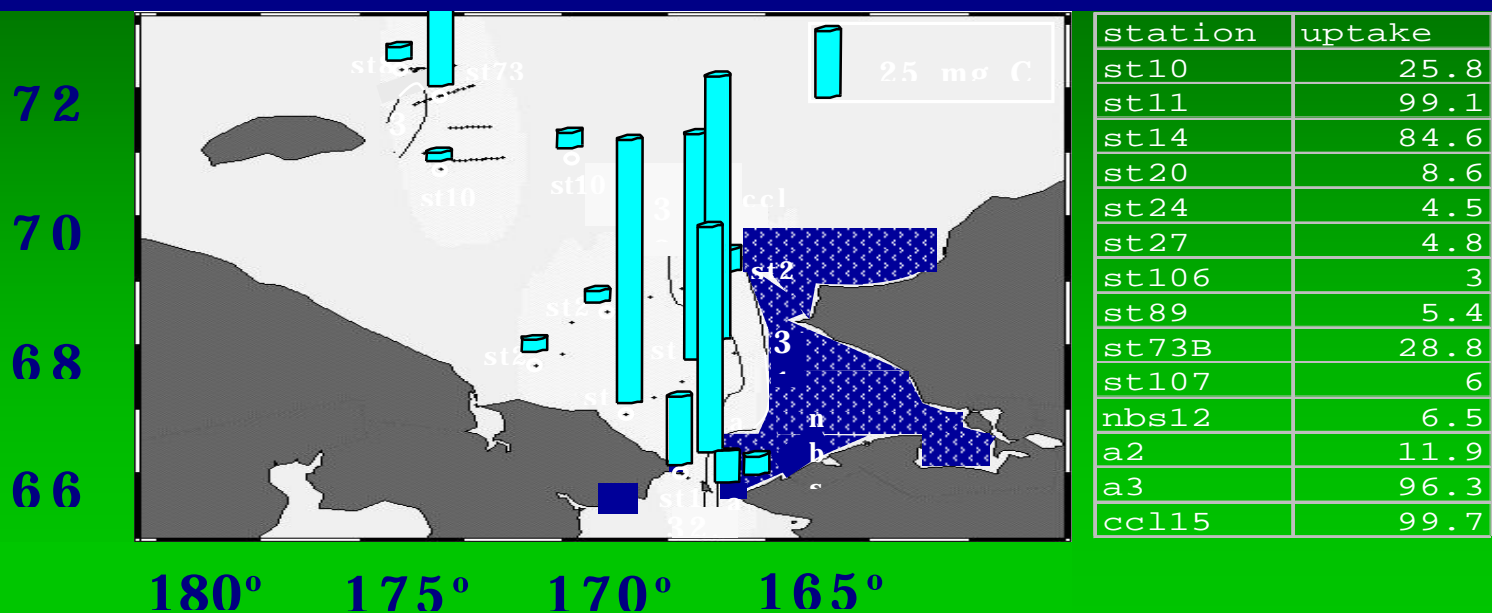


Figure 2. Primary production rates (mg C/m²/hr) in the Chukchi Sea during September 2004.

Future studies are still needed to understand the basic physical and biological processes as well as more detail of overall nutrient budgets and the species/abundance of major phytoplankton and zooplankton species that support the benthic and pelagic upper trophic levels. These observations need to be collected throughout the seasons and preferably as often as monthly during spring through early winter to provide accurate estimates of annual levels of biomass and rates. Additional biological measurements that should be concurrently collected are described below.

In order to assess the effects of climate change on the biological production in the western Arctic an increased effort must be taken with respect to the physical/chemical conditions that support productivity processes. As ice is removed the depth of mixing and stratification, the quantity of subsurface radiation and nutrient species can greatly influence the primary production in the newly open waters. However, the simple decrease of ice thickness and increase of light penetration can possibly inflate the normally low rates of primary production of phytoplankton under the ice. A special effort needs to be undertaken to obtain measurements of the light environment under the ice and snow during all seasons of potential growth. This may be effectively accomplished with AUV/ROV deployments under ice to collect light data over relatively large areas to assess the mean and range of transmission of PAR through ice to the water column.

Additional measurements that are needed to understand the composition and dynamics of the lower trophic levels are 1) all forms of carbon, nitrogen, phosphorus and silicon macronutrients as well as trace nutrients such as iron and manganese; 2) taxonomic

composition and abundance of major phytoplankton groups including genetic analyses; 3) physiological rates of major phytoplankton groups including critical light and nutrient conditions; 4) composition and rates of microbial populations that consume the microplankton and regenerate nutrients; 5) assessment of abundance and rates of micrograzers that can consume small plankton to produce dissolved organic matter; and 6) rates of sinking of organic matter (both live and dead) that support benthic populations and enhance organic concentrations in sediments.

The addition of many of the above observations will provide the specific rates and biomass values that are needed to a vastly improved ability to model the productivity of plankton populations under the scenario of continued changing climate conditions of reduced ice cover, higher temperatures, more surface layer wind mixing, greater salinity stratification from meltwater and/or increased freshwater discharge and a possible increased tolerance of more southerly species to survive in the Arctic.

MECHANISM OF CATASTROPHIC CLIMATE CHANGES IN THE ARCTIC OCEAN
A recommendation to future observational research to understand the fate of
Arctic Ocean and global climate

Koji Shimada

Faculty of Marine Science, Department of Ocean Sciences,
Tokyo University of Marine Science and Technology
koji@kaiyodai.ac.jp

INTRODUCTION

Recent sea ice reduction in summer is not spatially uniform, but is disproportionately large in the Pacific sector of the Arctic Ocean. This asymmetric reduction is a key to understand the acceleration of reduction of sea ice (e.g., Figure 3). The center of the maximum retreat in recent years is on the Northwind Ridge and Chukchi Plateau region where the warm Pacific Summer Water enters the central Canada Basin (Sumata and Shimada, 2007). The upward heat flux from Pacific Summer Water just beneath the surface mixed layer retards the sea ice formation during winter. In this region, sea ice thickness at the melt onset is much less than the surrounding region. As the results, the sea ice was easy to be disappeared there under the nearly the same atmospheric condition and solar radiation. The zonal asymmetric disappearance sea ice in western Arctic settled a dipole sea level pressure pattern there, which brings a warm air from south toward central Arctic from Pacific side. This wind anomaly drives the sea ice motion from Pacific sector to the Atlantic sector in addition to melt. These joint effects of the retreat pattern of the sea ice enhance the reduction of sea ice (e.g. sea ice cover in the summer of 2007).

Why the warming of the upper Arctic Ocean was initiated. This is a key issue to understand the initiation of positive feed back loop for sea ice reduction. Shimada et al. (2006) proposed a new ice-ocean feedback system to understand the recent catastrophic reduction of sea ice (Figure 1). The warming of the Pacific Summer Water in the Canada Basin is not directly associated with warming of upstream inflow through the Bering Strait. The oceanic heat is crucially controlled by the volume transport of the oceanic Beaufort Gyre. In the Arctic Ocean, the upper ocean is not directly driven by the wind stress, but by the motion of sea ice. Although the sea ice is driven by the wind forcing, but the amplitude of the motion is also affected by the stress from the coastal boundary. If the Arctic Ocean is completely covered by sea ice, the wind forcing does not hardly penetrate into the sea ice due to friction of sea ice against coastal boundary.

However, less sea ice cover just near the coastal boundary establishes more free-slip condition for large-scale sea ice motion. This means that the sea ice motion depends not only on the wind forcing but also on the sea ice cover itself.

R/V MIRAI INTERNATIONAL POLAR YEAR 2008 CRUISE

The summer minimum sea ice extent in 2008 was resulted in the second minimum record after the passive microwave observation since 1979. The sea ice extent is slightly smaller than that in 2007. This was caused by a further activation of sea ice motion associated with fragmentation of sea ice near the coast of the Banks and Queen Elizabeth

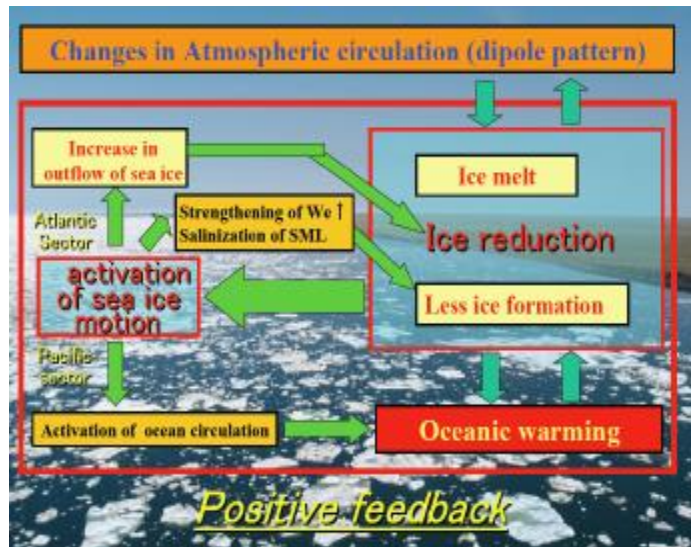


Figure 1. New positive feed back system

Islands. The fragmentation of sea ice suggest the thinning if sea ice associated with less ice formation and increase of sea ice transport from Pacific side of the Arctic Ocean to the Atlantic side of the Arctic Ocean. The anti-cyclonic oceanic Beaufort Gyre driven by the strong sea ice motion in 2007/2008 winter was anomalously accelerated. These preconditioning was identified before the MR08-04 cruise in the summer of 2008. In this circumstance, MR08-04 entitled as “R/V Mirai International Polar Year 2008 cruise”, was conducted as a mission of 4th International Polar Year (IPY). This was the first Japanese IPY cruise that entered the Arctic basins. The core science mission was organized to capture the mechanism of the drastic Arctic changes and their influences on the biogeochemical environment. In addition the science on the recent drastic changes, paleo-oceanographic observation was also involved to learn the history of Arctic climate system. The science station occupied by MR08-04 covered full span of the southern Canada Basin and Eastern Makarov Basin, especially focusing on the Chukchi Borderland area where the main pathway of the Pacific Water and western margin of oceanic Beaufort Gyre. The data acquired by MR08-04 cruise shows a fruitful feature of the changes in the ocean which was not identified by remote sensing and numerical simulation. The data of MR08-04 would be a basis to progress our knowledge on Arctic changes.

CRUISE SUMMARY

1. Ship

R/V Mirai

L x B x D 128.58m x 19.0m x 13.2m

Gross Tonnage 8,672 tons

Call Sign JNSR

2. Cruise Code

MR08-04

3. Project Name

R/V Mirai International Polar Year 2008 cruise

4. Undertaking Institute

JAMSTEC

2-15 Natsushima-cho, Yokosuka 237-0061, Japan

5. Chief Scientist

Koji Shimada

(Tokyo University of Marine Science and Technology / JAMSTEC)

6. Periods and Ports of Call

Aug. 15, 2008 ~ Oct. 9, 2008 (Sekine-hama ~ Hachinohe ~ Dutch Harbor ~ Dutch Harbor)

7. Observation Summary

CTD (+ water sampling) 204 stations

CTD (only) 56 stations

XCTD 195 stations

ADCP Observation Continuously

Oceanic Environment Monitoring Continuously

Surface Meteorology Continuously

Mooring recoveries 6

Mooring deployments 3

Plankton Net Sampling (Multi layer) 14 stations

Plankton Net Sampling (Single layer) 54 stations

Piston core 5 stations

Multiple core 4 stations

Sea Floor Topography (Seabeam) Continuously

Radiosonde Launching 95 times

Doppler Radar Observation Continuously

Aerosol measurement Continuously

Dual polarization lidar Continuously

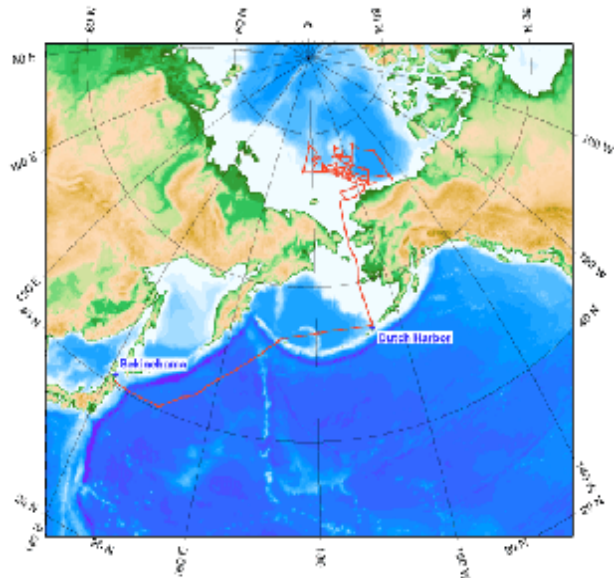


Figure 2a. Cruise track of MR08-04



Figure 2b. Cruise track of MR08-04 in the Arctic Ocean

RESULTS AND DISCUSSION

Interpretation of second sea ice minimum in 2008 - further activation of sea ice motion and ocean circulation -

How can we understand second minimum in 2008? Figure 3 shows the sea ice motion for the winter of 2002/2003-2006/2007 winters mean and 2007/2008 winter. The sea ice motion in 2007/2008 winter showed two times larger than that in 2002/2003-

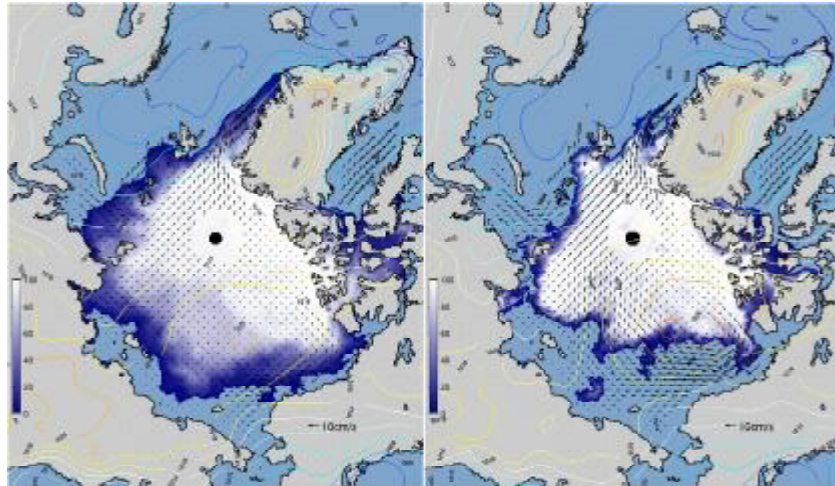


Figure 3. Sea ice concentration (September), sea ice motion and sea level pressure (previous November-April) for 2002-2007 and 2008. After Shimada (2009)

2006/2007 winters mean. Major difference between the two periods is identified in the sea ice cover near the Banks and Queen Elizabeth Islands. The less ice cover in this area established more free slip condition in the eastern Canada Basin. The local changes in the sea ice cover affect the activation of large basin scale sea ice motion (Shimada and Kamoshida, 2008; Shimada, 2009). The underlying ocean is strengthened by the further activation of sea ice motion. Figure 4 showed ocean dynamic topography at 100 dbar referred to 800dbar. The upper ocean circulation is anomalously accelerated (Shimada and Kamoshida, 2008; Shimada, 2009). The accelerated upper ocean circulation delivered huge amount Pacific Water from the shelf region into the central basin. Especially, the oceanic heat transport of the warm Pacific Summer Water onto the Chukchi Borderland area is crucial for the fate of the newly formed sea ice that drifts over the ocean hot spot. The ocean warming would retard sea ice formation during winter. The sea ice thickness at the beginning of summer becomes to be thin. The thin sea ice is easy to be disappeared without increase in solar radiation, i.e., huge retreat sea ice cover occurs in thin ice area. Once huge sea ice retreat occurs, sea ice formation in the vicinity of the coast is retarded. Then slip condition for sea ice motion is established again. The positive feedback system continues on. The stored heat in the western Canada Basin reached maximum value in the summer of 2008 (Figure 5). The second ice minimum extend is just a record of extent. The sea ice is originated from ocean. Hence the fate of the sea ice should be examined as a system of Arctic Water involving ice and ocean.

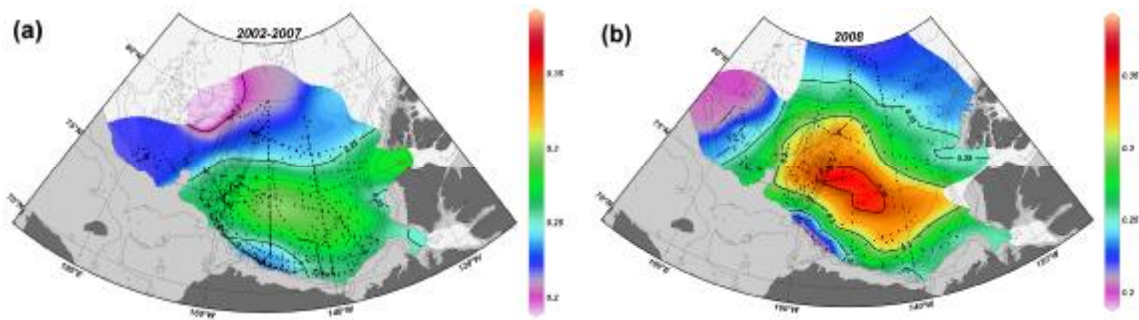


Figure 4. Oceanic dynamic topography (dynamic meter) at 100 dbar referring to 800 dbar for (a) 2002-2007 average and (b) 2008. Ocean currents along the contours of dynamic topography show the high values to the right. The upper ocean circulation in 2008 was enhanced by the activation of sea ice motion. A huge amount of Pacific Water was delivered into the central Arctic Ocean via the longitude band of 150-180W. After Shimada (2009)

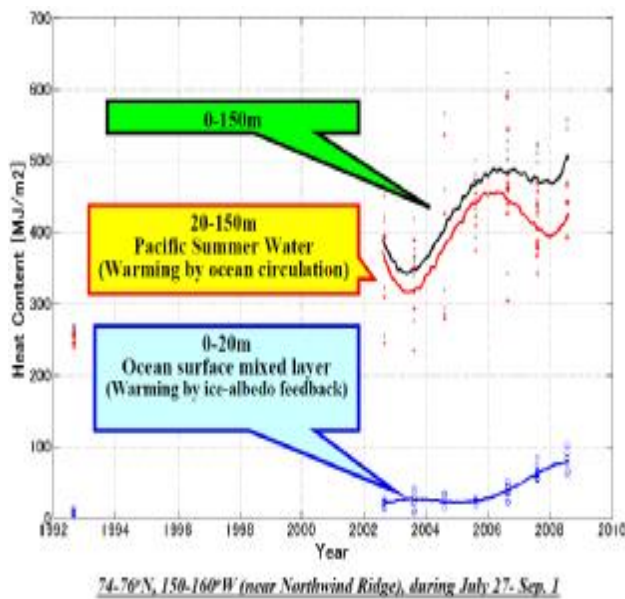


Figure 5. Time series of ocean heat content within a region of 74-76N and 150-160W near the major pathway of Pacific Summer Water from shelf region into the central Canada Basin. The value is divided into two parts. One is surface to 20m deep, which corresponds to ocean surface mixed layer. The warming of this layer mainly is caused by surface heating by atmosphere and short wave radiation. The second part is from bottom of surface mixed layer in summer to the upper minimum temperature in Pacific Winter Water layer near 150m. After Shimada (2009)

FUTURE DIRECTION AND RECOMMENDATION

Now in the Pacific sector of the Arctic Ocean, relatively heavy ice condition is in the eastern area while the less ice condition is in the western area. In other words, cold surface condition is in the eastern area, while warm surface condition is in the western area. This asymmetry establishes high atmospheric pressure field over the cold (eastern) area, while warm pressure field in the warm (western) area. This spatial distribution of atmospheric circulation pattern that is modulated by sea ice distribution brings southerly wind around the international data line (Figure 6). This atmospheric modulation helps the retreat of sea ice cover in addition to the contributions of strengthening of ice/ocean circulation. In the near future, if the heavy ices near the Canadian Archipelago disappear; asymmetric sea ice distribution in zonal direction disappears. Then the rate of sea ice reduction would slow. Next 5-10 years will be a significant duration to identify key features of Arctic changes and to understand the fate of the Arctic climate associated with climate of northern hemisphere. International collaborations to understand climate system are urgent issues.

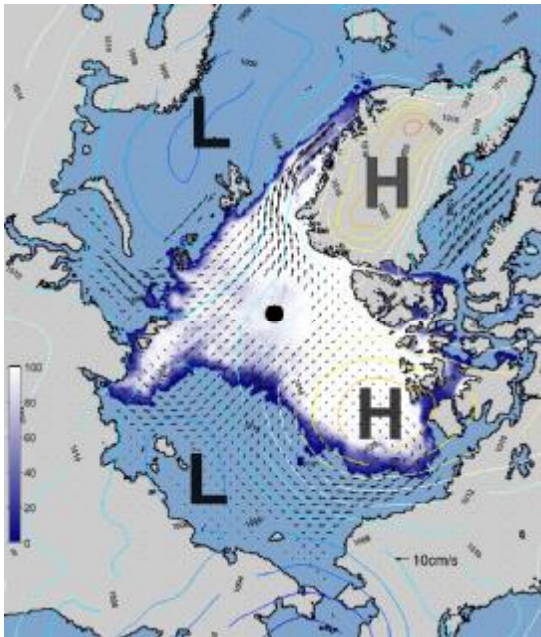


Figure 6. Sea ice cover with sea level atmospheric pressure field in September, 2007. Asymmetric sea ice cover in zonal direction establishes meridional atmospheric circulation pattern north of the Bering Strait. This enhances further retreat of sea ice cover in the Pacific sector of the Arctic Ocean. After Shimada (2009)

REFERENCES

- Shimada, K., T. Kamoshida, M. Itoh, S. Nishino, E. Carmack, F. McLaughlin, S. Zimmerman, and A. Proshutinsky (2006), Pacific Ocean Inflow: influence on catastrophic reduction of sea ice cover in the Arctic Ocean. *Geophys. Res. Lett.*, 33, L08605, doi:10.1029/2005GL025624.
- Shimada and Kamoshida (2008), Further Catastrophic Reduction of Sea Ice Caused by Activations of Sea Ice Motion and the Upper Ocean Circulation in the Arctic Ocean, *Journal of Geography*, vol 117, No 6, pictorial page xix-xx.
- Shimada (2009), Catastrophic changes in the Arctic Ocean toward blue ocean, *Jour. Japan Soc. Mar. Surv. Tech.*, Vol 21, No. 1, 53-59.
- Sumata, H. and K. Shimada (2007), On northward transport of Pacific Summer Water along the Northwind Ridge in the western Arctic Ocean, *J. Oceanogr.*, 63,363-378.

SESSION II

TECTONICS AND HYDROTHERMAL VENT

COMPARISONS BETWEEN MID OCEAN RIDGES AND BACK ARC BASIN

Sang-Mook Lee

School of Earth and Environmental Sciences, Seoul National University, Seoul 151-747,
Korea
smlee@snu.ac.kr

Mid-ocean ridges and back-arc basins are different in many ways. Scientists have noted the compositional differences of back-arc basin crusts resulting from influx of water and other components derived from the melting of slab. In this presentation, I focus on the structural and evolutionary difference between back-arc basins and mid-ocean ridges. While back-arc basins follow the well-known age versus depth relationship same as the mid-ocean ridges, they are deeper by 800 m or so on average than mid-ocean ridges.

I explore various possibilities that might have led to back-arc basins being deeper, including negative dynamic pressure generated by retreat of subducting slab. Generation of back-arc basin must involve subduction or collision at some plate boundary because if not the surface area of the earth would not remain constant. I speculate that back-arc basins are produced contemporaneously with the retreat of the trench (trench rollback). It appears that there are two different modes of trench rollback, fast and slow. The slow trench rollback occurs when the slab retreats uniformly along the strike of the trench. This type of rollback produces a slow back-arc opening. On the other hand, if the retreat of slab is not uniform along the strike and is much faster on one side than the other, there is a sudden fall back of slab and this produces a fast-opening back-arc basin. Izu-Bonin-Mariana and Tonga-Kermadec belong to this sudden rollback example. It is difficult to model the nonuniform case because the problem is inherently three dimensional and involves understanding of lateral mantle flow. Most of the back-arc basins in the western Pacific exhibit some degree of rotation and oblique spreading. These observations are thought to be a result of back-arc basins trying to accommodate new space, similar to micro-plates as they try to expand. However, our understanding of the exact cause and process is still very much at its infancy and further study needs to be conducted.

THE PACIFIC-ANTARCTIC RIDGE : GEOPHYSICAL AND GEOCHEMICAL RESULTS FROM THE FRENCH EXPEDITIONS OBTAINED WITH R/V L'ATALANTE (1996 AND 2004)

Louis Géli¹, H el ene Ondr eas¹, Laure Dosso², Frauke Klingelhoefer¹, Anne Briaais³,
Daniel Aslanian¹ and the Pacantartic 1&2 Groups

¹Marine Geosciences Department, BP 70, 29280, Plouzan e, France

²CNRS/IUEM, UMR6538, 1 Place Copernic, 29280 Plouzan e, France

³LEGOS-GRGS, CNRS UMR 5566, 18 Ave E. Belin, 31401 Toulouse, France

Anne.Briaais@ntp.obs-mip.fr

We here report the major results of two french expeditions conducted with R/V L'Atalante to study the geophysical and geochemical characteristics of the Pacific-Antarctic Ridge.

The first expedition (february 1996) collected multibeam bathymetric data and rock samples between the Pitman FZ and the Udintsev FZs, where small variations in plate kinematics are fully recorded in the axial morphology and in the geometry of the Ridge, due to the proximity of the Euler pole of rotation. Swath bathymetry and magnetic data show that clockwise rotations of the relative motion between the Pacific and Antarctic plates over the last 6 million years resulted in rift propagation or in the linkage of ridge segments, with transitions from transform faults to giant overlapping spreading centers. This bimodal axial rearrangement has propagated southward for the last 30 to 35 million years, leaving trails on the seafloor along a 1000-kilometer-long V-shaped structure south of the Udintsev fracture zone.

The second expedition (december 2004 – january 2005) surveyed and densely sampled the ridge crest as well as obliquely oriented, off-axis structures between the Vacquier FZ (52 30'S) and 42 S. Analysis of the bathymetric, gravity and geochemical data reveal three ridge segments separated by overlapping spreading centers south of the Menard transform fault (MTF) and five segments north of it. Calculation of the cross-sectional area allows quantification of the variation in size of the axial bathymetric high. Together with the calculation of the mantle Bouguer anomaly, these data provide information about variations in the temperature of the underlying mantle or in crustal thickness. Areas with hotter mantle are found north and south of the MTF. Geochemical analyses of samples dredged during the survey show a correlation of high cross-sectional area values and negative mantle Bouguer anomalies in the middle of segments with relatively less depleted basalts.

APPLICATION OF U- AND Th- DECAY SERIES DISEQUILIBRIA TO DATING SUBMARINE BASALTS

Kenneth W. W. Sims^{1,2}, Chris Waters¹, Jeff Standish^{1,3}

¹Department of Geology and Geophysics, Woods Hole Oceanographic Institution, Woods Hole, MA, USA

²Department of Geology and Geophysics, University of Wyoming, Laramie, WY, USA
ksims@whoi.edu

³Earth and Planetary Sciences, Harvard University, Cambridge, MA

INTRODUCTION

Time is the essential parameter required to answer many key questions about spreading center construction and how the various geological, hydrothermal and biological aspects of the ridge system relate to one another. For example: *What is the width of the neo-volcanic zone? How do lava ages vary with spatial position along and across a ridge segment? What is the frequency of eruption? How significant is off-axis volcanism? How does hydrothermal activity vary with length of time since an eruption? What are the differences in biological and hydrothermal systems built on young versus old volcanic terrain? And, on a global scale, how do these processes vary with spreading rate and tectonic environment?* Although high-resolution spatial observations provide us with a context necessary for understanding the evolution of the mid-ocean ridges, they cannot provide quantitative constraints on time.

The dating of young oceanic submarine basalts is not trivial: the half-lives of isotopic systems traditionally used for dating basalts (U-Pb, Sm-Nd, Rb-Sr) are much too long; K(Ar)-Ar methods are limited by the low abundances of K in most oceanic basalts; and, cosmogenic nuclides are not applicable. Fortunately, the relevant isotopes of the U- and Th-decay series have a wide range of appropriate half-lives (138 days up to 75ka) and differing chemical affinities (i.e. variable solid/melt and gas/melt partitioning), thereby providing a means to determine unique and essential ages for young oceanic volcanism.

In this talk, I will provide an overview of U-decay series systematics and its application to dating young ocean-floor basalts using two different MORB locales with contrasting spreading rates as examples—the fast-spreading East Pacific Rise at 9-10°N and the ultraslow-spreading Southwest Indian Ridge.

9-10°N EAST PACIFIC RISE

In Sims et al. (2002; 2003), we show that isotopic measurements constrain the degree to which the architecture of the fast-spreading EPR crust is controlled by growth at ridge crests alone or is embellished by off-axis magmatism (or volcanism?). Using U-Th and Th-Ra disequilibria to date off-axis lava flows at 9°-10°N EPR, our studies (Figure 1) show that lavas were recently erupted (< 8 ka) up to ~4 km from the center of seafloor

spreading and volcanism along the axial summit trough (AST). These studies further establish the use of U-series model ages as a valid dating technique and provide temporal evidence confirming both geological and geophysical observations that MOR volcanic construction is not limited to the AST. An important strength of this work is that the high-resolution imaging and bathymetry put these samples in geologic context and their collection by Alvin allowed us to compare U-series ages with qualitative geological indices of relative age. The use of ($^{226}\text{Ra}/^{230}\text{Th}$) model ages also improved the temporal resolution by almost an order of magnitude over previous off-axis studies (Goldstein et al, 1993; 1994). We continue to build upon our previous work using U-series methods to date off-axis samples at 9°-10° N EPR (Sohn and Sims, 2007; Waters et al, in prep). Our previous results provide a critical baseline that enable us to carry out these efforts, and our subsequent Alvin dives (Schouten et al., 2004) obtained sample suites that address specific stratigraphic problems related to near-axial volcanic construction and the interplay between magmatism and tectonism.

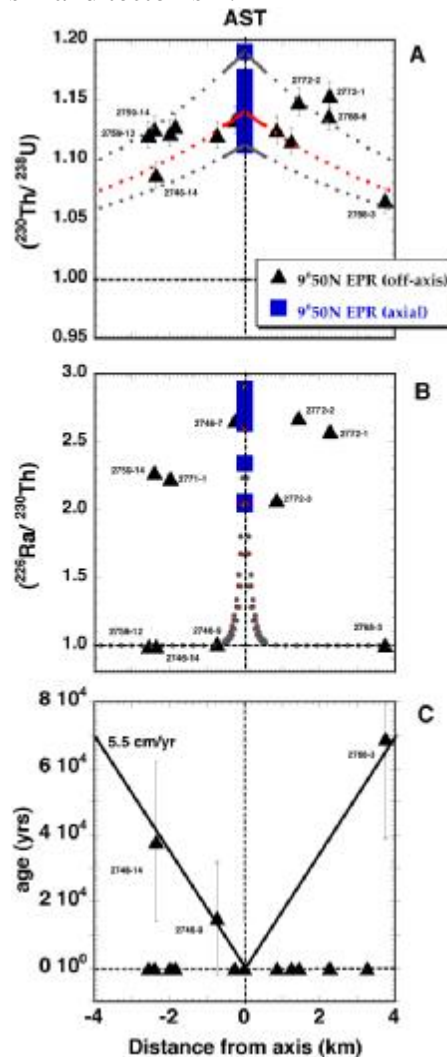


Figure 1 a) 9°50'N EPR samples ($^{230}\text{Th}/^{238}\text{U}$) versus their location, relative to the AST. Decay curves show how ($^{230}\text{Th}/^{238}\text{U}$) decreases as a function of distance from the AST. Initial values for decay curves come from the average (1.385 ± 0.02), shown in red, and high (1.425) and low (1.362) values of ($^{230}\text{Th}/^{238}\text{U}$) for the 9°50'N EPR axial samples reported in Sims et al. [2002]. **b)** 9°50'N EPR samples ($^{226}\text{Ra}/^{230}\text{Th}$) versus their location relative to the AST. Decay curves show how ($^{226}\text{Ra}/^{230}\text{Th}$) decreases as a function of distance from the AST. The initial values for

these decay curves come from the average (2.5 ± 0.3), shown in red, and high (2.89) and low (2.01) values of ($^{226}\text{Ra}/^{230}\text{Th}$) for the $9^\circ 50' \text{N}$ EPR axial samples taken from Sims et al. [2002]. c) U-Th and Th-Ra trend-line ages for the $9^\circ 50' \text{N}$ off-axis samples compared with ages calculated from spreading rate (5.5 cm/yr), as determined from paleomagnetic data [Carbotte and Macdonald, 1992].

SOUTH WEST INDIAN RIDGE

Crustal accretion occurs via the interaction of tectonic and magmatic mid-ocean ridge (MOR) processes. The standard model for MOR accretion is axial-centric and dominantly magmatic, thereby producing a linear relationship between crustal age and distance from the spreading axis. From a regional perspective, fast-spreading ridges tend to fit this paradigm, as magmatism is focused to a relatively narrow ridge axis. On the ultraslow-spreading Southwest Indian Ridge (Dick et al., 2003), however, detailed investigation of rift valley accretion finds that more than half of the measured lavas have U-series eruption ages significantly younger than their predicted spreading rate ages (Figure 2; Standish and Sims, submitted). This initial application of U-series eruption dating to an ultraslow spreading environment reveals two important findings, 1) magmatic crustal accretion occurs over a wider zone than previously recognized and 2) off-axis magmatism on ultraslow spreading ridges likely comprises a larger proportion of the total erupted lava volume than on faster spreading ridges. We also observe an association between young volcanism and faulting, suggesting that increased permeability associated with extensional tectonics may provide a mechanism(s) for the distribution of melt throughout the rift valley.

Standish&Sims_Figure_2

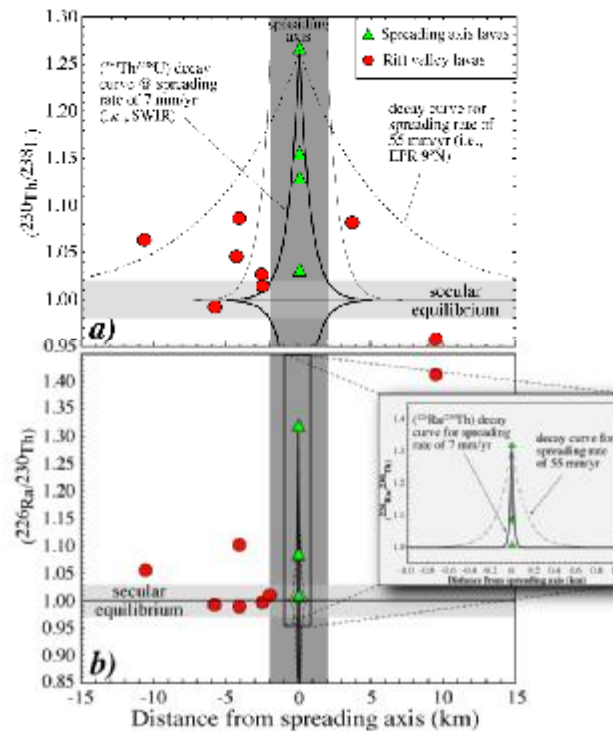


Figure 2. a) Measured ($^{230}\text{Th}/^{238}\text{U}$) for ‘spreading axis’ lavas (blue) and ‘rift valley’ lavas (red) for SWIR lavas, as a function of distance from the center of the ‘spreading axis’. Dark grey vertical field shows width of spreading axis. Decay paths for

maximum ^{230}Th basalt excess erupted at center (thick solid curve) and edge (thin solid curve) of the spreading axis, assuming half-spreading rate of 7.1 mm/yr. Dashed line indicates decay curve for same initial excess, using 9°N EPR spreading rate of 55 mm/yr. Light grey field represents $2s$ associated with $(^{230}\text{Th}/^{238}\text{U}) = 1$. **b)** Measured $(^{226}\text{Ra}/^{230}\text{Th})$ as a function of distance from the center of the 'spreading axis'. Fields as in panel a. Decay paths for maximum ^{226}Ra basalt excess erupted at center (thick solid curve) and edge (thin solid curve) of the spreading axis, assuming half-spreading rate of 7 mm/yr. Dashed line indicates decay curve for same initial excess, using 9°N EPR spreading rate of 55 mm/yr. Light grey field represents 2 associated with $(^{226}\text{Ra}/^{230}\text{Th}) = 1$

CONCLUSION

These studies show how U-decay series measurements on well-located samples, combined with high-resolution imaging and bathymetry, can constrain the extent to which the architecture of ocean crust is controlled by growth at ridge crests alone or is embellished by off-axis magmas. This information not only provides critical time-constraints on the details of ridge construction, but also leads to a better understanding of magma genesis and melt transport for off-axis lavas, which can be used to test 2-D models of mantle melting and flow.

REFERENCES

- Carbotte S.M. and Macdonald K.C. (1992) East Pacific Rise 8° - $10^\circ 30'\text{N}$: Evolution of ridge segments and discontinuities from SeaMARC II and three-dimensional magnetic studies. *J. Geophys. Res.* **97**, 6959-6982.
- Dick, H., J. Lin, and H. Schouten (2003), An ultraslow-spreading class of ocean ridge, *Nature*, **426**, 405-412.
- Goldstein, S. J., Murrell, M. T. and Williams, R.W., ^{231}Pa and ^{230}Th chronology of Mid-Ocean Ridge Basalts, *Earth Planet. Sci. Lett.*, **115**, 151-160, (1993).
- Goldstein, S.J., Perfit, M.R., Batiza, R., Fornari, D.J., and Murrell, M.T, Off-axis volcanism at the East Pacific Rise detected by uranium-series dating of basalts, *Nature*, **367**, 157-159, (1994).
- Schouten H., M. Tivey, D.J. Fornari, W. Seyfried, and Ship Board Science and Technical Teams. (2004) Central Anomaly Magnetic High and Volcanic Processes on Fast-spreading Mid-Ocean Ridges. *Cruise Report R/V Atlantis Voyage 11 Leg 7, 1/26-2/24/2004*.
- Sims, K.W.W. S.J. Goldstein, J. Blichert-Toft, M.R. Perfit, P. Kelemen, D.J. Fornari, P. Michael, M.T. Murrell, S.R. Hart, D.J. DePaolo, G. Layne, and M. Jull., Chemical and isotopic constraints on the generation and transport of magma beneath the East Pacific Rise. *Geochimica et Cosmochimica Acta*, **66**, 3481-3504, 2002.
- Sims, K.W.W., J. Blichert-Toft, D.J. Fornari, M.R. Perfit, S.J. Goldstein, P. Johnson, D.J. DePaolo, S.R. Hart, M.T. Murrell, P.J. Michael, G.D. Layne, and L. Ball, Aberrant youth: Chemical and isotopic constraints on the origin of off-axis lavas from the East Pacific Rise, 9° - 10°N . *Geochem. Geophys. Geosyst.*, **4**, 2003.
- Sohn, R. and K. W. W. Sims, "Bending as a mechanism for triggering off-axis volcanism on the East Pacific Rise", *Geology* **33**, 93-96, 2005.
- Standish, J. J., H. J. B. Dick, P. J. Michael, W. G. Melson, and T. O'Hearn (2008), MORB generation beneath the ultraslow spreading Southwest Indian Ridge (9 - 25°E): Major element chemistry and the importance of process versus source,

Geochem. Geophys. Geosyst., 9(Q05004).

Standish, J.J. and K.W.W. Sims, Dispersed MOR volcanism: Implications from U-series age dating for crustal accretion at ultraslow spreading ridges, *Nature - Geosciences* (in revision).

AUTONOMOUS DISCOVERY, MAPPING, AND SAMPLING OF DEEP SEA HYDROTHERMAL VENTS

Dana R. Yoerger

Senior Scientist, Deep Submergence Laboratory Dept. of Applied Ocean Physics and
Engineering, Woods Hole Oceanographic Institution, Woods Hole, MA 02543
dyoerger@whoi.edu

This talk will begin by presenting a future concept for hydrothermal vent discovery, exploration, and sampling. In the near future, we may be able to go to an unexplored ridge segment, launch one or more autonomous underwater vehicles, and locate, survey, and sample biota from all the vents on that segment. How much of this problem is presently solved, and how much remains?

Recently, we have succeeded in locating undiscovered hydrothermal vent sites using our autonomous underwater vehicle ABE. These discoveries include vent sites in the Lau Basin (20S,176W) and the first vents found on the Southern Mid Atlantic Ridge (5S, 12W) and Southwest Indian Ridge (38S, 50E). During this process, ABE makes maps of the water column, creates detailed bathymetric maps, and takes bottom photos of the vent sites. While the vehicle runs autonomously, we execute at least three dives with substantial data interpretation and planning by the science party between each dive. In this presentation, these results will be reviewed, the underlying engineering presented, and the role of human decision-makers explained.

Based on these experiences, we believe these results can be extended to enable fully autonomous vent discovery, mapping, and even sampling. The capabilities of autonomous underwater vehicles are improving in many aspects, including range, navigational capability, and in-situ sensing. In this talk, our initial attempts to improve efficiency through autonomous decision making will be reviewed, and candidate paradigms that can enable fully autonomous search will be presented. Plans for autonomous sampling will also be discussed.

LARVAL SUPPLY, COLONIZATION, AND FAUNAL COMMUNITY DEVELOPMENT AT HYDROTHERMAL VENTS ON THE EAST PACIFIC RISE

Stace Beaulieu¹, Lauren Mullineaux¹, and Diane Adams²

¹ Biology Department, Woods Hole Oceanographic Institution (WHOI), Woods Hole, MA, USA

stace@whoi.edu

² National Institutes of Health, 30 Convent Dr., Bldg 30, Room 523, Bethesda, MD 20892 USA

INTRODUCTION

This lecture provides a general summary of questions asked by ecologists interested in larval dispersal, colonization, and community structure at hydrothermal vents. We highlight recent studies at the East Pacific Rise 9° N site as specific examples. We begin the lecture with a summary of the six biogeographic provinces of hydrothermal vent macrofauna along the global mid-ocean ridge system (Van Dover et al., 2002; Bachraty et al., 2009). As Coordinator of the InterRidge program (<http://www.interridge.org>), Beaulieu is currently revising the Global Hydrothermal Vents Database and will point to a few of the most recently discovered vents. Biogeography is a focus of the Census of Marine Life project for Deep-Sea Chemosynthetic Ecosystems (ChEss; <http://www.noc.soton.ac.uk/chess>). However, processes affecting biogeography occur over very long / evolutionary time scales, while ecologists are often concerned with questions on much shorter time scales of one to several generations.

The bulk of the lecture will focus on studies on ecological time scales. The three questions that are posed in the lecture may be applied to any vent habitat:

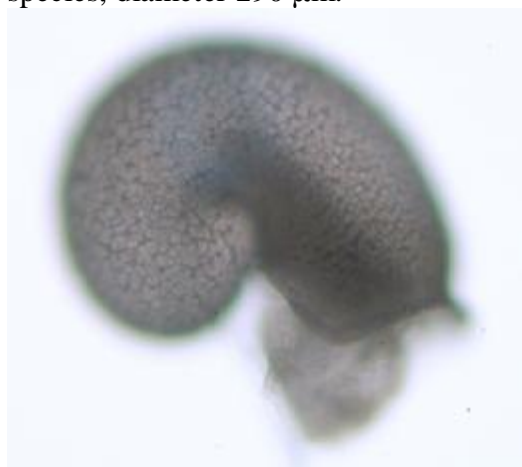
- 1) How far do larvae of vent-endemic fauna disperse?
- 2) How quickly are new vent sites colonized?
- 3) How do communities change over the “life time” of a vent?

LARVAL DISPERSAL AND SUPPLY

For Question 1, we first must address the technical challenge of: How do we quantify larval dispersal and supply to hydrothermal vents? Recent studies have indicated that large-volume plankton pumps are an excellent tool to quantify the concentration of larvae in the water column near hydrothermal vents (e.g., Mullineaux et al., 2005). Measuring the concentration simultaneously with flow velocity allows for an estimate of advective flux, which can be used in modeling dispersal of larvae. Time-series sediment traps are a promising tool for assessing the larval supply to hydrothermal vents (Beaulieu et al., 2009), with a recent short-term study utilizing sediment traps and simultaneous current measurements to demonstrate larval supply from relatively local sources (i.e., nearby vents; Adams and Mullineaux, 2008). However, a subsequent long-term study, also utilizing time-series sediment traps, indicated that weekly larval supply appeared to be driven by larger spatial scales through losses associated with cross-axis flows and the passage of mesoscale eddies (Adams 2007). In terms of an answer to Question 1, the best estimate that we have so far for the EPR is for the tubeworm, *Riftia pachyptila*, which has been estimated to have a dispersal potential of up to 100 km in its ~1 month larval period (Marsh et al., 2001). For an atlas of photographs of larvae from vents at the EPR (Fig. 1), go to: <http://www.whoi.edu/vent-larval-id> (Mills et al., 2007).

Figure 1. Larvae collected at the East Pacific Rise 9° N site.

A. Gastropod, unknown neomphalid species, diameter 290 μm . B. Polychaete, unknown species similar to chaetosphaerid, length ~300 μm .

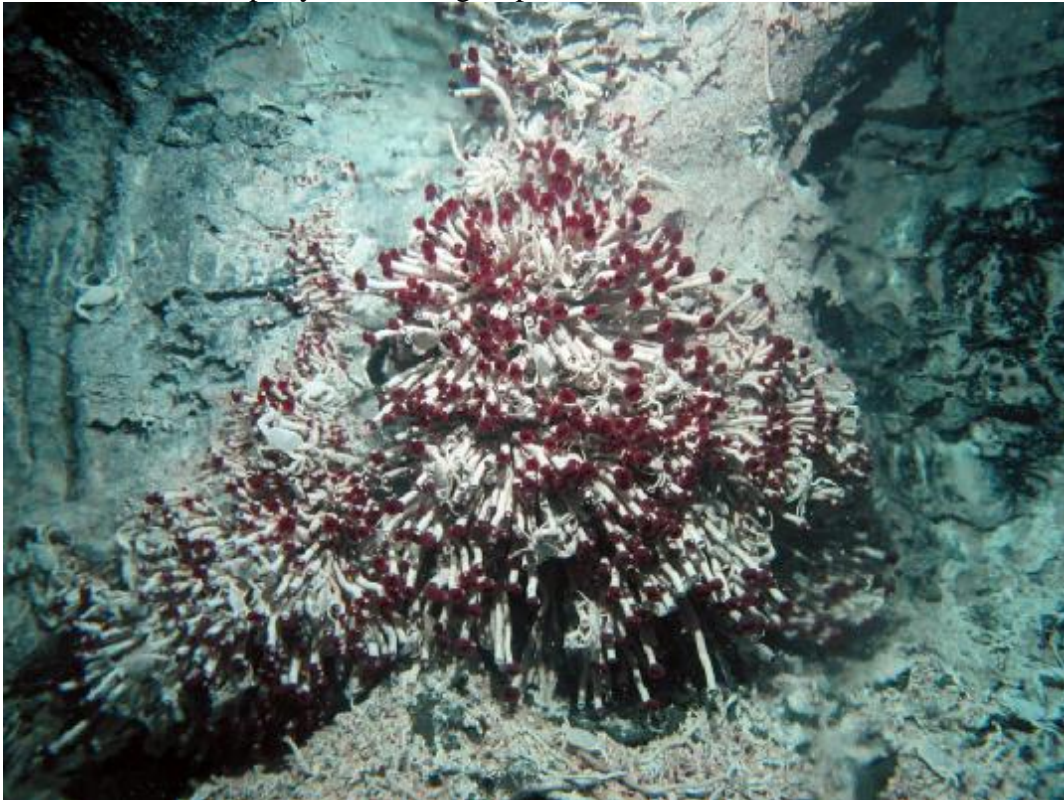


COLONIZATION AND COMMUNITY DEVELOPMENT

Question 2 requires the serendipity of discovering a new vent site, or the observation of a vent site over a long enough time period to capture a major disturbance such as an eruption event. Fortunately, the EPR 9° N site was under investigation when it experienced seafloor eruptions in 1991 and most recently in 2005/2006, and in both cases we have repeated visits to observe colonization and, for Question 3, subsequent community development. After the 1991 eruption, a transect of site markers was deployed and enabled visual observations of the succession of fauna, indicating a pattern from microbial mats and mobile vent fauna to the colonization of sessile tubeworms *Tevnia jerichonana* to *Riftia pachyptila* to the mussel *Bathymodiolus*

thermophilus within 5-10 years (Shank et al., 1998). After the eruption in 2005/2006, without the site markers we were dependent on precise navigation to relocate sites that had changed very much in visual appearance. We deployed sediment traps and settlement panels to continue time-series monitoring of larval supply and colonization. Although the megafauna observed from submersible appeared to be following a similar sequence as observed after the 1991 eruption (Fig. 2), to our surprise the species composition of larvae and smaller, macrofaunal colonists changed dramatically after the eruption (Mullineaux, unpub. data). We will describe some of the changes in larval supply that occurred after the eruption, and suggest implications for community development to be observed in the coming years.

Figure 2. Tubeworm *Tevnia jerichonana*, an early colonist following the eruption at the East Pacific Rise 9° N site in 2005/2006. Photograph taken October 2006, courtesy LADDER 1 cruise party and Alvin group, WHOI.



CONCLUSION

We will end the talk by returning to the global map of hydrothermal vents and pointing to other sites at which experiments and time-series observations are allowing ecologists to observe changes in communities over time. We conclude by highlighting the mission of the InterRidge Working Group for Vent Ecology.

REFERENCES

- Adams, D.K. (2007) Influence of hydrodynamics on the larval supply to hydrothermal vents on the East Pacific Rise. Thesis (Ph.D.), Massachusetts Institute of Technology, <http://hdl.handle.net/1721.1/38988>.
- Adams, D.K. and Mullineaux, L.M. (2008) Supply of gastropod larvae to hydrothermal vents reflects transport from local larval sources. *Limnology and Oceanography* 53: 1945-1955.
- Bachraty, C., et al. (2009, in press) Biogeographic relationships among deep-sea hydrothermal vent faunas at global scale. *Deep-Sea Research I*.
- Beaulieu, S.E., et al. (2009) Comparison of a sediment trap and plankton pump for time-series sampling of larvae near deep-sea hydrothermal vents. *Limnology and Oceanography: Methods* 7: 235-248.
- Marsh, A.G., et al. (2001) Larval dispersal potential of the tubeworm *Riftia pachyptila* at deep-sea hydrothermal vents. *Nature* 411: 77-80.
- Mills, S. W., Beaulieu, S. E. and Mullineaux, L.S. 2007. Photographic identification guide to larvae at hydrothermal vents in the eastern Pacific. Published at: <http://www.whoi.edu/vent-larval-id>.
- Mullineaux, L.S., et al. (2005) Vertical, lateral and temporal structure in larval distributions at hydrothermal vents. *Marine Ecology Progress Series* 293: 1-16.
- Shank, T.M., et al. (1998) Temporal and spatial patterns of biological community development at nascent deep-sea hydrothermal vents (9 degrees 50'N, East Pacific Rise). *Deep-Sea Research II* 45(1-3): 465-515.
- Van Dover, C.L., et al. (2002) Evolution and biogeography of deep-sea vent and seep invertebrates. *Science* 295: 1253-1257.
- General references for hydrothermal vent ecology:
- Desbruyeres, D. et al. (2006) Handbook of Deep-Sea Hydrothermal Vent Fauna. *Denisia* 18 (available online at: http://www.biologiezentrum.at/biophp/de/band_det.php?litnr=23702).
- Van Dover, C.L. (2000) *The Ecology of Deep-Sea Hydrothermal Vents*. Princeton Univ. Press.

TECTONO-MAGMATIC ACTIVITY AND ICE DYNAMICS IN THE BRANSFIELD STRAIT BACK-ARC BASIN, ANTARCTICA

Robert P. Dziak¹, Minkyu Park², Won Sang Lee², Haru Matsumoto¹, DelWayne R.
Bohnenstiehl³, Joseph H. Haxel¹

¹Oregon State University, NOAA Cooperative Institute for Marine Resources Studies,
Newport, Oregon 97365-5258, USA

robert.p.dziak@noaa.gov

²Polar Environmental Research Division, Korea Polar Research Institute, Incheon 406-840,
Republic of Korea

³Department of Marine, Earth and Atmospheric Sciences, North Carolina State University,
Raleigh, North Carolina 27695-8208, USA

ABSTRACT

An array of moored hydrophones was used to monitor the spatio-temporal distribution of small- to moderate-sized earthquakes and ice-generated sounds near the Bransfield Strait, Antarctica. During a two-year period, a total of 3,900 earthquakes, 5,925 icequakes and numerous ice-tremor events were located throughout the region. The seismic activity included eight space-time earthquake clusters, positioned along the central rift zone of the young Bransfield back-arc system. These sequences of small magnitude earthquakes, or swarms, suggest ongoing magmatic activity that becomes localized along isolated volcanic features and fissure-like ridges in the southwest portion of the basin. A total of 122 earthquakes were located along the South Shetland trench, indicating continued deformation and possibly ongoing subduction along this margin. The large number of icequakes observed show a temporal pattern related to seasonal freeze-thaw cycles, and a spatial distribution consistent with channeling of sea ice along submarine canyons from glacier fronts. Several harmonic tremor episodes were sourced from a large (~30 km²) iceberg that entered northeast portion of the basin. The spectral character of these signals suggests they were produced by resonance of a small chamber of fluid within the iceberg, rather than by resonance of the entire berg. These pressure waves appear to have been excited by abrasion of the iceberg along the seafloor as it passed Clarence and Elephant Islands.

INTRODUCTION

The Bransfield Strait is geographically located between the South Shetland Islands and western Antarctic Peninsula, in an area of evolving tectonics driven by the interaction of the Antarctic, Scotia and South American plates (Figure 1). The Bransfield Strait seafloor is a Quaternary back-arc basin and is one of only two back-arc basins forming in continental crust that are opening without a large strike-slip component [Lawver *et al.*, 1996]. Fresh volcanic rocks occur on numerous submarine features distributed along the rift-axis, including a discontinuous neovolcanic ridge

similar to the nascent spreading centers seen in some other back-arc basins.

For the first time, an array of moored hydrophones was deployed within the Bransfield Strait, with 7 instruments from December 2005-2006 and 6 instruments from 2006 to December 2007. The hydrophones record the acoustic Tertiary (T -) waves of sub-seafloor earthquakes that propagate in the ocean-water column, primarily as surface-related phases at these high southern latitudes. Using regional T -waves to detect submarine earthquakes typically provides a complete catalog of $\geq 3.0 m_b$ earthquakes from remote ocean basins [Dziak *et al.*, 2004], a significant improvement over the $\sim 4.5 m_b$ detection limit of land-based seismic networks for the southern ocean. In addition to seismo-acoustic signals, the hydrophones record the broadband arrivals of “icequakes” that result from cracking, collision, and breakup of icebergs, iceflows and icesheets within and along the periphery of the strait (Figure 2). The goal of this study is to use hydrophone recorded seismicity to provide insights into the style of rifting (volcanic versus tectonically dominated) along the Bransfield back-arc, identify centers of recent magmatic activity within the basin, and evaluate the meteorological or possible geophysical processes influencing icequakes (breakup) in the region.

BRANSFIELD SEISMICITY

From December 2005 to December 2007, a total of 3,146 earthquakes were located in the Bransfield back-arc spreading center, and another 754 earthquakes were located throughout the region including the South Shetland Trench and Drake Passage (Figure 3). Bransfield earthquakes locate throughout the basin and along the neovolcanic zone of the back-arc spreading center. The hydroacoustically-determined source locations were estimated using an iterative non-linear regression algorithm that minimizes the error between observed and predicted travel time by incrementing an event’s latitude, longitude, and origin time. Travel times and velocities along acoustic paths are estimated by applying propagation models to the U.S. Navy ocean sound-speed database, the Generalized Digital Environmental Model [Davis *et al.*, 1986]. The sound propagation field in the Bransfield is surface-limited, meaning sound velocity decreases linearly from the seafloor to the sea surface. This causes all rays from both seafloor and shallow water sources to turn up toward the sea-surface and then propagate laterally through multiple reflections from the sea-surface, and possibly seafloor.

An acoustic magnitude, or source level (SL), is calculated for each earthquake by removing the effects of geometric spreading along the propagation path and the hydrophone instrument response [Dziak, 2001]. Source levels for Bransfield earthquakes range from 170.8-234.1 decibels (dB), where dB is relative to 1 μPa (pressure) at 1m. There were no teleseismically recorded earthquakes from the Bransfield during 2005-2007 to allow for a robust estimate of seismic to acoustic magnitude relationships; however, seismic magnitudes of the Bransfield earthquakes can be estimated using an empirical source level to body-wave magnitude (m_b) relationship developed for the north Atlantic hydrophone array of $SL = 18.95m_b + 151.91$ [Dziak *et al.*, 2004]. This equation provides an estimate of magnitude range for Bransfield events of 1.0-4.4 m_b , where the magnitude of completeness is 208 dB or 3.0 m_b . Since none of these hydroacoustic events were recorded on global, land-based seismic networks, this implies a $>4.4 m_b$ earthquake detection threshold for the Bransfield-South Shetland Island region.

The levels of continuous background seismicity vary through the two-year experiment, with long-term peaks in activity observed from December 2005 to March 2006 and December 2006 to October 2007. The majority of seismicity also appears to be spatially limited along the back-arc to within the 225 km distance between Deception

and Bridgeman Islands (Figure 3). Given that the rift basin extends beyond Elephant Island, significant earthquake activity might be expected to the northeast of the array. The dearth of events to the east of Bridgeman Island therefore may in part reflect locally increasing location errors and higher detection thresholds.

There also appear to be eight distinct spatio-temporal clusters, or swarms, of seismicity along the neo-volcanic zone of the back-arc. All eight earthquake swarms occurred at, or along the flanks of, major volcanic centers within the back-arc basin implying the seismicity was caused by magmatic activity (Figure 4). The swarms occurred at (in temporal order) Hook Ridge, Three-sisters, Edifice-A, Bridgeman Island, Wordie volcano, Orca volcano, Three-Sisters, and Deception Island. The three earthquake swarms at Edifice-A and Three-sisters show some indication of earthquake migration, which is observed during magma injection events at mid-ocean ridges [Dziak *et al.*, 2007]. However, the apparent direction of earthquake propagation is oblique to the strike of the rift zone, and given the location error, the epicenter migration may not be statistically significant. The five other earthquake swarms remained equidistant from the nearest volcanic center during the duration of activity, implying that magma was not injected laterally along the rift zone during these episodes. It is also interesting to note that four of the swarms occurred during a three-week period in August 2006 (Figure 4). In total these four swarms are distributed over nearly the entire 400 km length of the Bransfield back-arc rift, from Deception Island to Wordie Volcano. This also represents the only time during the experiment when significant seismicity was observed in the section of the rift between Wordie Volcano and the intersection with the Shackleton Fracture Zone.

In addition to the Bransfield rift-related seismicity, the hydrophone array detected a large amount of seismicity along the northern and southern margins of the Bransfield Strait, as well as 122 earthquakes from the South Shetland Trench (Figure 3). The margin events are likely related to normal fault processes due to back-arc extension. The earthquakes oceanward from the South Shetland Islands implying there is active, gravity driven subduction beneath the South Shetland Islands. Since the Phoenix Ridge is extinct and the slab is not actively converging, subduction seismicity is being driven by the slab roll-back processes. However with the lack of focal depth and fault parameter information from the hydroacoustic it is not clear where in the slab and what exact slab deformation process is involved in producing the trench earthquakes.

The possible correlation of Bransfield seismicity with tidal stresses also was investigated. The triggering of microearthquakes ($M_L < 2$) at spreading centers due to the removal of vertical loads (ocean tidal loading) [Wilcock, 2001; Tolstoy, 2001] or the direct solid Earth tide [Stroup *et al.*, 2007] has been demonstrated in previous studies. We calculated the ocean tidal load and solid-Earth tide using the GOTIC2 model of Matsumoto *et al.* [2001]. Time series representing the tidal sea-surface height (maximum of 1 m) and tidally-induced stress changes (maximum of 20 kPa) were cross-correlated with the Bransfield seismic database, both before and after catalog declustering. No statistically significant correlation was found, indicating that the nucleation of small-to-moderate magnitude earthquakes along the Bransfield fault systems is insensitive to

BRANSFIELD ICEQUAKES AND ICEBERG TREMOR

Icequakes are impulsive, broadband, short-duration (< 30 s) signals with dominant energy in the 40-125 Hz band, in contrast to earthquake generated T-waves that exhibit energy over the 1-50 Hz band. Icequakes may be caused by thermal stresses, as well as physical deformation of the ice from wind, currents, waves and collisions

(Figure 2). These external forcing factors result in shear failure of the ice-crystal lattice, generating pressure waves that emanate into the water column.

A total of 5,925 icequake locations were derived from the hydrophone dataset. The icequake locations (Figure 2, bottom) parallel the coast of the Antarctic Peninsula, and are distributed throughout the Bransfield Strait. The icequake locations southeast of the Bransfield also separate into six lobes that trend toward the Antarctic Peninsula. These lobes are not interpreted as artifacts of the location algorithm, since they are perpendicular to the error surface and exceed location error. Notably, they appear to parallel the trends of submarine canyons, suggesting that sea ice may accumulate in areas of glacial outflow. A similar correlation between ice-tremor and outlet glaciers has been noted for the Wilkes Land coast [Chapp *et al.*, 2005].

The number of icequakes recorded varies regularly with season, with more events being detected during the austral summer months. Auto-correlation of icequake activity indicates that the correlation has a maximum value at a lag of 207.3 days, with other peaks at 103.6 and 310.9 days. This is consistent with an approximately six-month seasonal periodicity, which likely reflects variable thermal and wind stress conditions during the annual freeze-thaw cycle.

The possible correlation of Bransfield icequakes with ocean and solid- Earth tidal stresses and sea-surface tidal height also was investigated. As with the earthquake data, no statistically significant correlation was found between tides and icequakes.

Another remarkable cryogenic sound recorded on the hydrophone array was produced by the grounding and subsequent movement of large icebergs along the Bransfield seafloor. The sliding of the iceberg along the seafloor, caused by a combination of winds and ocean currents, produces pressure waves that enter and resonate in the iceberg, presumably in discrete zones that are a quasi-liquid/crystal bounded by an impedance contrast with the remaining frozen portion of the iceberg. Thus these signals differ significantly from the icequakes, which correspond to the failure of cracks in the ice. Iceberg tremor was recorded on the Bransfield array in January 2006 and July-August 2006. The fundamental frequency of the tremor is between 40-50 Hz, with as many as 5 overtones at ~16 Hz integer spacing observed up to the filter cutoff of 125 Hz. This signal bandwidth places it within the upper frequency range of ice-generated tremor signals previously recorded, where tremor from large (>10 km) icebergs from other regions of Antarctica has been shown to exhibit signals with a fundamental frequency typically between 2–10 Hz [Talandier *et al.*, 2002; Chapp *et al.*, 2005]. The phenomenon of “gliding” is also visible in the spectrogram where the packet of ensemble spectral peaks varies in frequency through time while maintaining their harmonic spacing [Garces *et al.*, 1998], giving the signals a unique spectral character. We were able to use the August 2006 tremor signals to locate their source, which corresponded to a large (>10 km long) iceberg in the northern Bransfield region identified and named from satellite images as UK213.

DISCUSSION

Overall, the hydroacoustic earthquake data show the Bransfield to be a seismically active region, with both the central seafloor rift zone and surrounding basin margins producing thousands of earthquakes during the two-year recording period. The Bransfield region also exhibits thousands of icequakes and other cryogenic sound sources and clearly is an area of dynamic sea ice activity.

Eight swarms of seismicity were observed along the neovolcanic zone the back-arc. All occurred at, or along the flanks of, major volcanic centers, consistent with the events being triggered by intrusive magmatic activity (Figure 4). The swarms occurred

at (in temporal order) Hook Ridge, Three-sisters, Edifice-A, Bridgeman Island, Wordie volcano, Orca volcano, Three-Sisters, and Deception Island. The three earthquake swarms at Edifice-A and Three-sisters show some indication of earthquake migration, which is observed during magma injection events at mid-ocean ridges associated with intrusion, and lateral propagation, of magma into shallow crust [Einarsson and Brandsdottir, 1980; Dziak *et al.*, 2007]. However the earthquake propagation direction is oblique to the strike of the rift-zone, and given the location error, the epicenter migration may not be statistically significant. The five other earthquake swarms remained equidistant from the nearest volcanic center during the duration of activity, implying that magma was not injected laterally along the rift zone during these episodes. Yet, the presence of earthquake sequences that exhibit tight space-time clustering and contain many similar magnitudes events does indicate that magma intrusion likely initiated the activity.

The four swarms that occurred over a 3-week period in August 2006 (Figure 4) are distributed over nearly the entire 400 km length of the Bransfield back-arc rift-zone, from Deception Island to Wordie Volcano. This August 2006 rifting sequence began with two swarms in the southwest Bransfield back-arc that occurred within a 4-day period, while the other two occurred 10 days later and 150 km down-rift during August 26-28. Although speculatively these four swarms could be related, it is more likely given the distance separating the two clusters that they were not from one large, Bransfield-wide, extension event.

The icequake locations illustrate the dynamic behavior of sea ice in the Bransfield and Antarctic Peninsula region. The icequakes show a strong seasonal variability in occurrence, reflecting the freeze-thaw cycle with most icequakes being detected during the austral summer months. The lesser histogram peak in icequake activity during the austral winter likely reflects the increase in wind and wave stress rather than the thermal stress that dominates the summer months. The icequake locations southeast of the Bransfield show a clear separation into six lobes that trend toward the Antarctic Peninsula. These lobes are not interpreted as artifacts of the location algorithm, since they are perpendicular to the error surface, exceed location error (Figure 3), and appear to parallel the trends of submarine canyons. Thus we interpret the icequakes as likely being caused by impact of the icebergs with each other as well as with the seafloor as they are calved off the glacier fronts and are channeled along the shallow portions of the canyons toward the open ocean. The majority of the icequakes occur near the Antarctic Peninsula at depths less than the 500m bathymetric contour, consistent with retreat of the ice fronts from the 400 m ground line since the Last Glacial Maximum. Moreover, although we think the majority of earthquakes along the southeastern margin are due to active fault processes, several earthquakes also locate along the Antarctic Peninsula submarine canyons. This suggests either the trend of these canyons may be fault controlled morphologic features, or that some of the icequakes within the canyons may have been misidentified as earthquakes.

To understand better the relative contribution of earthquakes and icequakes to the overall ocean conditions in the Bransfield, we estimated the total energy release of each phenomenon. The total acoustic energy release from earthquakes and icequakes in the Bransfield can be estimated by converting source level to seismic magnitude (described in section 3), then to energy E using the equation $\text{Log}(E) = 5.8 + 2.4 m_b$ [Kasahara, 1981]. This yields the result that total icequake energy release (1.9×10^{17} ergs) exceeds total earthquake acoustic energy (1.1×10^{17} ergs) by roughly a factor of 2. Since these 2-yr energy estimates represent the combined release of mechanical energy, acoustic-wave energy and heat, these totals demonstrate the significant role icebreakup has not only on the ocean-sound field, but also on the physical oceanographic

conditions within the Bransfield Strait.

ACKNOWLEDGMENTS

The authors thank the captain and crew of the R/V Yuzhmorgeologiya, and captain and personnel of King Sejong Base, King George Island, Antarctica, for their support during staging and deployment of the hydrophone arrays. The authors also wish to thank B. Hanshumaker, T-K Lau, K. Stafford, S. Heimlich, M. Fowler, A. Young, and S. Yun for their at sea support and laboratory assistance. This project was made possible through support of the Korea Ocean and Polar Research Institute and the NOAA Ocean Exploration Program, KOPRI project number PP08020

REFERENCES

- Barker, D. H. N. and J. A. Austin, Rift propagation, detachment faulting, and associated magmatism in Bransfield Strait, Antarctic Peninsula, *J. Geophys. Res.*, 103(B10), 24,017-24,043, 1998.
- Chapp, E., D.R. Bohnenstiehl and M. Tolstoy, Sound channel observations of ice-generated tremor in the Indian Ocean, *G-cubed*, 6, Q06003, doi:10.1029/2004GC000889, 2005.
- Davis, T.M., K.A. Countryman, and M.J. Carron, Tailored acoustic products utilizing the NAVOCEANO GDEM (a generalized digital environmental model), in *Proceedings, 36th Naval Symposium on Underwater Acoustics*, Naval Ocean Systems Center, San Diego, CA, 88pp., 1986.
- Dziak, R.P., Empirical relationship of T-wave energy and fault parameters of northeast Pacific Ocean earthquakes, *Geophys. Res. Lett.*, 28, 2537-2540, 2001.
- Dziak, R.P., D. R. Bohnenstiehl, H. Matsumoto, C.G. Fox, D.K., Smith, M. Tolstoy, T-K Lau, J. Haxel and M.J. Fowler, P- and T- wave detection thresholds, Pn velocity estimate, and detection of lower mantle and core P-waves on ocean sound-channel hydrophones at the Mid-Atlantic Ridge, 94, No.2, 665-677, *Bull. Seism. Soc. Am.*, 2004.
- Dziak, R.P., D. R Bohnenstiehl, J. P. Cowen, E.T. Baker, K. H. Rubin, J. H. Haxel, M. J. Fowler, Rapid dike injection leads to volcanic eruptions and hydrothermal plume release during seafloor spreading events, *Geology*, 35, 579-582, July 2007.
- Einarsson, P. and B. Brandsdottir, Seismological evidence for lateral magma intrusion during the July 1978 deflation of Krafla Volcano in NE Iceland, *J. Geophys.*, v: 47, 160-165, 1980.
- Kasahara, K., *Earthquake Mechanics*, University of Cambridge, 248pp, 1981.
- Lawver, L. A., et al., Distributed active extension in Bransfield Basin, Antarctic Peninsula: Evidence from multibeam bathymetry, *GSA Today*, 6(11), 1-6, 1996.
- Matsumoto, K., T. Sato, T. Takanezawa, and M. Ooe (2001), GOTIC2: A program for computation of oceanic tidal loading effect, *J. Geod. Soc. Jpn.*, 47, 243– 248, 2001.
- Talandier, J., O. Hyvernaud, E.A. Okal, P-F. Piserchia, Long-range detection of hydroacoustic signals from large icebergs in the Ross Sea, Antarctica, *Earth Planet. Sci. Lett.*, 203, 519-534, 2002.
- Tolstoy, M., Vernon, F.L., Orcutt, J.A. and F.K. Wyatt, The breathing of the seafloor: Tidal correlations of seismicity on Axial volcano, 30:503-506, *Geology*, 2002.
- Wilcock, W. S. D., Tidal triggering of microearthquakes on the Juan de Fuca Ridge, *Geophys. Res. Lett.*, 28, 3999-4002, 2001.

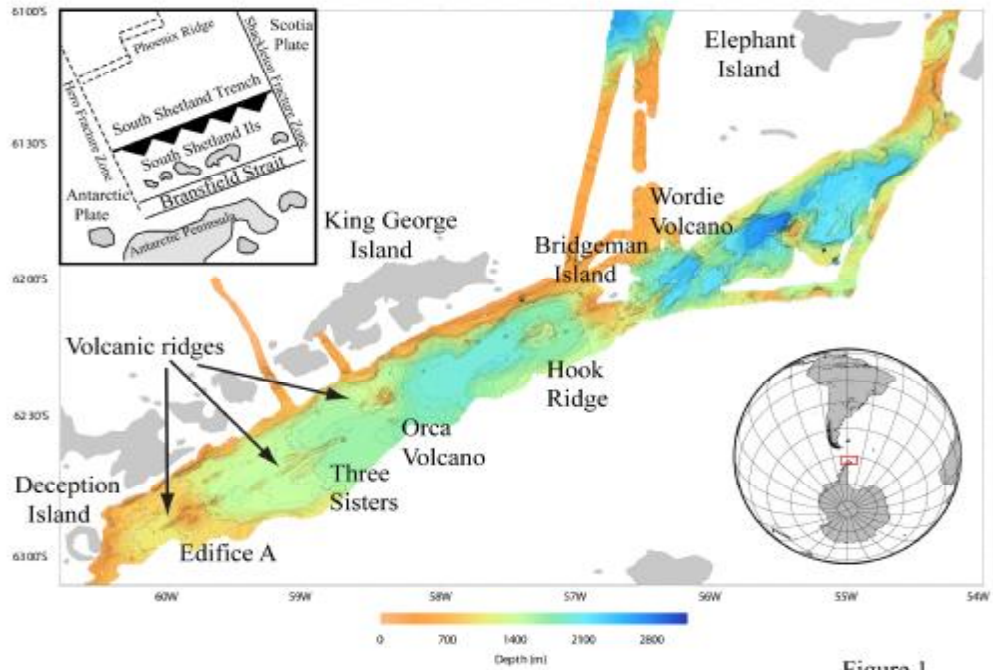


Figure 1

Figure 1: Bathymetric map of Bransfield Strait and Drake Passage, along west coast of Antarctic Peninsula [Lawver *et al.*, 1996]. Names of major volcanic centers and significant islands are labeled. The “neo-volcanic” zone of the Bransfield back-arc spreading center is the elongate bathymetry in center of basin. Inset map shows simple tectonic map of the region. The Phoenix ridge and Hero Fracture Zone are currently extinct, with roll-back of the slab at the trench leading to back-arc extension

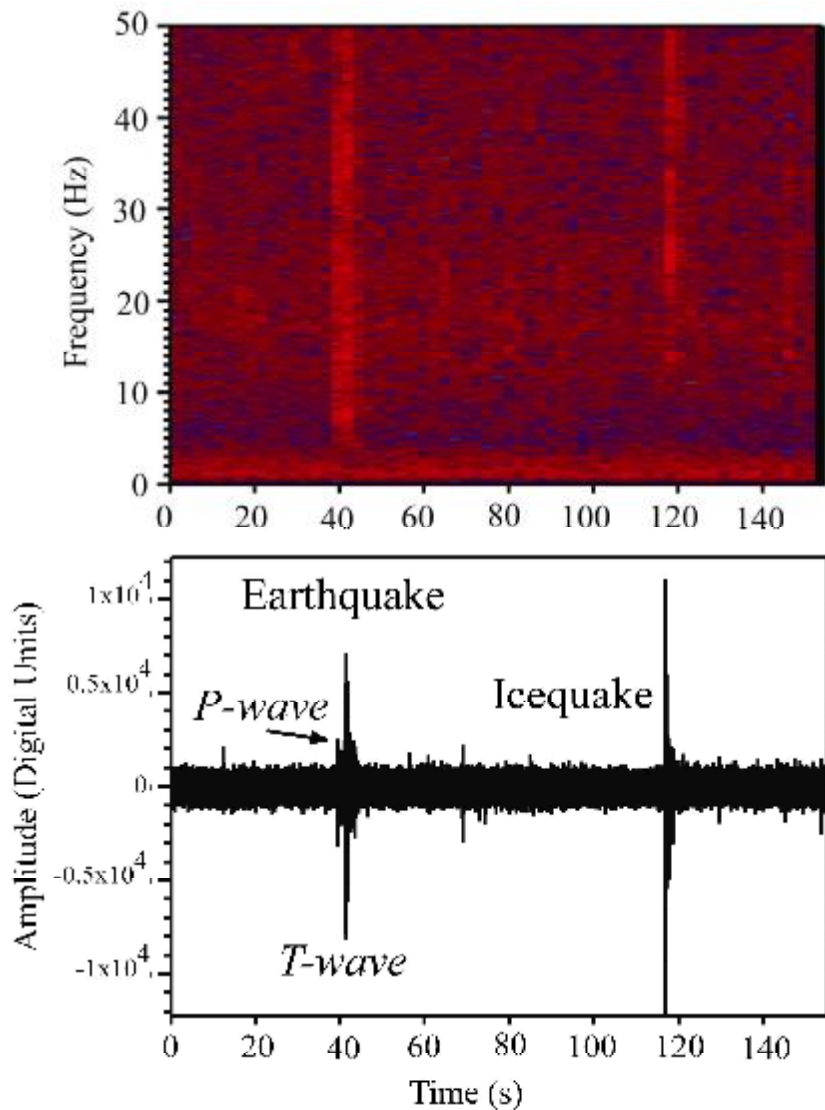


Figure 2

Figure 2: Time-series and spectrogram of hydrophone data (station 5) examples of an earthquake (a) and icequake (b) acoustic arrivals. The earthquake shown occurred on 5 April 2007 and was a 4.7 m_b event that occurred at the southwest Bransfield Strait (event mechanism within box of Figure 3). Earthquakes produce seismic phases that convert to an acoustic phase at the seafloor-ocean interface. This acoustic earthquake phase propagates laterally through the water-column as a broadband (3-50 Hz) arrival referred to as a *T*-wave. The faster direct P-wave arrival is also recorded by the hydrophone as a locally converted acoustic phase. Icequakes originate in sea-surface ice and produce acoustic phases that propagate solely in the water-column downward toward the hydrophone. Icequake arrivals are distinguished from earthquakes by their impulsive, short-duration coda (~ 10 s) and higher frequency content (>10 -50 Hz).

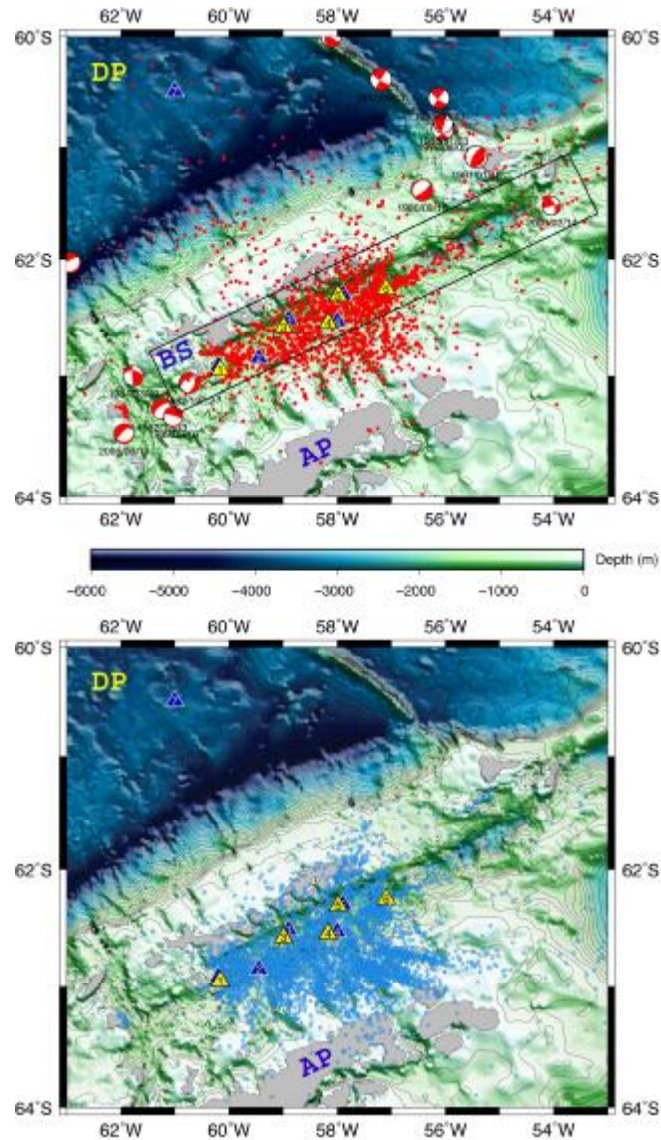


Figure 3: Top diagram shows earthquakes, bottom diagram shows icequakes located using the hydrophone arrays during the two-year deployment. Blue and yellow triangles represent for 2005-2006 hydrophone mooring deployments (7 instruments) and 2006-2007 deployments (5 instruments), respectively. Only 5 hydrophones were used to estimate locations from 2005-2006 data due to clock errors (see Figure 4). Labels indicated the Drake Passage (DP), Bransfield Strait (BS) and Antarctic Peninsula (AP). Box shows earthquakes used to make Figure 5. Bathymetry is from Sandwell and Smith [1997] satellite altimetry. Red focal mechanisms show the 14 Harvard Centroid Moment-Tensor solutions that were determined for this region from 1976-2008. Earthquakes range in magnitude from 5.0-6.0 m_b , showing strike-slip motion along the Shackleton Fracture Zone and normal fault motion at the southwest Bransfield basin.

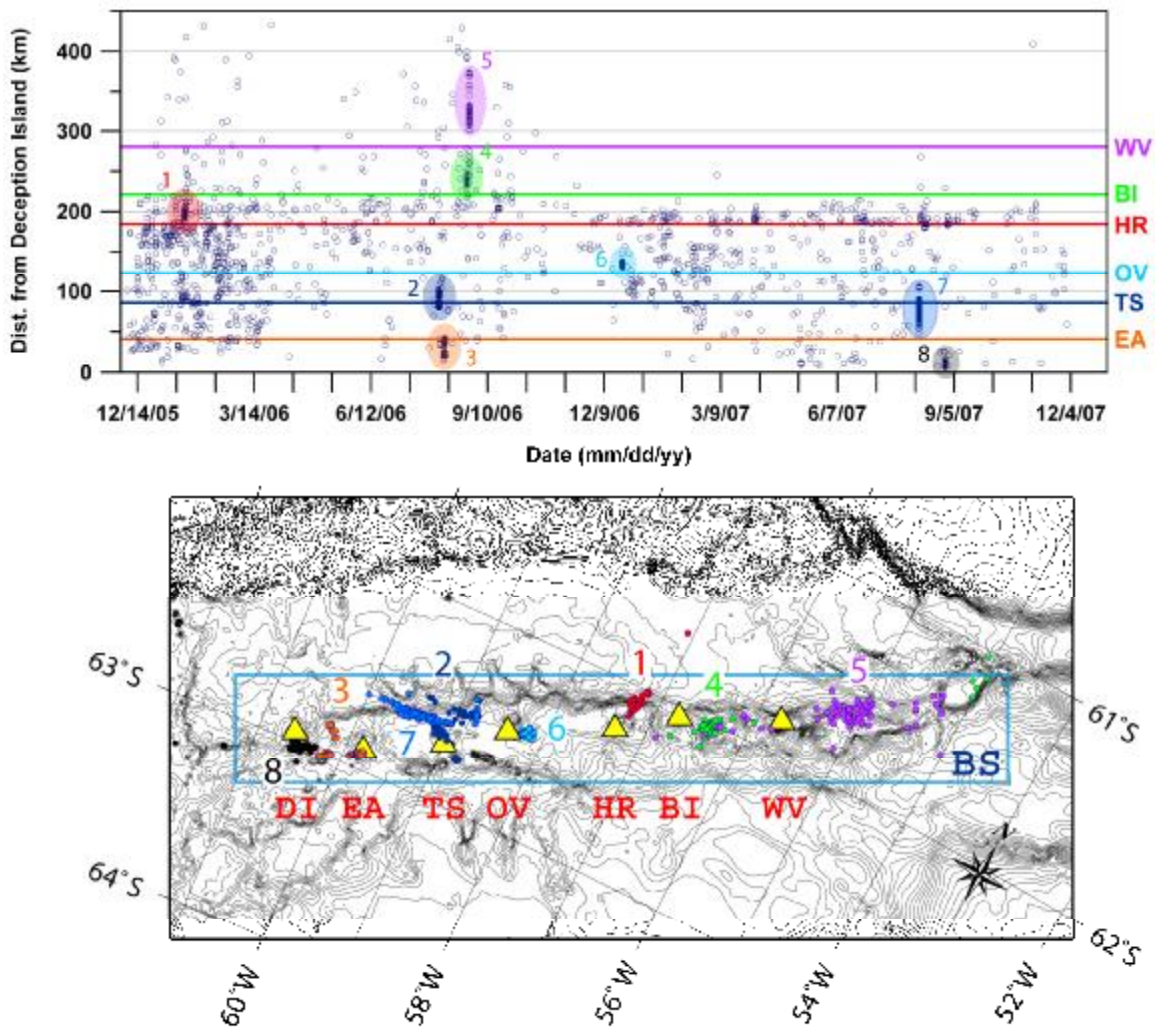


Figure 4: (Top) Diagram shows distribution in time and distance of hydroacoustic earthquake locations. The time axis is the entire two-year hydrophone deployment, distance is in km uprift along Bransfield neo-volcanic zone, with Deception Island as the reference point. (Bottom) Earthquakes show temporal clustering in eight distinct swarms occurring at the volcanic centers, with each earthquake cluster color coded to appropriate volcanic center. Swarms are numbered by date of occurrence. The major Bransfield seafloor volcanoes are labeled and triangles give their locations: EA=Edifice-A volcano, TS=Three Sisters, OV=Orca Volcano, HR=Hooks Ridge, WV=Wordie Volcano. Bottom diagram shows map-view distribution of earthquake swarm in relation to volcanic centers.

CENOZOIC TECTONICS OF THE WESTERN ROSS SEA REGION

F J Davey

GNS-Science, P O Box 30368, Lower Hutt, New Zealand
f.davey@gns.cri.nz

INTRODUCTION

The western margin of the Ross Sea is formed by the Transantarctic Mountains, a rift mountain range considered to have formed in the Cretaceous and marking the margin between the East Antarctic craton and the extended, thinned continental lithosphere of the Ross Sea. Subsequent Cenozoic lithospheric extension along the rift margin in the western Ross Sea region (Figure 1) has formed the Northern Basin (NB) in the north (Brancolini et al., 1995) and the Victoria Land Basin (VLB) to the south (Cooper and Davey 1987). A major east-west trending magnetic anomaly, the Polar-3 anomaly (Bosum et al., 1989), coincides with an offset of the VLB from the NB. Off north-western Ross Sea, marine magnetic anomalies have defined an episode of seafloor spreading from about 43 – 26 Ma that formed the Adare Basin (Cande et al 2000). About 170 km of ENE-WSW extension occurred.

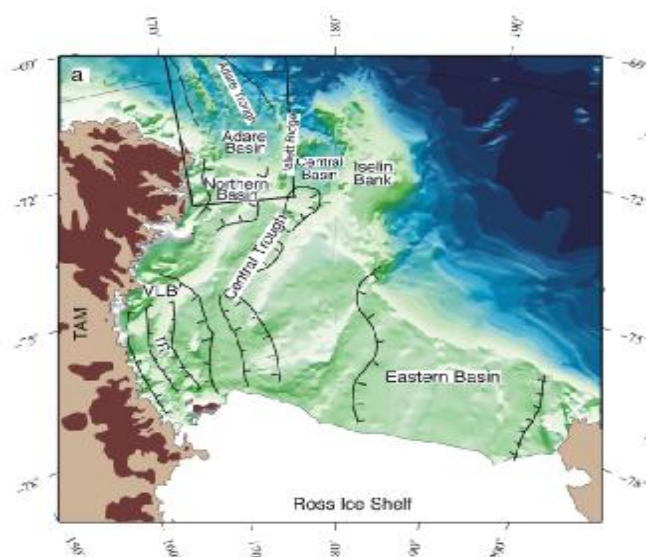


Figure 1. Ross Sea morphology and major structures

DATA

The morphology of the western Ross Sea continental shelf and slope is well known (Davey 2004). The major features of the whole shelf region are a series of N to NNE trending broad banks and troughs from the Ross Ice Shelf to the shelf edge (Figure 2). These features generally cross obliquely the geological structures underlying the shelf and are inferred to be caused by erosion by grounded icesheets, possibly ice streams (Houtz and Davey 1975, Shipp et al., 1995).

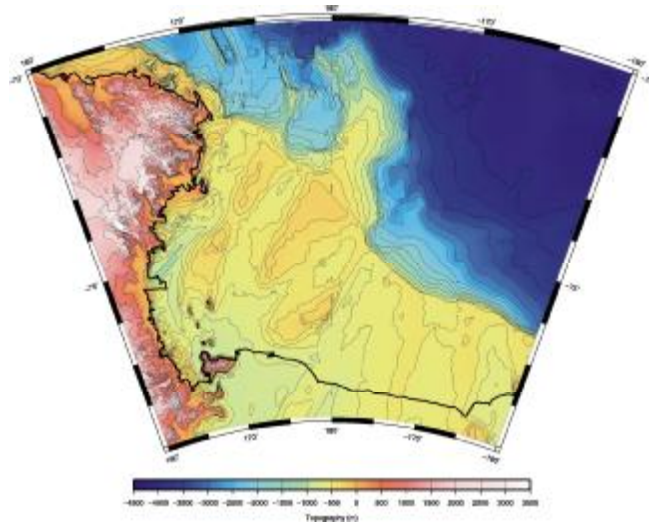


Figure 2. Ross Sea morphology (100 m contours on shelf)

Detailed morphology delineate icesheet erosional features such as sub-ice linear grooves and roche moutonees under the inner shelf; random, often sinuous, shallow channels or furrows on the outer shelf, interpreted to be caused by iceberg keels; terminal moraines; and shelf break gullies just downslope of the continental shelf edge inferred to be caused by meltwater streams from under a continental ice sheet grounded to the shelf edge (Davey and Jacobs, 2007; Shipp et al., 1999; Wellner et al., 2006).

An extensive data base of multichannel and single channel seismic reflection data exists for the Ross Sea. Several major erosional unconformities can be mapped across the shelf and onto the slope and rise. The major structural features are a series of deep troughs or rift basins delineated by major faulting (Figure 3). The Victoria Land Basin contains up to 14 km of sedimentary rocks at least 36 Ma in age, perhaps as old as Cretaceous, and extending up to the present. It lies along the southwest Ross Sea margin and is inferred to be caused by rifting along the Transantarctic Mountains. Further north

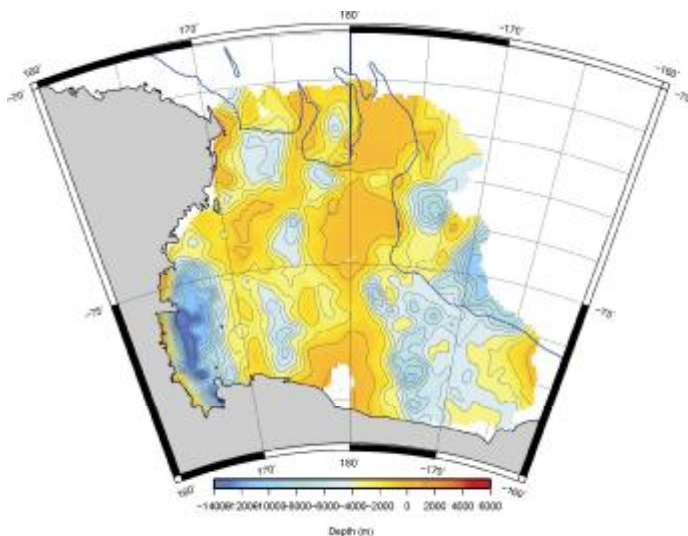


Figure 3. Depth to basement (1 km contours)

and east is the Northern Basin, possibly of the same age but only about 6 km deep. The sediment infill is not well dated but is probably at least 26 Ma in age. Parallel to and east of these two basins lies the Central Trough. Its age is not well constrained, but it is inferred to contain Cretaceous sediments and deformation appears to have mainly been mid Cenozoic or older (Decesari et al., 2007). It is also offset to the east at about the same latitude as the offset between the VLB and NB

Aeromagnetic data cover a large part of the western Ross Sea (Bosum et al. 1989, Damaske et al. 1994, 2007). East-west trending bands of large magnetic anomalies coincide with the northern (the Polar 3 anomaly) and southern limits of the VLB, and a series of magnetic anomalies corresponds with the young extensional feature (the Terror Rift – TR in Figure 1) that marks the centre of the VLB. 15 Ma and younger volcanics of the McMurdo volcanic province and the older (45 – 30 Ma) intrusives of the Cape Washington region (Rocchi et al. 2002) correspond closely to the magnetic anomalies.

Age control for the Cenozoic sediments and tectonics is poor. Few Cenozoic rocks are exposed on land. A limited number of offshore drill holes exist, particularly in the McMurdo Sound region, and constrained the age of the sedimentary section back to about 36 Ma but it is often difficult to extrapolate these dates regionally using seismic data due to intervening complex tectonics or the onlapping of the older section on intervening basement ridges. Uplift of the TAM has been constrained by apatite fission track dating indicating unroofing (and inferred uplift) of this region starting in the Cretaceous and mainly in the early Cenozoic (Fitzgerald and Stump, 1997) To the north, the oceanic crust of the Adare basin has been dated by marine magnetic anomalies to have been formed from 43 to 26 Ma (Cande et al., 2000)

TECTONICS

The development of the Ross Sea region is largely one of rift tectonics and subsequent thermal subsidence associated with break-up of Gondwana and subsequent adjustments along plate boundaries through the region associate with the plate tectonic development of the Pacific –Antarctic region. Miocene and younger glacial processes has had a major effect on the younger sedimentary deposition patterns.

The earliest event was Jurassic rifting during the earliest Gondwana break-up processes associated with the intrusion of the Ferrar dolerites into the Beacon Supergroup sediments and eruption of Kirkpatrick basalts. These rocks are only documented in the Transantarctic Mountains and its immediate margin (e.g. CRP3 drill site) and have not been found in the Ross Sea.

The major lithospheric thinning of the Ross Sea region (and West Antarctic rift system) occurred in Cretaceous times associated with the cessation of subduction along the Pacific margin at about 115 – 100 Ma and the break-up of New Zealand region from Gondwana at about 83 Ma. Rifting was generally amagmatic. No sediments of Cretaceous age are known from the Ross Sea region although rocks of this age have been inferred for the deepest sediments in the western and eastern parts of Eastern Basin that underlies eastern Ross Sea (e.g. Luyendyk et al. 2001), under the Central Trough (Decesari et al. 2007), and Victoria Land Basin (Cooper and Davey 1987).

The major rifting in western Ross Sea and immediately north occurred in the mid-Cenozoic. Spreading in the Adare Basin off north-western Ross Sea (43 -26 Ma) with extension of at least late Eocene –Oligocene age in the Northern Basin (NB) immediately south and extension in the Victoria Land Basin (VLB) starting before 36 Ma. Seismic data indicates that the major extension of these rift basins occurred during this time (Davey et al., 2007). Two major phases appear to have occurred – about 43 Ma to 35 Ma, possibly asymmetric rifting and associated with major magmatic intrusives (Polar 3 anomaly) and offset in rifting between VLB and NB, and from 35 Ma to about 26 Ma with only minor intrusives.

A later rifting phase, largely vertical faulting but with extensive extrusive volcanism, occurred in the late Cenozoic, with active faulting occurring from VLB (focussed on the Terror Rift) to the southern Adare Basin where its trend changes to

NNE from the Cape Adare region to the southern end of the Adare Trough. This change may in part be related to the change in Pacific –Antarctic spreading direction about 6 m.y. ago. Active hydrothermal features occur in the VLB.

REFERENCES

- Brancolini, G., A.K. Cooper, and F. Coren, 1995. Seismic Facies and Glacial History in the Western Ross Sea (Antarctica), in *Geology and seismic stratigraphy of the Antarctic margin*, edited by A.K. Cooper, P.F. Barker, and G. Brancolini, pp. 209-234, Amer. Geophys. Union, Washington, D. C.
- Bosum, W., Damaske, D., Roland, N.W., Behrendt, J.C., Saltus, R., 1989. The GANOVEX IV Victoria Land/Ross Sea aeromagnetic survey: interpretation of the anomalies, *Geol. Jb.* E38: 153-230.
- Cande, S.C., J.M. Stock, D. Müller, and T. Ishihara, 2000. Cenozoic Motion between East and West Antarctica, *Nature*, 404, 145-150.
- Cooper A.K., Davey, F.J., 1987. The Antarctic Continental Margin: Geology and Geophysics of the Western Ross Sea. CPCEMR Earth Science Series Volume. 5B: Houston, Texas. Circum-Pacific Council for Energy and Mineral Resources. 230p.
- Damaske, D., Behrendt, J.C. McCafferty, A.M., Saltus, R., Meyer, U., 1994. Transfer faults in the western Ross Sea; new evidence from the McMurdo Sound/Ross Ice Shelf aeromagnetic survey (GANOVEX VI), *Antarctic Science*, 6 (9), 359-364.
- Damaske, D., Läufer, A.L., Goldmann, F., Möller, H-D., Lisker, F , 2007. Magnetic Anomalies Northeast of Cape Adare, Northern Victoria Land (Antarctica), and their Relation to Onshore Structures, in *Antarctica: A Keystone in a Changing World – Online Proceedings of the 10th ISAES*, edited by A. K. Cooper and C. R. Raymond et al., USGS Open-File Report 2007-1047, Short Research Paper 016, DOI: 10.3133/of2007-1047.srp016.
- Davey, F.J. 2004. Ross Sea bathymetry, 1:200,000. Geophysical map, Institute of Geological & Nuclear Sciences 16, Institute of Geological & Nuclear Sciences Limited, Lower Hutt.
- Davey, F. J., Cande, S. C., Stock, J. M. 2006. Extension in the western Ross Sea region-links between Adare Basin and Victoria Land Basin, *Geophys. Res. Lett.*, 33, L20315, doi:10.1029/2006GL027383.
- Davey, F. J., Jacobs, S.S., 2007. Influence of submarine morphology on bottom water flow across the western Ross Sea continental margin, in *Antarctica: A Keystone in a Changing World – Online Proceedings of the 10th ISAES*, edited by A. K. Cooper and C. R. Raymond et al., USGS Open-File Report 2007-1047, Short Research Paper 067, 5p.; doi: 10.3133/of2007-1047.srp067.
- Decesari, R.C., Sorlien, C.C. Luyendyk, B.P. Wilson, D.S., Bartek, L., Diebold J., Hopkins. S.E., 2007. Regional seismic stratigraphic correlations of the Ross Sea: Implications for the tectonic history of the West Antarctic Rift System, in *Antarctica: A Keystone in a Changing World – Online Proceedings of the 10th ISAES*, edited by A.K. Cooper and C.R. Raymond et al., USGS Open File Report 2007-1047, Short Research Paper 052, 4 p.; doi:10.3133/of2007-1047.srp052
- Fitzgerald, P.G., Stump, E., 1997. Cretaceous and Cenozoic episodic denudation of the Transantarctic Mountains, *Antarctica: New constraints from apatite fission track thermochronology in the Scott Glacier region*, *J Geophys. Res.*, 102(B4), 7747-7765.

- Houtz, R.E., Davey, F.J., 1973. Seismic profiler and sonobuoy measurements in Ross Sea, Antarctica. *Jl Geophys. Res.* 78: 3448-68.
- Luyendyk, B. P., Sorlien, C.C., Wilson, S., Bartek, L. R., Siddoway, C. H., 2001. Structural and tectonic evolution of the Ross Sea rift in the Cape Colbeck region, Eastern Ross Sea, Antarctica, *Tectonics*, 20, 933-958.
- Rocchi, S., Armienti, P., D'Orazio, M., Tonarini, S., Wijbrans, J.R., Di Vincenzo, G., 2002. Cenozoic magmatism in the western Ross Embayment: Role of mantle plume versus plate dynamics in the development of the West Antarctic Rift System, *Journal of Geophysical Research* 107, B9, 2195, doi:10.1029/2001JB000515.
- Shipp, S., J. B. Anderson, and E. Domack, 1999. Late Pleistocene- Holocene retreat of the West Antarctic Ice-Sheet system in the Ross Sea: Part 1-Geophysical results, *GSA Bulletin*, 111(10), 1486-1516.
- Wellner, J. S., D. C. Heroy, and J. B. Anderson, 2006. The death mask of the Antarctic Ice Sheet: comparison of glacial geomorphic features across the continental shelf: *Geomorphology*, v. 75, p. 157-177.

**WORKSHOP ON
GEOLOGY & GEOPHYSICS**

SESSION 1

**ICE-SHELF, SEDIMENTATION
& PALEOCLIMATE**

LARSEN ICE SHELF SYSTEM (LARISSA): A MULTI-DISCIPLINARY EARTH SYSTEMS APPROACH TO ANTARCTIC ENVIRONMENTAL CHANGE

Eugene W. Domack & LARISSA team

Department of Geosciences, Hamilton College, Clinton New York 13323 USA
edomack@hamilton.edu

LARISSA is an international, multi-disciplinary field program to address the rapid changes occurring in the Antarctic Peninsula region as a consequence of the abrupt collapse of the Larsen B Ice Shelf (<http://www.hamilton.edu/news/exp/LARISSA/>). The overarching goal of this project is to describe and understand the basic physical and geological processes active in the Larsen embayment that **a)** contributed to the present phase of massive, rapid environmental change; **b)** are participating in that change as part of the coupled climate-ocean-ice system; and **c)** are fundamentally altered by these changes. LARISSA includes a comprehensive, interdisciplinary project composed of geologists, glaciologists, oceanographers, and biologists. Because of this broad scope, three separate but interrelated projects are part of LARISSA. This paper addresses Marine and Quaternary Geosciences, while two others include Marine Ecosystems and Cryosphere & Oceans. Our geoscience research addresses five major questions.

- (1) What does the stratigraphic record from prior to the Last Glacial Maximum reveal about the extent of the Larsen Ice Shelf under climate conditions of the penultimate interglacial (approximately ~125 ka) when global conditions of sea level and average climate were higher and warmer, respectively, than today?
- (2) What was the detailed configuration of the northern Antarctic Peninsula Ice Sheet (APIS) during the Last Glacial Maximum and subsequent retreat?
- (3) Why has the Larsen B Ice Shelf been a stable component of the cryosphere through the Holocene epoch, while other ice shelves have apparently come and gone during periods of natural climate variability?
- (4) What controls the dynamics of ice-shelf grounding-line systems and what role does meltwater or oceanic processes play in their stability?
- (5) What changes in sediment flux (both lithogenic and biogenic) accompany large scale ice shelf disintegration and post break up surge of tributary glaciers, and what is the temporal and spatial pattern of this pulse of sediment across the basin?
- (6) Finally, what role does biotic isolation beneath ice shelf basins play in the establishment of chemotrophic ecosystems and, how are such systems impacted by ice shelf disintegration and increased sediment flux to the seafloor.

Given the importance of ice shelf dynamics to both popular and scientific debate relating to climate change, the Larsen B ice shelf system is an important focus for investigation, learning, and education during and after the International Polar Year (IPY). The results of this international, multi-disciplinary effort will significantly advance our understanding of linkages amongst the earth's systems in the Polar Regions and are proposed in the true spirit of IPY.

**STUDY OF DRY AND MELT SNOW ZONES OF LAMBERT GLACIER –
AMERY ICE SHELF, ANTARCTICA USING TEM+ DATA**

Jaehyung Yu¹, Samuel Cantu¹, Joonghyeok Heo², Hongxing Liu²

¹Department of Physics and Geosciences, Texas A&M University-Kingsville,
Kingsville, TX, USA

²Department of Geography, Texas A&M University, College Station, TX, USA
jaehyung.yu@tamuk.edu

The surface area of an ice sheet or a glacier is subdivided into four distinct snow zones: the bare ice zones, the wet snow zone, the percolation zone, and the dry snow zone. The balance between accumulation and melt in different snows also affects the runoff and discharge of stream systems fed by snow and glacier melt water. In addition, snow pack is extremely sensitive to atmospheric temperature. Spatial extent and geographical position of different snow zones indicate regional climate condition. Moreover Blue-ice areas represent zero accumulation and the surface mass loss to the atmosphere by sublimation. Due to its importance in surface accumulation and mass balance of Antarctic ice sheet, it is necessary to quantify the spatial extent of Blue-ice areas and different snow zones.

The Lambert Glacier-Amery Ice Shelf, located in the East Antarctic Ice Sheet, is one of the largest glacial systems on Earth. Because of its large size and dynamic nature, the Lambert Glacier-Amery Ice Shelf system plays a fundamental role in the study of mass budget of the Antarctic Ice Sheet in response to present and future climate changes. In spite of its importance in mass balance study and snow accumulation, the blue ice areas and different snow are never fully mapped for the entire Lambert Glacier-Amery Ice shelf system from the Landsat ETM+.

This study utilizes Landsat ETM+ data acquired from 1999 to 2003 to map the extent of Blue-ice area and different snow zones. Normalized Difference Snow Index is effective to differentiate snow and ice features using the spectral differences of snow and ice in the visible green wavelength region (ETM+2) and the MIR region (ETM+5). The spectral signatures show ETM+3 and ETM+4 work the best to differentiate surface features in Antarctica. Both supervised (maximum likelihood and parallel piped) and unsupervised (ISODATA) classification methods are carried out to map the extents of Blue-ice, snow zones, and rock exposures. As a result, 23,000 km² are mapped as blue ice, and 3,000 km² rock exposure areas are identified. Moreover, no wet snow zones are identified whereas wide range of percolation zones is distributed over the Amery Ice Shelf.

**UNFINISHED BUSINESS; CAPTURING THE VALUE OF EXTENDED
CONTINENTAL SHELF DATA SETS TO UNDERSTAND THE HISTORY OF
THE ARCTIC OCEAN**

Bernard Coakley¹, Larry Mayer², Kelley Brumley¹, Martin Jakobsson³, Betsy Baker⁴

¹Geophysical Institute, University of Alaska, Fairbanks, AK 99775 USA

²Center for Coastal and Ocean Mapping, Durham, NH 03824 USA

³Department of Geology and Geochemistry, Stockholm University, Stockholm 106 91,
Sweden

⁴Vermont Law School, South Royalton, VT 05068-0096, USA

bernard.coakley@gi.alaska.edu

Scientists and lawyers are working together to map the extended continental shelf (ECS) in all of the world's oceans. For better or worse, lawyers wrote the rules that scientists are now trying to apply: Article 76 of the UN Convention on the Law of the Sea. Negotiated more than 30 years ago, Article 76 lays out procedures for coastal states to establish exclusive exploitation rights over seabed and subsoil resources – primarily oil and gas – beyond 200 nautical miles from their territorial sea baselines. The rules involve simple, measurable quantities from geodesy (position), hydrography (depth) and marine geology (sediment thickness). With a data set in hand, it is possible to come up with a document that could, with assigned numerical uncertainty (position, depth and sediment thickness +/- so many meters), apply the rules and establish the limits of a coastal state's seabed entitlement.

The bathymetric features used to establish the extent of the ECS are the 2500 meter isobath or depth contour and the foot of the slope (FOS). The FOS is the point at which a bathymetric profile has maximum curvature or the largest change in slope. It might correspond, in the real world, to what is known as the top of the continental rise. Sediment thickness data are also needed to identify the point where the sediment thickness is 1% of the distance back to the FOS.

The Article 76 process must somehow reconcile the great diversity of seafloor structure and composition that has been recognized with the simplistic language of the treaty itself. While this process relies on scientific data, it is not hypothesis testing. In the ECS context the data are material for advocacy. The data are a means to achieve a particular objective; in the typical situation, the goal is to make a positive case for a particular limit line, and thereby maximize the claimed area.

Bathymetry data and multi-channel seismic reflection data are among the classical data sets of marine geology and geophysics. As a result the marine geology community is heavily involved in data acquisition for determination of ECS limits. The scientist's skills and tools used to study the history of the Arctic Ocean are necessary to establish ECS assertions, but the applications are distinct. An ECS survey is not a science cruise. No hypothesis is asserted or tested. The data collected to establish a nation's ECS are collected in particular locations to define certain characteristics of the seafloor. Despite being collected for a non-scientific purpose, these data are useful for exploration of the arctic. By going places scientists would not have reason to visit, these

data will reveal some unexpected aspects of Arctic Ocean structure and history and form the basis for the next round of science programs. In this, there is an opportunity to use R/V Aaron to maximum effect.

ECS mapping and scientific cruises all supported by the icebreaker USCGC Healy have fortuitously encountered a number of unexpected features in the Arctic Ocean. These cruises, pursuing other purposes, have left these discoveries behind to complete their diverse missions. The R/V Aaron, with its' multi-beam system and coring capability, could, by extending these data sets, test particular hypotheses about how these features formed. This would leverage the substantial investment of USCGC Healy time in the Arctic Ocean and yield good results from a relatively limited amount of R/V Aaron time.

For example;

1) There are a number of large pockmarks on the elevated parts of the Chukchi Borderland. Using data collected during multiple LOS cruises and Larry Lawver's cruise in 2006, Kelley Brumley has mapped these and argues that they are associated with underlying faults in the deeper sections of the Chukchi Borderland.

Systematic investigation of these features, mapping and coring could do a lot to establish the important processes, controls and source of gases.

2) Focusing on the edges of the Chukchi Borderland. This would have two important science impacts;

a) Mapping out the limits of the glacial erosion on the shallower portions of the borderland.

b) Improving the data set we have on the transitions between this obviously continental block and the adjacent blocks of oceanic and/or distinct continental crust.

3) Mapping the shelf edge transition to establish how the canyons on the Beaufort Slope connect with other sedimentary features on the shelf. If there is a chirp sub-bottom profiler on board, it would also be possible to learn a lot about the history of glacial flow parallel to the coast as established with data collected from the USS Hawkbill during the last SCICEX mission in 1999.

All 3 efforts would expand existing data sets into more useful products for testing real hypotheses.

THE BARENTS SEA PALEOENVIRONMENTS OVER THE LAST 15 KA

Elena V. Ivanova¹, Ivar Murdmaa¹, Natalia Chistyakova¹, Bjorg Risebrobakken² and Galina Alekhina¹

¹Shirshov Institute of Oceanology, Russian Academy of Sciences, 36 Nakhimovskiy Prospekt, 117997, Moscow, Russia
e_v_ivanova@ocean.ru

²Bjerknes Centre for Climate Research, University of Bergen, 5007 Bergen, Norway

The study of more than 30 sediment cores from the Barents Sea (Ivanova et al., 2002; Murdmaa et al., 2006) provides a robust framework for the recognition of three major lithostratigraphic units in postglacial sections of shelf depressions. Hence, the major paleoclimatic and paleoceanographic events in this basin can be correlated with global changes and with the variability of the Atlantic Meridional Overturning. The Atlantic Water input via the surface and subsurface water layers (Fig. 1) strongly affects the Barents Sea climate and, in turn, is modulated by the outflow of the Arctic Waters (e.g. Pfirman et al., 1994). Two of the three mentioned lithostratigraphic units recover the last ~ 15 ka, as it is confirmed by AMS-14C dates in a few cores from different locations (e.g. Lubinski et al., 2001; Ivanova et al., 2002; Slubowska et al., 2005; Chistyakova et al., in press). However, the paleoenvironmental reconstructions are strongly limited by generally very scarce microfossil occurrence in the shelf sediments, except for the fjords, prior to the Holocene. A 5-m long sediment core PSh 5159R from the Ingøydjupet Depression, within the passage of the surface Atlantic Water inflow, contains rather diverse foraminiferal assemblages and rare mollusks in the last 16 ka interval. Combined with a well-dated 3.5-m long twin core PSh 5159N this enables the high resolution (about 100-200 years) record of the bottom and surface (over the last 12 ka) water environments in the south-western Barents Sea (Fig. 2-3; Chistyakova et al., in press; Risebrobakken et al., in prep.). The Holocene environments are studied with about the same time resolution in AMS-14C dated cores ASV 880 from the Franz Victoria Trough and ASV 1200 from the Persey Trough (Fig. 1-2) according to the age model by Duplessy et al. (2005). Time series of indicative benthic foraminiferal species, oxygen isotopes and paleotemperature from these cores are compared to the corresponding data from other locations in the Barents Sea (Fig. 1) to highlight paleoenvironmental variability through the Holocene with respect to changes in regional climate (in particular, sea ice extent) and Atlantic Water inflow.

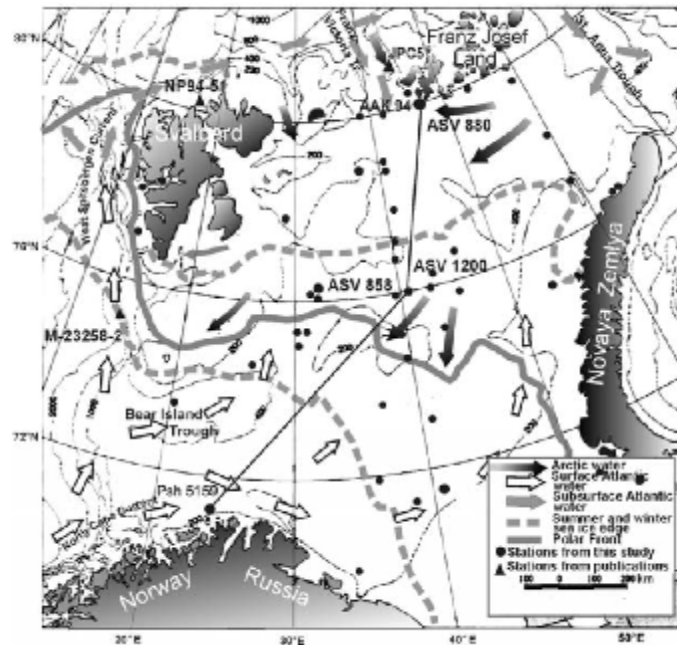


Fig. 1. Location of transect, sediment cores and modern hydrography of the Barents Sea. Surface circulation simplified after Pfirman et al.(1994), summer and winter sea ice edges after Vinje and Kvambekk (1991). Triangles indicate cores studied by Lubinski et al. (2001), Sarnthein et al. (2003) and Slubowska et al. (2005).

In the south-western part of the Barents Sea, unstable bottom settings and ice rafting are characteristic of the Oldest Dryas. Saline but chilled Atlantic Water inflow increased noticeably during the Bølling-Allerød interstadial and then decreased during the Younger Dryas, as indicated by benthic assemblages. Our foraminiferal records reveal a generally strong dominance of typical arctic species in the Holocene assemblages, except for the south-western part of the Barents Sea where so-called ‘atlantic’ species are common since ~ 11.2 cal. ka (Fig. 2). Relatively scarce planktic foraminifera are represented by subpolar *N. pachyderma* sin. in the northern and central parts of the basin, whereas more abundant assemblages in the south-west contains also boreal species, notably abundant *T. quinqueloba*. In Core PSh 5159N/R, arctic species, especially *C. reniforme* and *E. clavatum*, dominate through the YD/Holocene transition. High amounts of Atlantic species like *C. teretis*, *M. barleeanus*, *P. bulloides*, *P. quinqueloba*, *T. angulosa* and boreal planktic foraminifera point to a relatively persistent Atlantic water transport into the Barents Sea along the Norwegian coast during the last ~ 11.2 ka. The Earliest Holocene was characterized by an abrupt warming of both bottom and surface waters (from ~ 6 to 11°C) with the thermal optimum ~ 9.8 – 7.6 cal. ka BP. A similar magnitude of SST changes with a longtime optimum in the Early Holocene was reconstructed by Sarnthein et al. (2003) in Core M-23258-2 obtained ~ 3° northward of our core (Fig. 1 and 3). Stable relatively warm conditions prevailed in the south-western Barents Sea during the Middle Holocene whereas variable temperatures in the water column are characteristic of the last ~2.5 ka.

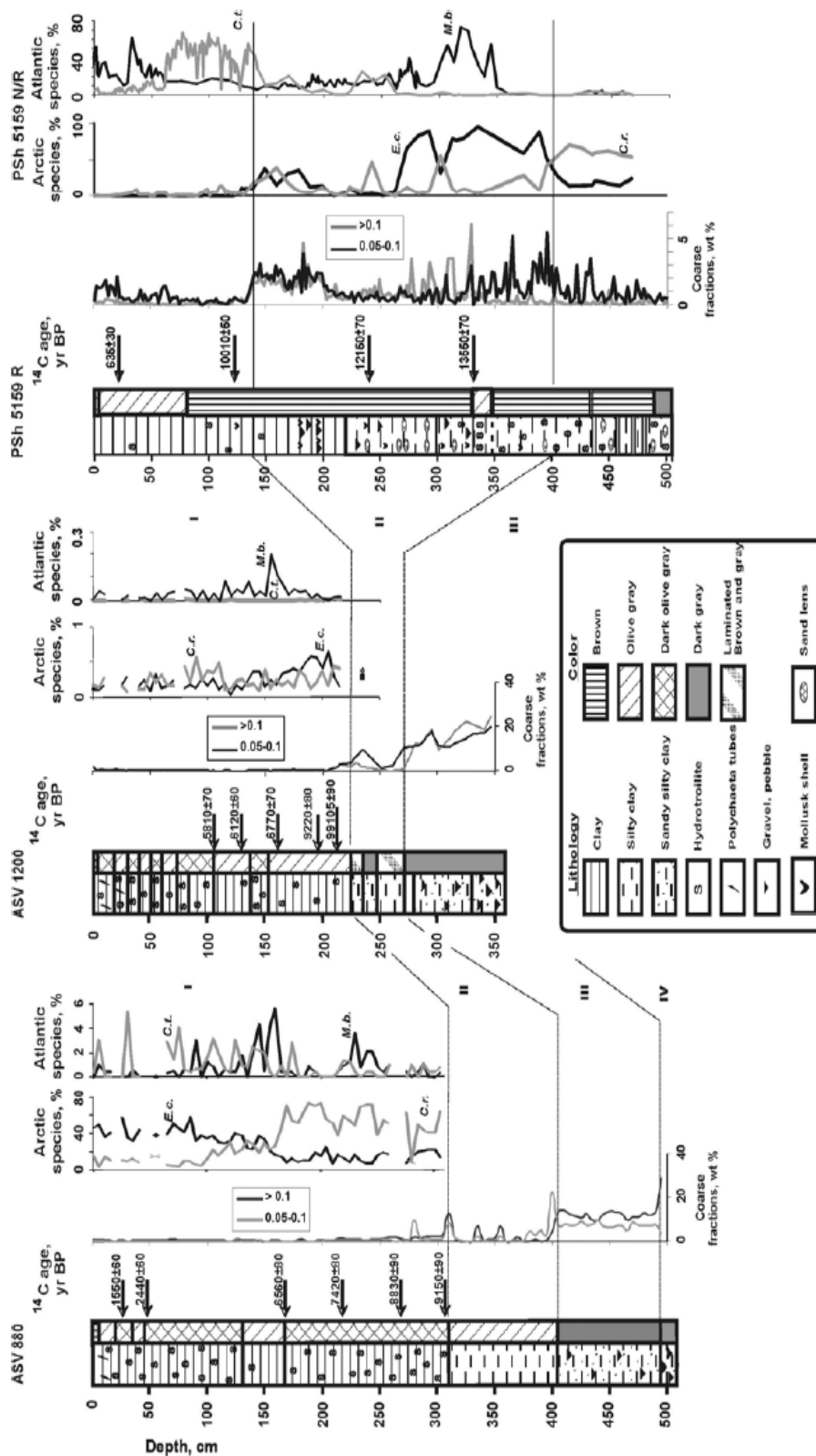


Fig. 2. Lithology, AMS-14C dates, distribution of two sediment fractions and indicative arctic and atlantic foraminiferal species in the three reference sediment cores along the SW-NE transect shown on Fig. 1. Data from (Ivanova et al., 2002; Ivanova, 2006; Chistyakova et al., in press). *E.c.* - *Elphidium clavatum*, *C.r.*-*Cassidulina reniforme*, *M.b.*-*Melonis barleeanus*, *C.l.*-*Cassidulina teretis*.

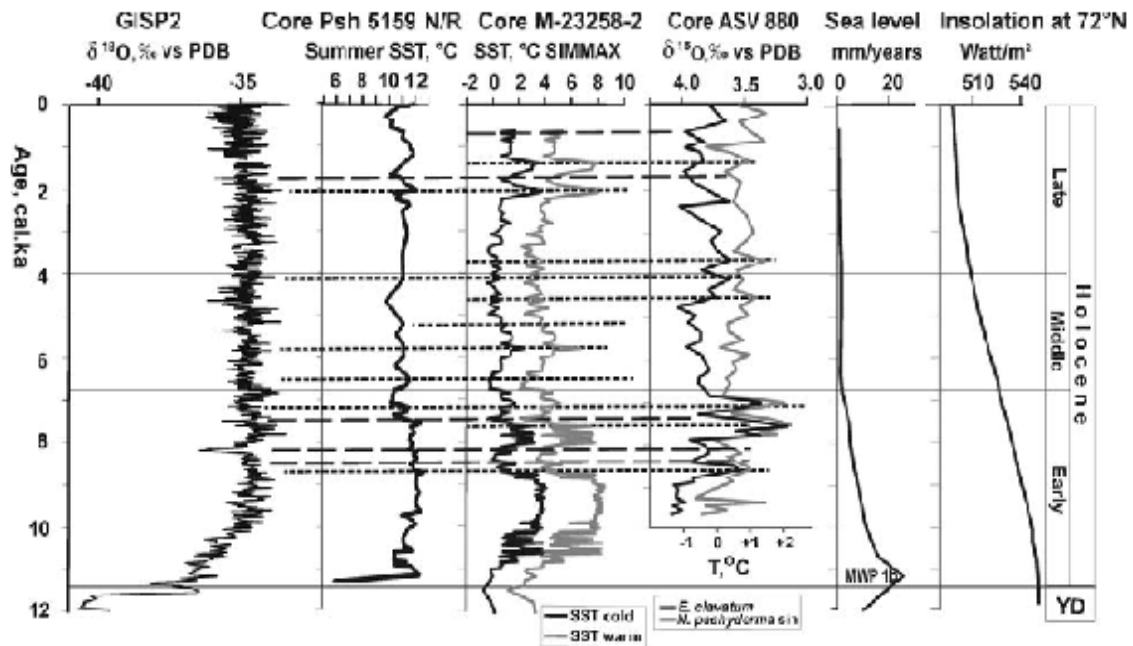


Fig. 3. Correlation of paleotemperature time series in the Barents Sea cores with GISP2 oxygen isotope record, June insolation at 72°N and sea-level record over the last 12 ka (after Ivanova, in press). Paleotemperature records from core ASV 880 (Duplessy et al. 2001) correspond to subsurface and bottom water layers, for core M-23258-2 (Sarnthein et al. 2003) winter (cold) and summer (warm) sea-surface temperatures (SST) are shown, for core PSh 5159N/R (Chistyakova 4 et al., in press) summer SST (at 10m w.d.) is shown. Short-term warming and cooling episodes are indicated by dotted and dashed lines respectively. YD- Younger Dryas. MWP 1b- melt water pulse 1b at the end of the last deglaciation.

In the Franz Victoria Trough, the thermal optimum in subsurface to bottom layer is inferred from the planktic and benthic oxygen isotopes at 7.8-6.9 cal. ka (Duplessy et al., 2001). It is also reflected by an increase in occurrence of benthic species *Islandiella helenae/norscrossi* as a result of a longer ice free season during the strong Atlantic water influx along the northern continental slope of the Barents Sea. Subsurface water temperature varied from ~ -0.5 to 2.4°C during the last 10 ka (Fig. 3). In other northern cores JPC5 (Lubinski et al., 2001) and AAK 94, an increased Atlantic water input during this optimum and at the beginning of Holocene is indicated by enhanced amount of the Atlantic benthic species. A dominance of opportunistic *E. clavatum* in cores ASV 880 (Fig. 2) and NP94-51 (Slubowska et al., 2005) points to the gradual paleoenvironmental deterioration through the Middle to Late Holocene. In Core ASV 1200 from the Persey Trough, both isotope and foraminiferal records are rather smoothed. Thus, all the above mentioned data suggest a remarkable spatiotemporal variability of the postglacial Barents Sea environments to a significant extent controlled by the variability of Atlantic Water input via the southern and northern branches into the Barents Sea.

REFERENCES

- Chistyakova, N., Ivanova, E., Risebrobakken, B. et al. Reconstruction of Postglacial environments in the south - western Barents Sea. *Oceanology*, in press. Duplessy, J.C., Ivanova, E.V., Murdmaa, I.O. et al. Holocene paleoceanography of the Northern Barents Sea and variations of the northward heat transport by the Atlantic Ocean. *Boreas*, 2001, 30(1): 2-16.
- Duplessy, J.C., Cortijo E., Ivanova E. Et al. Paleoceanography of the Barents Sea during the Holocene. *Paleoceanography*, 2005, 20, doi:10.1029/2004PA001116.
- Ivanova E.V. The Global Thermohaline Paleocirculation. Scientific World, Moscow, 2006, 320p. (in Russian).
- Ivanova E.V. The Global Thermohaline Paleocirculation. Springer, 2009 (in press).
- Ivanova E.V., Murdmaa I.O., Duplessy J.C., Paterne M. Late Weichselian to Holocene Paleoenvironments in the Barents Sea. *Global and Planetary Change*. 2002, 34 (3-4): 69-78. Lubinski D.J., Polyak L., Forman S.L. Freshwater and Atlantic water inflows to the deep northern Barents and Kara seas since ca 13 14C ka: foraminifera and stable isotopes. *Quat. Sci.Rev*, 2001, 20: 1851-1879.
- Murdmaa I.O., Ivanova E.V., Duplessy J.C., et al. Facies System of the Central and Eastern Barents Sea since the Last Glaciation to Recent. *Mar.Geology*, 2006, 230 (3-4): 273-303.
- Pfirman S.L., Bauch D., Gammelsrod T. The Northern Barents Sea: Water mass distribution and Modification. In: *The Polar oceans and their role in shaping the global environment*. AGU Geophys. Monogr., 1994, V. 85: 77-94.
- Risebrobakken B., Moros M., Ivanova E., Chistyakova N., Rosenberg R. Holocene climate extremes in the south-western Barents Sea (in prep.).
- Sarnthein M., van Kreveld S., Erlenkeuser H., Grootes P. M., Kucera M., Pflaumann U., Schulz M. Centennial-to-millennial-scale periodicities of Holocene climate and sediment injections off the western Barents shelf, 75°N. *Boreas*, 2003, 32: 447-461.
- Slubowska M.A., Koç N., Rasmussen T.L., Klitgaard-Kristensen D. Changes in the flow of Atlantic water into the Arctic Ocean since the last deglaciation: Evidence from the northern Svalbard continental margin, 80°N. *Paleoceanography* 2005, 20, doi:10.1029/2005PA001141.
- Vinje T., Kvambekk E.S. Barents Sea drift ice characteristics. *Polar Res.*, 1991, 10: 59 - 68.

**WORKSHOP ON
GEOLOGY & GEOPHYSICS**

SESSION 2

**GEOLOGY & GEOPHYSICS IN
ANTARCTICA**

**JAPANESE MARINE GEOPHYSICAL AND GEOLOGICAL RESEARCH
ACTIVITIES
IN THE ANTARCTIC OCEAN**

Yoshifumi Nogi¹, Hideki Miura¹, Minoru Ikehara², Nobukazu Seama³

¹National Institute of Polar Research, Tokyo, Japan
nogi@nipr.ac.jp

²Center for Advanced Marine Core Research, Kochi University, Kochi, Japan

³Research Center for Inland Seas, Kobe University, Kobe, Japan

Marine geophysical and geological research in the Indian Ocean sector of the Antarctic Ocean is vital to understanding the process of Gondwana fragmentation and also essential for revealing change in paleoenvironment due to seafloor spreading. Marine geophysical data, such as magnetic anomalies, have been obtained in the Southern Indian Ocean by the Japanese Icebreaker under the JARE (Japanese Antarctic Research Expedition). New constraints for the seafloor spreading process during the Initial Gondwana breakup are presented by those data, and complicated seafloor spreading history are suggested.

In February 2008, the R/V Hakuho-maru cruise KH-07-4 Leg3 have been carried out in the Southern Indian Ocean between Cape Town, South Africa, and off Lützow-Holm Bay, Antarctica. Swath bathymetry, gravity and magnetic anomaly data are also obtained during the cruise, although the R/V Hakuho-maru is not ice capable vessel. These data mostly support new seafloor spreading history estimated from the data obtained by Japanese Icebreaker, and provide new constraints for the fragmentation process of the Gondwana. Sediment core samplings are also performed during the KH-07-4 Leg3 cruise to understand mechanisms and processes of sub-systems in the Antarctic Cryosphere. Three sediment cores have been collected from the Conrad Rise, the Gunnerus Ridge and off Lützow-Holm Bay.

Concerning the area covered by sea ice, gravity corer were used to obtain the sediment cores under the sea ice during the JARE47 in Lützow-Holm Bay where Japanese Antarctic Station, Syowa, situated. However, long sediment cores more than about 1m have never been acquired, possibly due to ice rafted debris, even though heavy weight were used for gravity corer. Therefore, we are now developing rotary coring system, which is operational from Icebreaker and assembled on the seafloor, to penetrate more than 1m and get long sediment cores. Marine geophysical and geological surveys under sea ice using AUV and ROV are also planed in the next phase of the JARE in cooperation with JAMSTEC.

New Icebreaker Shirase will be in service in 2009, this year. She equips newly with the multi narrow beam echo sounder. Swath mapping, gravity and magnetic anomaly measurements will be conducted on her route. Marine geophysical and geological surveys in the Southern Indian by the R/V Hakuho-maru are also scheduled during 2010-2011 season. We will present marine geophysical and geological activities including future plan, such as mantle imaging by marine electromagnetic survey, and hydrothermal vent research activities in Japan will also be briefly introduced.

**BROADBAND SEISMIC DEPLOYMENTS IN EAST ANTARCTICA:
IPY CONTRIBUTION TO UNDERSTAND EARTH'S DEEP INTERIOR
- AGAP/GAMSEIS -**

Masaki Kanao¹, Douglas Wiens², Satoru Tanaka³, Andrew Nyblade⁴, and Seiji Tsuboi³

¹ National Institute of Polar Research, Research Organization of Information and Systems, 1-9-10 Kaga, Itabashi-ku, Tokyo, 173-8515, Japan
kanao@nipr.ac.jp

² Dept. of Earth and Planetary Sciences, Washington University, St. Louis MO 63130 USA

³ Institute for Research on Earth Evolution, Japan Agency for Marine-Earth Science and Technology, 2-15 Natsushima-cho Yokosuka 237-0061, Japan

⁴ Dept. of Geosciences, Pennsylvania State University, University Park, PA 16802 USA

INTRODUCTION

Existing permanent seismic stations belonging to the Federation of Digital Seismographic Network (FDSN) allows resolution of the structure beneath Antarctica at a horizontal scale of 1000 km, which is sufficient to detect fundamental differences in the lithosphere beneath East-West Antarctica, but not to clearly define the structure within each sector. While, observation of seismicity around the Antarctic is limited by the sparse station distribution and the detection level for earthquakes remains inadequate for full evaluation of tectonic activity (Reading, 2002). In addition to lithospheric studies, the observed teleseismic waveforms have advantages in investigating the deeper part of Earth's interior such as lower mantle, D" layers, the core-mantle boundary (CMB) and the inner core as they are effectively a large span array located in the southern high latitude.

The justification for developing broadband arrays addresses both the unique aspects of seismology and general issues that would be common to global Earth sciences; for example: - lithospheric dynamics in an ice-covered environment;- how lithospheric processes drive and may be driven by global environmental change (sea level, climate);- the scale and nature of rifting as a process that has shaped the continent and dominated its evolution;- the role of Antarctica as the keystone in the super-continent formation and break-up throughout Earth's history;- how the tectonic and thermal structure of the Antarctic lithosphere affect current ice sheet dynamics;- age, growth, and evolution of the continent and processes that have shaped the lithosphere;- the effect of improved seismic coverage on global models of the lithosphere, together with deep interior of the Earth.

The International Polar Year 2007-2008 provides a good opportunity to make significant advances in seismic array deployment to achieve these science targets.

SIGNIFICANT ADVANCE AT IPY

Discussions at the SCAR / ANTEC (Siena, Italy, 2001) and SEAP (Structure and Evolution of the Antarctic Plate, Boulder, Colorado, 2003) workshops have led to the development of a strategy to improve our knowledge of the Antarctic by using broadband deployments. The originally named ‘Antarctic Arrays’ is an ambitious program to improve seismic instrumentation on and around the Antarctica (<http://www.antarcticarrays.org>). A science plan designed to improve the understanding of the Antarctic Plate with this array deployment had been developed prior to the initiation of the IPY when it was transferred into the chief category of the ‘POLER observation NETWORK (POLENET)’ (IPY project #185).

The original idea of ‘Antarctic Arrays’ strategy has several components, including 1) process-oriented experiments such as 3D-arrays; 2) evolving regional arrays; and 3) an enhanced permanent backbone network. The strategy of attaining a sufficient density of stations (20-30) in symmetrically disposed sectors of the continent allows optimal ray path coverage across Antarctica and improves tomographic resolution (Ritzwoller, et al., 2001).

Several temporary field broadband experiments have been carried out in the past a decade around continental marginal areas of Antarctica (e.g., Bannister and Kennett, 2002; Muller and Eckstaller, 2003; Reading, 2003; Robertson, et al., 2002; Kanao et al., 2002). The broadband monitoring observations at several outcrops around the LHB area also contribute to the improvements of spatial resolution of the stations in Antarctica over the marginal part of Eastern Dronning Maud Land.

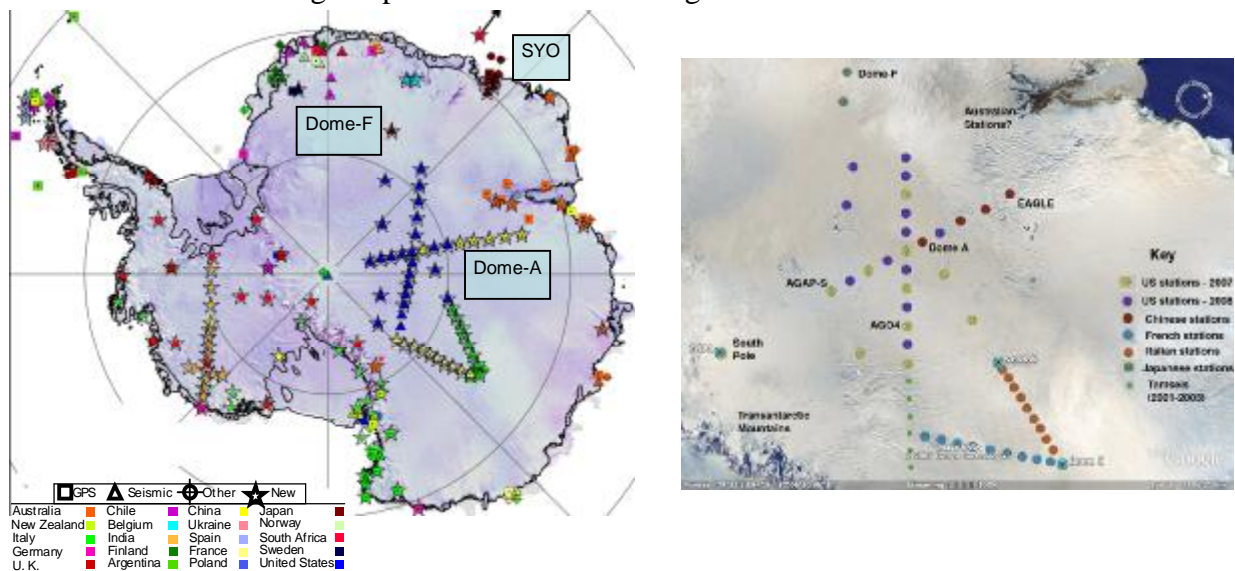


Fig. 1 Distribution map of stations during IPY 2007-2008 (left; whole continent; POLENET, right; East Antarctica; AGAP/GAMSEIS)

FIELD ACTIVITIES

The main field area targeted by the Japanese contribution is Eastern Dronning Maud Land - Enderby Land, East Antarctica. Several distinctive geophysical observations that reveal structure and evolution of this area have been made by Japanese Antarctic Research Expedition (JARE) in the last few decades. By carrying out broadband deployments on this area, more detailed signatures can be obtained concerning tectonics and structure from lithosphere to ascenosphere, together with heterogeneous characteristics of deep interior of the Earth.

A northern part of the Eastern Dronning Maud Land, particular from Mizuho Plateau to Dome-F area, would be the most plausible place with enough logistical support to make a deployment of the portable seismic stations. The temporary stations along the inland traverse routes on the continental ice-sheet on the Plateau would be installed for the IPY periods by using snow terrain vehicles with support from aircraft. These temporary observation stations, that have long-term batteries and large capacity digital data-loggers, can be utilized for the other science purposes, such as geophysical, meteorological, glaciological and biological studies.

The 'Antarctica's Gamburtsev Province / Gamburtsev Mountain SEISmic experiment (AGAP / GAMSEIS) (IPY project # 147)' project, in contrast, is an internationally coordinated deployment of 25-35 broadband seismographs over the crest of the Gambursev Mountains (Dome-A area). The proposed seismological investigations would provide detailed information on crustal thickness and mantle temperatures and thus provide key constraints on the origin of the Gamburtsev Mountains, and more broadly on the structure and evolution of the entire East Antarctic craton. Understanding the origin of the Gamburstev Mountains and the structure of the East Antarctic craton is also vitally linked to other first-order problems, such as the geological history of East Antarctica, the role of its topography and heat flow on Earth's climate and glacial history, and the geophysical and geological controls on subglacial lakes.

STUDY OF THE DEEP INTERIOR

In addition to the crust – upper mantle studies, the teleseismic waveforms observed with the GAMSEIS have a great advantage for investigating the deep Earth interior, such as the lower mantle, the D" region and the CMB by using the seismographs as a large aperture array located in the southern high latitude. Many earthquakes will be observable at the GAMSEIS planned area. The epicentral distance range from 60° to 90° would be especially suitable for the observation of the D" reflected phases as well as the core reflected phases of ScS and PcP. That from 90° to 130° would be appropriate for the observation of the core diffracted phases of Pdiff, and Sdiff, and a core phase of SKS. So far we have only a few regions in the southern hemisphere where the deep mantle structure has been examined in detail. Thus a new broadband observation program in Antarctica is expected to be an important opportunity to get valuable data.

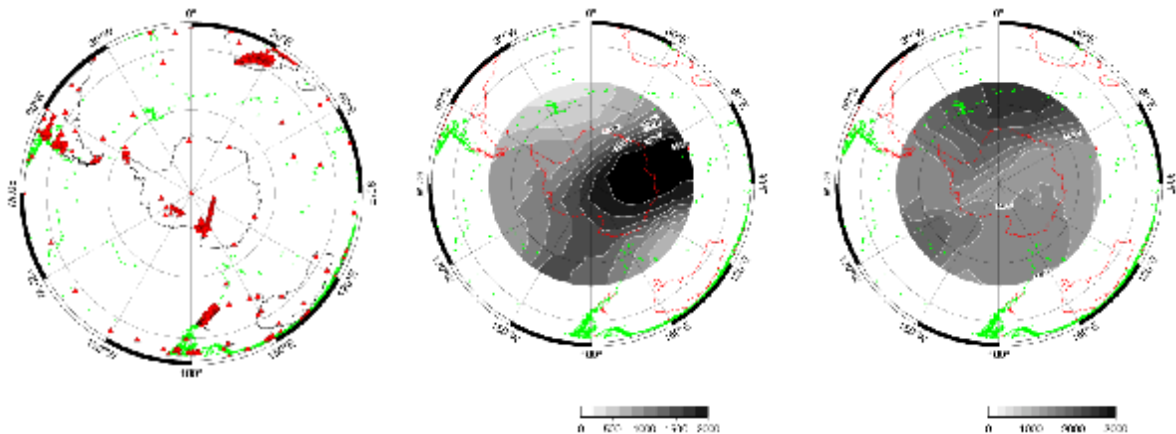


Fig. 2 (left) Distribution map of the permanent and temporary stations in Antarctica (red color; from IRIS/DMS and PASSCAL). Hypocentral data collected in 1990-2004 (green color). Maps of observable earthquake numbers for the epicenter distances of 60°-90° (central), 90°-130° (right), respectively. Gray scales show the earthquake numbers that are counted at each location using an earthquake list for the period from 1990 to 2004.

INTERNATIONAL COLLABORATION

The broadband deployment project is endorsed by several national Antarctic committees and contribute to individual international program of ‘TransAntarctic Mountain SEISMic experiment (TAMSEIS; Lawrence, et al., 2006)’, ‘AGAP / GAMSEIS (IPY project # 147)’ and ‘POLENET (IPY project #185)’ during the IPY 2007-2008. The data set observed during the IPY will be initially stored and available for all the related cooperatives and the other geo-scientists by Internet service from the data library server of the National Institute of Polar Research (POLARIS system). Then it will immediately be offered to the world data centers of seismology, such as Incorporated Research Institute of Seismology / Data Management System (IRIS/DMS), FDSN/ GSN, PACIFIC21 centers. The web-pages are available in general and also contribute to the Joint Committee on Antarctic Data Management / Antarctic Master Directory (JCADM/AMD).

REFERENCES

- Bannister, S., and B. L. N. Kennett (2002), Seismic Activity in the Transantarctic Mountains - Results from a Broadband Array Deployment. *Terra Antarctica*, 9, 41-46.
- Kanao, M., A. Kubo, T. Shibutani, H. Negishi and Y. Tono (2002), Crustal structure around the Antarctic margin by teleseismic receiver function analyses, Gamble J.A., Skinner D.N.B. and Henrys S. (eds) *Antarctica at the close of a millennium*, Royal Society of New Zealand Bulletin 35, 485-491.
- Lawrence, J. F., D. A. Wiens, A. A. Nyblade, S. Anandakrishan, P. J. Shore, and D. Voigt (2006), Upper mantle thermal variations beneath the Transantarctic Mountains inferred from teleseismic S-wave attenuation. *Geophys. Res. Lett.*, 33, L03303, doi:10.1029/2005GL024516.

- Muller, C., and A. Eckstaller (2003), Local seismicity detected by the Neumayer seismological network, Dronning Maud Land, Antarctica: tectonic earthquakes and ice-related seismic phenomena. IX Intern. Sympo. Antarc. Earth Sci. Programme and Abstracts, 236.
- Reading, A. M. (2002), Antarctic seismicity and neotectonics. Antarctica at the close of a millennium. ed. by J. A. Gamble et al. Wellington, The Royal Soc. of New Zealand Bull., 35, 479-484.
- Reading, A. M. (2003), The SSCUA broadband seismic development, East Antarctica. IX Intern. Sympo. Antarc. Earth Sci. Programme and Abstracts, 270.
- Ritzwoller, M. H., N. M. Shapino, A. L. Levshin, and G. M. Leahy (2001), Crustal and upper mantle structure beneath Antarctica and surrounding oceans. J. Geophys. Res., 106, 30645-30670.
- Robertson, S. D., D. A. Wiens, P. J. Shore, G. P. Smith, and E. Vera (2002), Seismicity and tectonics of the South Shetland Islands and Bransfield Strait from the SEPA broadband seismograph deployment. Antarctica at the close of a millennium, ed. by J. A. Gamble et al. Wellington, The Royal Soc. of New Zealand Bull., 35, 549-554.

INVESTIGATION OF THE DEEP EARTH, FROM ANTARCTICA

Genti Toyokuni¹, Hiroshi Takenaka², Masaki Kanao¹

¹National Institute of Polar Research, Research Organization of Information and Systems, Tokyo, Japan
toyokuni.genchi@nipr.ac.jp

²Department of Earth and Planetary Sciences, Faculty of Sciences, Kyushu University, Fukuoka, Japan

We provide a numerical method for accurate and efficient computations of global seismic wavefield which will be a powerful tool for inverting observed seismic data from Antarctica to investigate the Earth's deep interior. Antarctica is ideally located for observations of deep Earth structures such as the inner core due to its weak seismicity, wide extent, and novelty of the data. Approved projects of the IPY 2007-2008 such as the POLENET and AGAP/GAMSEIS have been installing broad-band seismographs on intra-Antarctic region, which will provide unique observational results exploiting the vantage points of Antarctica.

In cooperation with such high-quality data, images of the Earth's interior can be obtained through waveform inversion, a method to detect structures by minimizing residuals between observed and synthetic seismograms. The inversion method iteratively calculates synthetic seismograms as for the structural model changed each time, so that it requires an accurate and computationally efficient method for numerical computation of seismic waveforms.

A traditional approach suited this requirement is the axisymmetric modeling. It assumes the structure to be axisymmetric with respect to the axis through a seismic source and solves the elastodynamic equation in spherical coordinates on a cross section of the Earth. The only drawback of this approach is restriction on structural models and seismic sources within axisymmetry. We had, therefore, extended the traditional axisymmetric approach for arbitrary asymmetric structures and moment-tensor sources, developing numerical schemes with the finite-difference (FD) method. Our FD scheme had also incorporated the anelastic attenuation for the first time for axisymmetric global FD computation of seismic wavefield in spherical coordinates.

This time, we have succeeded in introducing the Earth's center, a singularity point of equations in spherical coordinates. It enables to simulate realistic seismic wave propagation on a whole cross section of the Earth including the core passing phases. We show several numerical examples to demonstrate validity and feasibility of our scheme in this presentation.

HYDROACOUSTIC MONITORING IN THE SCOTIA SEA, ANTARCTICA

Won Sang Lee¹, Minkyu Park¹, Robert P. Dziak², Haru Matsumoto², DelWayne R. Bohnenstiehl³, Joseph H. Haxel², f Yun¹

¹ Polar Environmental Research Division, Korea Polar Research Institute, Incheon 406-840, Republic of Korea

² Oregon State University, NOAA Cooperative Institute for Marine Resources Studies, Newport, Oregon 97365-5258, USA

³ Department of Marine, Earth and Atmospheric Sciences, North Carolina State University, Raleigh, North Carolina 27695-8208, USA

Since December 2005, KOPRI and OSU/NOAA have collaboratively operated an Autonomous Underwater Hydrophone (AUH) array in the Southern Ocean, mostly in the Bransfield Strait, Antarctica. During the period, however, from December 2007 to February, we moored five AUHs in the Scotia Sea to monitor seismicity and ice-related signals in the vicinity of the South Sandwich Islands. The array takes advantage of the efficient propagation of sound in the oceans to detect, locate and analyze the temporal and spatial distribution of small- to moderate-size earthquakes and cryospheric sounds along the study region. A total of 793 earthquakes were identified from an automated-detection-association algorithm during the mooring period. In this presentation, we will show our preliminary analysis of hydroacoustic observation and discuss tectonics in the Scotia Sea.

**WORKSHOP ON
GEOLOGY & GEOPHYSICS**

SESSION 3

**TECTONICS AND MAGMATISM
AT POLAR RIDGES**

RECENT PROGRESS IN MID-OCEAN RIDGE RESEARCH IN CHINA

John Chen¹ and Jiabiao Li²

¹InterRidge China Office
School of Earth and Space Sciences, Peking University, Beijing, 100871, China
johnyc@pku.edu.cn

²The Second Institute of Oceanography, SOA, Hangzhou, China

We report significant recent progress in China in mid-ocean ridge research. China joined the InterRidge, an interdisciplinary international science program, as an Associate Member in 2003, following the 1st InterRidge workshop in China in October 2003. In 2007, China became an InterRidge Principal Member, the first from a developing country. Rapid advances in multi-disciplinary deep-sea research in China are reflected in the following highlights of recent cruises and other activities.

THE FIRST AROUND-THE-GLOBE EXPEDITION IN 2005

The first around-the-globe marine geoscience expedition by a modern Chinese research ship was conducted in 2005 and early 2006. The 297-day expedition travelled more than 40,000 nautical miles in the Pacific, Atlantic, and Indian Oceans. The expedition was organized and funded by the China Ocean Mineral Resources R & D Association (COMRA) and was carried out on its research ship R/V *DaYangHiHao* (meaning "Ocean #1"). The goal of the expedition was to survey and investigate regions of abundant manganese nodules and cobalt-rich ferromanganese crusts in the western and central Pacific Ocean, as well as to collect samples of hydrothermal deposits and to search for new hydrothermal vents along mid-ocean ridges in the eastern Pacific Ocean, the Atlantic Ocean, and the Indian Ocean. R/V *DaYangYiHao* is a well-maintained modern research ship. It has a weight capacity of 5,600 tons, measures 105 meters in length, and is equipped with a ship dynamic positioning control system and a variety of geophysical, geological, and microbiological instruments. Out of the six legs in the 2005-2006 around-the-globe expedition, two legs (cruise DY105-17A) were devoted to COMRA's cooperative projects with international institutions. The first was a China-US cooperative leg to investigate hydrothermal vents on the East Pacific Rise (EPR). The second was a China-US-Germany cooperative leg to investigate hydrothermal vent processes of the Southwest Indian Ridge and Central Indian Ridge.

The EPR leg successfully collected samples of hydrothermal deposits near the EPR 13°N region using a Chinese built TV-guided grab and recovered relic hydrothermal-vent chimney fragments. A significant accomplishment of the leg was the discovery, for the first time, of strong evidence for active water column plumes on the EPR immediately south of the equator (Chen et al., 2006). This discovery was made during a comprehensive water column survey program using six MAPR (Miniature Autonomous Plume Recorder) instruments from Dr. Ed Baker of NOAA/PMEL. A WHOI built deep-tow magnetometer was also used in the cruise surveys.

The Indian Ocean leg conducted comprehensive survey of water columns along the ultraslow spreading Southwest Indian Ridge (SWIR) and the Central Indian Ridge (CIR), which is of intermediate spreading rate. Along the CIR, the cruise surveyed and imaged the Kairei and Edmond hydrothermal vent sites and collected hydrothermal deposit samples. A survey program was also conducted along the CIR between the Kairei and the Edmond hydrothermal vent sites to measure water column anomalies using the MAPR sensors and the METS instrument (Zhu et al., 2008). Along the Southwest Indian Ridge, the cruise discovered, for the first time, a region of major hydrothermal plume anomalies on a ridge segment west of the Gallieni Fracture Zone. The measured turbidity anomalies by the MAPR instruments were by far the strongest known anomalies along the SWIR (*Guo and Han, 2006; Lin and Zhang, InterRidge News, vol. 15, pp. 33-34, 2006*). This cruise led to a 2007 cruise that imaged the first black smoker on the SWIR.

DISCOVERY OF THE FIRST ACTIVE VENT FIELD ON THE ULTRASLOW SPREADING SOUTHWEST INDIAN RIDGE (SWIR) IN 2007

Two 2007 cruises on board the Chinese research vessel R/V *DaYangYiHao* have successfully located and investigated the first active hydrothermal vent field along the ultraslow spreading SWIR and collected hydrothermal sulfide deposit samples. The discovered active vent field is located on the western end of a magmatically robust spreading segment immediately west of the Gallieni transform fault. The vent field was precisely located, mapped, and photographed in great detail in February-March 2007 using WHOI's autonomous underwater vehicle ABE. A high-resolution bathymetric map, more than 5,000 near-bottom color photos, and several types of water column data were all obtained during three phases of ABE dives. Within the approximately 120-m-long by 100-m-wide hydrothermal field, three groups of active high-temperature vents were identified and color images of black smokers and associated biological communities were obtained. Hydrothermal sulfide deposits were then successfully obtained using a TV grab (Tao et al., *InterRidge News*, <http://www.interridge.org/node/4897> 2007; *Oceanus* article by K. Kusek, <http://www.who.edu/oceanus/viewArticle.do?id=26106§ionid=1021>). In 2007, R/V *DayangYihao* also surveyed the SWIR further east and identified evidence of new hydrothermal deposit sites (Han, <http://interridge.who.edu/RidgeCrestNews>). Multi-leg cruises including OBS experiments are planned to return to the SWIR in the coming years to conduct multi-disciplinary studies.

THE FIRST CHINESE EXPEDITION TO LAU BASIN AND SOUTHEAST INDIAN RIDGE (SEIR)

In 2007, Chinese scientists on board R/V *DaYangYiHao* also conducted a month-long cruise to the back-arc spreading center at Lau Basin. A new active hydrothermal vent field was detected with a deep-tow video system along the spreading center between two known sites. In January 2007, a strong hydrothermal plume was also detected at the segment K on the Southeast Indian Ridge by a Chinese expedition, about 250-km southeast of the St. Paul-Amsterdam hotspot. This plume is near the hydrothermal plume detected at this segment 10 years ago.

NEW HYDROTHERMAL VENT FIELDS DISCOVERED ON THE EQUATORIAL SOUTHERN EAST PACIFIC RISE (SEPR) IN 2008

Chinese scientists and a WHOI team successfully completed a 25-day research cruise in Aug- Sept 2008 on board R/V *DayangYihao* to the SEPR near the equator. The joint cruise was equipped with WHOI's ABE vehicle. This expedition follows the work of a 2005 expedition by R/V *DayangYihao*, during which strong water column turbidity anomalies were measured in the region. Several new high-temperature hydrothermal vent fields were discovered along the SEPR ridge axis and on an off-axis seamount located between 1.4°S to 2.2°S. A significant portion of the hydrothermal activity at the ridge axis appears to be concentrated along the edges of a seafloor fissure system. High-resolution bottom bathymetry, deep-tow magnetics, color photography, water column data, as well as hydrothermal sulfide deposit samples were obtained during the cruise (*Tao et al.*, 2008; <http://www.interridge.org/node/5703>).

OTHER ACTIVITIES

The Qingdao Ocean Sciences Summer School on "International Advances in Geo-Biological Research" was held in Qingdao, China, July 14-20, 2008. Several InterRidge scientists helped to co-organize this well-attended summer school and gave lectures (<http://www.interridge.org/node/5580>).

Chinese scientists also co-organized and contributed abstracts to a special session on "Recent multidisciplinary studies of mid-ocean ridges and ophiolites", 5th Asia Oceania Geosciences Society Conference, Busan, Korea, June 17, 2008 (<http://www.interridge.org/node/4893>).

The recent rapid progress in mid-ocean ridge and exploration by the Chinese science community mark a milestone event in Chinese programs of ocean research and exploration of ocean mineral resources. It reflects China's increasing contributions to international ocean ridge research since China became an InterRidge Associate Member nation in late 2003. It is anticipated that China will play an increasingly important role in mid-ocean ridge research and exploration in the coming years and will continue to strengthen its cooperation with the InterRidge program and the international community.

SOUTHEAST INDIAN OCEAN-RIDGE EARTHQUAKE SEQUENCES FROM CROSS-CORRELATION ANALYSIS OF HYDROACOUSTIC DATA

Sukyoung Yun^{1,2}, Sidao Ni³, Minkyu Park² and Won Sang Lee²

¹SEES, Seoul National University, Seoul, Korea

²Korea Polar Research Institute, Incheon, Korea

³Mengcheng National Geophysical Observatory, University of Science and Technology of China, Hefei, Anhui, China

ABSTRACT

Parameters of earthquake sequences, for instance location and timing of foreshocks and aftershocks, are critical for understanding dynamics of mid-ocean ridge and transform faults. Whole sequences including small earthquakes in the ocean cannot be well recorded by land-based seismometers due to large epicentral distances. Recent hydroacoustic studies have demonstrated that T-waves are very effective in detecting small submarine earthquakes because of little energy loss during propagation in Sound Fixing and Ranging channel. For example, an M_w 6.2 (2006/03/06, 40.11°S/78.49°E) transform-fault earthquake occurred at the Southeastern Indian Ocean Ridge, but National Earthquake Information Center only reported three aftershocks in the first following week. We applied cross-correlation method to hydroacoustic data from the International Monitoring System arrays in the Indian Ocean to examine the whole earthquake sequence. We detected 14 aftershocks and none foreshock for the earthquake and locations of these aftershocks show an irregular pattern. From the observation, we suggest that the feature could be caused by complicated transcurrent plate-boundary dynamics between two overlapped spreading ridges, which is possibly explained by the bookshelf faulting model.

GENERATION OF ²³¹PA, ²²⁶RA, ²³⁸U, AND ²³⁰TH EXCESSES IN ARCTIC MID-OCEAN RIDGE BASALTS FROM THE KOLBEINSEY, MOHNS, KNIPOVICH, AND GAKKEL RIDGES

L.J. Elkins¹, K.W.W. Sims¹, J. Prytulak², J. Blichert-Toft³, J. Blusztajn¹, S. Fretzdorff⁴, K. Haase⁵, T. Elliott², S. Humphris¹, J.-G. Schilling⁶

¹ Woods Hole Oceanographic Inst., Woods Hole, MA, USA

ksims@whoi.edu

² University of Bristol, Bristol, UK

³ l'École Normale Supérieure de Lyon, Lyon, France

⁴ Division of marine science, BMFT, Rostock, Germany

⁵ GeoZentrum Nordbayern, Erlangen, Germany

⁶ Univ. Rhode Island, Narragansett, RI, USA

We present U-Th-Pa-Ra isotopic data for mid-ocean ridge basalts (MORB) from the slow- to ultraslow spreading Kolbeinsey, Mohns, Knipovich, and Gakkel Ridges. In general, in Arctic MORB we find variable radiogenic and U-series isotope signals. All Arctic samples have (²³¹Pa/²³⁵U) excesses, in keeping with observations from global MORB. MORB from Kolbeinsey R. have uniformly high ²³⁰Th excess for a narrow range of (²³⁰Th/²³²Th) and formed in a long, deep, homogeneous mantle melting column. A relatively uniform degree of ²³⁰Th-²³⁸U disequilibrium is observed for isotopically enriched Kolbeinsey R. samples north of 70.6°N, the Mohns R., and the Knipovich R. (mean (²³⁰Th/²³⁸U) = 1.17 ± 6%). Age-constrained ((²²⁶Ra/²³⁰Th) values out of equilibrium) samples from Mohns R. cluster with mean (²³⁰Th/²³⁸U)=1.22, while both Knipovich R. samples and three samples from the Kolbeinsey R. north of 70.6°N form sloped arrays on a (²³⁸U/²³²Th) vs. (²³⁰Th/²³²Th) diagram (slopes of 1.0 and 1.9, respectively). Position on these arrays correlates with radiogenic isotope compositions (e.g. ⁸⁷Sr/⁸⁶Sr and ¹⁴⁷Nd/¹⁴⁴Nd), suggesting the influence of mantle source heterogeneities in this region. In contrast, on the ultraslow-spreading end member Gakkel R., we find homogeneous MORB from the 85°E volcano on the Eastern Volcanic Zone, with depleted radiogenic isotopic signatures (e.g. mean ⁸⁷Sr/⁸⁶Sr=0.702612±1) and age-constrained (²³⁰Th/²³⁸U) ranging from small (5%) ²³⁰Th excesses to small ²³⁸U excesses (5%). Gakkel R. (²²⁶Ra/²³⁰Th) and (²³⁰Th/²³⁸U) lie along a global negative correlation, supporting their production by mixing of melts from different depths.

Globally, mean (²³⁰Th/²³⁸U) vs. axial ridge depth lies on a negative correlation, supporting a global mantle temperature and peridotitic melting control on generation of U-Th disequilibrium in MORB. The variance of (²³⁰Th/²³⁸U) ratios in MORB formed by individual ridge segments result from variables such as melting of heterogeneous mantle sources.

GRAVITY ANOMALY COMPARISON OF SUBDUCTION ZONES IN THE WESTERN PACIFIC

Yoon-Mi Kim and Sang-Mook Lee

School of Earth and Environmental Sciences, Seoul National University, Seoul 151-747, Korea

The western Pacific is a key area to investigate subduction zones at different evolutionary stages. Among them, Izu-Bonin-Mariana and Tonga-Kermadec trenches are considered as well-developed or mature subduction zones, and Yap, Mussau and Hjort trenches constitute the young, incomplete or ultraslow-member in the spectrum of subduction evolution. We used satellite-derived gravity data to compare the two end-members, mature and immature subduction zones. The isostatic residual gravity anomaly shows that the width of non-isostatically-compensated region of the mature subduction zones is substantially wider than that of immature ones. When the gravitational effect due to the seafloor is removed from the free-air gravity anomaly, a large difference exists between the mature and immature subduction zones in the overriding plate side. Unlike immature subduction zones, mature ones show a low gravity anomaly of ~200-250 mGals at distances of 150-200 km from the trench in the overriding plate. We discuss the possible causes of the low gravity anomaly including: (1) the serpentinization in the upper mantle; (2) the presence of partial melt in the mantle wedge; (3) the difference in the density structure between the overriding and subducting plates caused by difference in slab age and thermal structure with and without compositional stratification between crust and mantle; and (4) the anomalous crustal structure of the arc. Serpentinization alone cannot explain the low gravity anomaly because its location does not match with the pattern of low gravity anomaly. Our simple calculation shows that despite the uncertainty in its degree and extent, the presence of the partial melting in the mantle wedge cannot be a major source of the low gravity anomaly. Also, the difference of gravity anomaly due to the difference in density structure reflecting temperature difference is insufficient to account for the total anomaly. The sinking of lighter crustal material into the mantle can produce a negative gravity anomaly of ~100 mGal, however, the location of this anomaly does not match the observed gravity anomaly. It seems that the total difference cannot be explained without considering the density contrast between crust and mantle. With acquisition of information on deep crust and upper mantle structure and property, gravity data is expected to provide a better constraint on the evolution of subduction system.

ANALYSIS OF THE SEISMICITY IN THE ANTARCTIC PLATE BY THE STATISTICAL METHOD

Tetsuto Himeno¹, Masaki Kanao¹

¹ National Institute of Polar Research, Research Organization of Information and System, Tokyo, Japan
himeno.tetsuto@nipr.ac.jp

A large earthquake (M 8.0) occurred in the Balleny Islands region (62.877°S, 149.527°E) around Antarctic plate on March 25, 1998. Before the occurrence of this earthquake, the earthquake with a magnitude more than 4.0 rarely occurred around this region. But many earthquakes are observed around this region after March 25, 1998. Therefore, we consider that the change of the Antarctic plate occurred.

We use observation data which occurred in the region bounded by 120°E and 180°E meridians and 50°S and 80°S parallels and with a depth less than 100km for the period 1980-2006. For examine the frequency of these earthquakes, we use the Gutenberg-Richter magnitude-frequency relation. The relation is as follows

$$\log n(M) = a - bM,$$

where $n(M)$ denotes the number of earthquakes with a magnitude more than M , and a and b are constants depending on the group of earthquakes considered. By this relation, the plot of $\log n(M)$ should fit the straight line. From the plot, we saw that there are few earthquakes with a magnitude less than 4.0. Thus, we analyze the earthquakes with a magnitude more than 4.0.

The number of earthquake increase in the Balleny Islands region after March 25, 1998. So, we compare b -value to verify this change. The b -value is a constant parameter of the Gutenberg-Richter magnitude-frequency relation. This value is derived by the maximum likelihood method. By the comparison of b -value, we see that the Balleny earthquake causes the change of seismicity around not only the Balleny earthquake region but also other region.

We also use the statistical method which is called Epidemic Type Aftershock Sequence (ETAS) model. This model is a point process representing the activity of earthquakes of magnitude M_0 and larger in a region during a period of time. This model includes background activity of constant occurrence rate μ in time and also includes aftershock activity. The aftershock activity is represented by the modified Omori formula. In this method, the frequency of earthquake at time t is represent by

$$m + \sum_{t_j < t} e^{a(M_j - M_c)} \frac{K}{(t - t_j + c)^p},$$

where μ , a , K , c and p are constant parameter and (t_j, M_j) denote time and magnitude of earthquake which occur before time t . We examine the time change of the activity of earthquakes by ETAS model.

On the other hand, we see that Balleny earthquake cause the change of the activity of earthquake in extensive region. Thus, we use the space-time ETAS model and examine the space change.

**THE TECTONIC EVOLUTION OF THE PACIFIC-ANTARCTIC RIDGE,
RECENT CHANGES IN PLATE MOTION, INTRAPLATE TECTONICS AND
AXIAL MORPHOLOGY**

Louis Géli¹, H el ene Ondr eas¹, Laure Dosso², Frauke Klingelhoefer¹, Anne Briais³,
Daniel Aslanian¹ and the Pacantartic^{1&2} Groups

¹Marine Geosciences Department, BP 70, 29280, Plouzan e, France

²CNRS/IUEM, UMR6538, 1 Place Copernic, 29280 Plouzan e, France

³LEGOS-GRGS, CNRS UMR 5566, 18 Ave E. Belin, 31401 Toulouse, France

Anne.Briais@ntp.obs-mip.fr

Due to the proximity of the Euler pole of rotation between the Pacific and Antarctic plates, the spreading rate at the Pacific-Antarctic Ridge (PAR) increases rapidly from 54 mm/yr near Pitman Fracture Zone (FZ) up to 76 mm/yr near Udintsev FZ, resulting in three domains of axial morphology: an axial valley south of Pitman FZ, an axial high north of Saint Exup ery FZ, and in between, the transitional domain extends over 650 km. It comprises sections of ridge with an axial valley or an axial high and generally displays a very low cross-sectional relief. It is also characterized by two propagating rifts. Two domains of different seafloor roughness appear south of Udintsev FZ: east of 157 W these two domains are separated by a 1000-km V-shaped boundary. West of 157 W, the boundary approximately coincides with Chron 3a or Chron 4. The southward migration of the transitional area during the last 35 Myr explains the V-shaped boundary: (1) increases in spreading rate above a threshold value produced changes in axial morphology; and (2) in the transition zone, rotations of the spreading direction were accommodated by the plate boundary, either by rift propagation or by transitions from fracture zones to non transform discontinuities, leaving trails on the seafloor that presently delineate the V. North of the Udintsev FZ, small kinematic changes in plate motions also play a key role, producing deformation processes and off-axis, oblique volcanic structures, such as the Hollister Ridge, located between the Udintsev FZ and the Eltanin FZ, and conjugated volcanic alignments on both parts of the Menard FZ.

**WORKSHOP ON
CLIMATE CHANGE
AND
POLAR OCEAN SYSTEM**

SESSION 1

THE SOUTHERN OCEAN

POLARSTERN: OPERATION OF AN ICEBREAKING MULTI-PURPOSE RESEARCH VESSEL IN THE ARCTIC AND ANTARCTIC

Eberhard Fahrbach¹

¹Alfred-Wegener-Institut für Polar- und Meeresforschung in der Helmholtz-
Gemeinschaft, Bremerhaven, Germany
eberhard.fahrbach@awi.de

The German multi-purpose icebreaking research vessel *Polarstern* was put into service in 1982. It is run by the Alfred-Wegener-Institut (AWI) and provides the possibility to the national and international polar research community to carry out marine research in both polar areas. It has to serve to the research programmes of universities sponsored by the Deutsche Forschungsgemeinschaft and the research programme of the Helmholtz Association of German Research Centres of which the Alfred-Wegener-Institut is a member. It provides berths and research facilities for 55 scientists and spends on average 320 days per year at sea. In addition to marine research *Polarstern* has to assure the supply of the Neumayer Station and support field work in Antarctica. The austral summer is normally dedicated to Antarctic research, the boreal summer to Arctic research. Twice per year *Polarstern* commutes between northern and southern hemisphere. Occasionally *Polarstern* stays over winter in Arctic or Antarctic to investigate the particular winter conditions. Access to *Polarstern* is possible by submitting proposals to the AWI which are submitted to a peer review process to decide about acceptance. The accepted proposals are grouped together according to the compatibility of the required facilities and regional aspects. Interdisciplinary projects in which about 10 different groups work on board to improve the cross-disciplinary understanding of the polar components of the Earth System are of high priority. The technical facilities including cranes and winches allow to apply gear to satisfy almost all disciplines investigating the atmosphere, the ocean, the biosphere and the geosphere. The 19 laboratories and space for 21 laboratory containers provide a wide range of possibilities to the scientists to install and operate their equipment to take samples or to deploy sensors. The crew and the technical services are provided by the shipping company Reederei F. Laeisz, Bremerhaven. Up to 44 crew members run the nautical and technical services and support the life and the work of the scientists on board.

VARIABILITY OF THE SURFACE TRANSPORT AT THE DRAKE PASSAGE

Jae Hak Lee

P.P.Box 29, Ansan, Korea
jhlee@kordi.re.kr

The variability of the surface transport through the Drake Passage is analyzed using the surface velocity derived from the sea surface height anomaly grid data merged TOPEX/Poseidon and ERS in the period from 1992 to 2006. The seasonal pattern is shown to exhibit its maximum and minimum in late summer to spring and in late winter, respectively. The result indicates that the magnitude of seasonal variation in the barotropic volume transport is about 20 Sv (1 Sv=10⁶ m³/s). The low-frequency variability of the transport is dominated by fluctuations with a period of about 4.6 years. The larger and smaller transports appear in 1993, 1997 and 2003 and in 1995 and 2000, respectively. The interannual fluctuation of the transport is statistically coherent with the El Niño-Southern Oscillation (ENSO) indexes with a phase lag of about 3 months and the transport variation leading the ENSO indexes. It is also shown that the transport variability is weakly correlated with the Southern Annular Mode (SAM).

**ANTARCTIC SEA ICE: INTERNATIONAL POLAR YEAR CRUISES-
RESULTS FROM THE SIMBA AND SIPEX FIELD CAMPAIGNS
(SEPT-OCT 2007)**

S.F. Ackley

UTSA, San Antonio TX USA, and A.P. Worby, ACECRC, Univ. of Tas., Hobart, Tas,
Australia
Stephen.ackley@utsa.edu

The keystone activity on Antarctic Sea Ice during International Polar Year was the coordination of two dedicated sea ice cruises during the late winter (Sept-Oct 2007). This period coincides with the annual maximum extension of Antarctic sea ice. The two cruises operated on opposite side of the Antarctic sea ice zone, the *NB Palmer* at 90W longitude in the Bellingshausen Sea and the *Aurora Australis* at 90-120E off East Antarctica. A common core of ice sampling, ice observations and biogeochemical sampling using similar protocols was conducted on both cruises, allowing a more detailed comparison and contrasting of the sea ice development within the same time period on opposite sides of the continent, not previously achieved. Important adjuncts to these measurements were dedicated satellite data acquisitions from the IceSAT laser altimeter and RadarSAT and EnviSAT ASAR active microwave sensors. Detailed ground truth, enhanced by airborne measurements made by helicopter from the *Aurora Australis*, allowed better validation of these satellite products and improves the monitoring of Antarctic sea ice in future from space. The third Antarctic sea ice drift station and the first in late winter, Ice Station Belgica, was conducted from the *NB Palmer* for nearly a month and gave time series measurements of the biogeochemical activity within the sea ice (e.g. CO₂, DMS/P, *chl a*, iron) during this critical period, coinciding with the onset of warming, higher light enhancing biological activity and maximum area coverage of sea ice.

SEA ICE OBSERVATIONS AND MODELING

Achim Stössel

Department of Oceanography, Texas A&M University, College Station, USA
astoessel@ocean.tamu.edu

Sea ice has been observed and monitored ever since mankind intruded the high latitudes. Meanwhile, we monitor sea ice routinely from (ice-strengthened or ice-breaking) vessels, from land stations, and through satellite remote sensing, mainly for navigational, exploitative, or military purposes. Such monitoring belongs to the tasks of national ice services. Furthermore, sea ice is measured for scientific purposes, e.g. to make judgments about long-term changes in the sea-ice cover and characteristics, as recently observed in the Arctic Ocean (e.g., Serreze and Stroeve, 2008). This involves more elaborate measurements from research ice breakers (e.g., Wadhams et al., 1987; Worby et al., 2008), and from moored upward-looking sonars (e.g., Strass and Fahrback, 1988), as well as products derived from various satellite sensors using sophisticated algorithms (e.g., Gloersen et al., 1992; Markus and Cavalieri, 2000; Zwally et al., 2008). Such measurements are augmented by comprehensive numerical models of sea ice, which exist since the 1970s (e.g., Parkinson and Washington, 1979; Hibler, 1979; Leppäranta, 1981). A fundamental difficulty in simulating sea ice arises from its rheology. While air and water can be readily treated as a Newtonian fluid, the dynamics of convergent sea ice are more accurately described by assuming plasticity. Furthermore, leads and polynyas make the large-scale horizontal sea-ice texture highly heterogeneous, in particular with regard to the development of unstable atmospheric boundary layers within an otherwise stably stratified environment. When described on a finite grid of a numerical model, this leads necessarily to subgrid-scale effects, and thus a challenge for a proper simulation of the associated sea-ice thermodynamics. Finally, due to the large heat capacity of the ocean, the quality of any coupled sea-ice-ocean simulation depends decisively on the ocean component, in particular on how oceanic heat is being advected or supplied by convection. Convective plumes normally not being resolved in large-scale ocean models, their parameterization has a major impact on the sea-ice simulation, and with that also on the surface buoyancy fluxes that in turn determine the ocean stratification in high latitudes, and thus the long-term deep-ocean properties.

REFERENCES

- Gloersen, P., Campbell, W.J., Cavalieri, D.J., Comiso, J.C., Parkinson, C.L., and Zwally, H.J. 1992. *Arctic and Antarctic sea ice, 1978-1987: Satellite passive microwave observations and analysis. Spec.Publ., NASA SP-511*, NASA, Washington, D.C.
- Hibler, III, W. D. 1979. A dynamic thermodynamic sea ice model. *J.Phys.Oceanogr.* 9, 815-846.
- Leppäranta, M. 1981. On the structure and mechanics of pack ice in the Bothnian Sea. *Finnish Marine Research No. 248*, 3-86.
- Markus, T. and Cavalieri, D.J. 2000. An enhancement of the NASA Team sea ice algorithm. *IEEE Trans.Geosc.and Remote Sens.* 38, 1387-1398.
- Parkinson, C.L. and Washington, W.M. 1979. A large-scale numerical model of sea ice. *J.Geophys.Res.* 84, 311-337.
- Serreze, M.C., and Stroeve, J.C. 2008. Standing on the brink. *Nature Reports Climate Change*, doi:10.1038/climate.2008.108.
- Strass, V.H. and Fahrbach, E. 1998. Temporal and regional variation of sea ice draft and coverage in the Weddell Sea obtained from upward looking sonars. In: *Antarctic sea ice: physical processes, interactions and variability. AGU, Antarctic Research Series 74*, 123-139.
- Wadhams, P., Lange, M.A., and Ackley, S.F. 1987. The ice thickness distribution across the Atlantic sector of the Antarctic ocean in midwinter. *J.Geophys.Res.*92, 14,535-14,552.
- Worby, A.P., Geiger, C.A., Paget, M.J., Van Woert, M.L., Ackley, S.F., and DeLiberty, T.L. 2008. Thickness distribution of Antarctic sea ice. *J.Geophys.Res.*113, C05S92, doi: 10.1029/2007JC004254.
- Zwally, H.J., Yi, D., Kwok, R., and Zhao, Y. 2008. ICESat measurements of sea ice thickness in the Weddell Sea. *J.Geophys.Res.*113, C02S15, doi: 10.1029/2007JC004284.

**ESTABLISHING A SOUTHERN OCEAN TIME SERIES PROGRAM FOR
BIOGEOCHEMISTRY AND CARBON CYCLING**

Tom Trull

Institute of Antarctic and Southern Ocean Studies, University of Tasmania, Australia
Tom.Trull@utas.edu.au

Particulate carbon fluxes to the deep sea south of Tasmania, as measured by moored sediment traps, reveal strong spatial and especially temporal variations. But ship-based observations on similar timescales for the surface ocean are insufficient to determine the ecosystem controls on the carbon export. Foraminifera samples from the traps reveal lower shell weights than observed in Holocene sediments, suggesting an impact from ocean acidification. But data to resolve the seasonal variations in upper ocean conditions that influence foraminifera growth are similarly unavailable. To address these and other important issues in carbon cycling, marine biogeochemistry and ecosystem research, we are developing moorings capable of high temporal resolution measurements and sample collection in the surface Southern Ocean, where high waves and strong currents present considerable difficulties. These moorings are part of the Integrated Marine Observing System (www.imos.org.au) Southern Ocean Time Series Facility. There are 3 different moorings: a surface meteorological mooring for air-sea flux measurements, a Pulse mooring for surface and mixed layer biogeochemical sensor measurements and water sample collections, and a deep-sea sediment trap mooring. These observations will also be augmented by profiling float, glider, and resupply vessel observations.

LONG-TERM VARIATION OF OCEANIC CO₂ AND POSSIBLE ACIDIFICATION IN THE INDIAN SECTOR OF THE SOUTHERN OCEAN

G. Hashida¹, T. Yamanouchi¹, S. Nakaoka², S. Aoki³, T. Nakazawa³

¹ National Institute of Polar Research, Tokyo, Japan

² National Institute for Environmental Studies, Tsukuba, Japan

³ Tohoku University, Sendai, Japan

gen@nipr.ac.jp

Long-term monitoring of the partial pressure of CO₂ in the surface seawater (*p*CO₂) on-board Japanese icebreaker SHIRASE has been carried out in the Indian sector of the Southern Ocean since 1987 as a part of Japanese Antarctic Research Expedition (JARE). Meridional distributions of *p*CO₂ along 110° E in early December and along 150°E in late March clearly show steep changes at such fronts as Subtropical Front, Subantarctic Front, and Polar Front. *p*CO₂ of each zone divided by the fronts can be distinguished from the others by the difference of averaged *p*CO₂ in the zone. Although *p*CO₂ of each zone shows interannual variation, secular trend is detectable. For example, estimated increasing rate of *p*CO₂ in the permanent open ocean zone between polar front (around 53°S) and northern edge of winter ice cover (63°S) is about 1.5 μatm/y which is almost same as the increasing rate of atmospheric CO₂ concentration. Oceanic acidification corresponding to *p*CO₂ increase is one of the most direct effects of increasing atmospheric carbon dioxide. Preliminary analysis of pH which has been observed on board SHIRASE and her predecessor FUJI shows gradual decrease from 1980 to 2005.

PHYTOPLANKTON COMMUNITY STRUCTURE AND PHOTOSYNTHETIC PHYSIOLOGY WITHIN A NATURAL IRON GRADIENT IN THE SOUTHERN DRAKE PASSAGE

Haili Wang, B. Greg Mitchell

Scripps Institution of Oceanography, La Jolla, California, USA
hwang@spg.ucsd.edu

During an interdisciplinary cruise near Elephant Island in the Southern Drake Passage (February – March, 2004) we studied the phytoplankton community and its physiology in a natural iron gradient. The 7-PI team deployed 40 surface drogued drifters and completed a 100-station survey that included hydrography, nutrients, trace metals (Fe, Al, Mn), ADCP currents, variable fluorescence and optics. A strong natural iron gradient was found in the photic zone with high Fe (1-4 nM) in shelf waters and low Fe (< 0.2 nM) in Southern Antarctic Circumpolar Current Front (SACCF) water that is often found northwest of Elephant Island. PvsE parameters (P^b , a), phytoplankton absorption and quantum yields of photosynthesis(f), and variable fluorescence (Fv/Fm) were determined. Values for photosynthetic parameters and Fv/Fm were low in SACCF waters (low Fe) and higher in shelf waters (elevated Fe). Values of P_{max}^b ranged from 0.4 to 2.5 (mgC/mg chl-a/hr); f_{max} ranged from 0.005 – 0.06 (molC/mol quanta); and Fv/Fm ranged from 0.1 – 0.6. Highest values of P^b and f_{max} were found in waters replete with Fe. Some off shore waters with as little as 15% shelf water mixed with SACCF water had moderate levels of Fe and intermediate to high values for photosynthetic parameters. Several off shore stations had low values of P_{max}^b and f_{max} but high concentrations of chl-a. Low dissolved Fe and Al for these stations, but moderate Mn concentrations, indicated that Fe that had supported the bloom was derived from the shelf, not the atmosphere or deep water upwelling. Hydrographic, drifter, current, nutrient and trace metal data supports the hypothesis that Fe in shelf water is mixed into SACCF water in this region before the SACCF moves back offshore toward the northeast. The processes of community response to natural iron gradients, the evolution and senescence of blooms, changes in community structure, and effects on parameters of photosynthetic photophysiology models all need to be better understood if we are to improve ecosystem and carbon cycle models for the Southern Ocean.

OPTICAL DISCRIMINATION OF PHYTOPLANKTON GROUPS TO DERIVE DIMETHYLSULFONIOPROPIONATE (DMSP) CONCENTRATION IN THE SOUTHERN OCEAN

T. Hirawake¹, N. Kagawa¹, N. Kondo¹, N. Kasamatsu², S. Saitoh¹

¹Graduate School of Fisheries Sciences, Hokkaido University, Hakodate, Hokkaido,
Japan

hirawake@salmon.fish.hokudai.ac.jp

²National Institute of Polar Research, Tachikawa, Tokyo, Japan

INTRODUCTION

Dimethylsulphide (DMS) is important sulfur compound to regulate radiant energy because it is oxidized and then create aerosols which act as cloud condensation nuclei (CCN) in atmosphere. Chemical precursor of DMS, dimethylsulphoniopropionate (DMSP), is created mainly by phytoplankton in the ocean. Therefore, modulation of marine clouds by DMS(P) of phytoplankton and their feedback mechanism to phytoplankton population has been proposed (e.g., Charlson et al., 1987). DMS is potential to become major CCN rather than anthropogenic and land materials in the Southern Ocean where is far from land and human activity. Thus, clear interaction between phytoplankton and marine clouds was expected in the Southern Ocean.

Estimation of DMS and DMSP concentrations using satellite data has benefit to reveal the large scale feedback mechanism. Some models based on chlorophyll *a* concentration (chl-*a*) have been developed (e.g., Belviso et al., 2004). However, DMSP/chl-*a* ratio of phytoplankton is quite different between its groups or species (Keller and Bellows, 1996) and it is little know about the ratio for natural phytoplankton community. Recent progresses of optics and ocean color have made it possible to discriminate dominant phytoplankton groups (e.g., Alvain et al., 2005). If we can detect the groups from satellite, it is effective tool to estimate DMSP concentration using DMSP/chl-*a* ratio of each group.

Here we attempted to discriminate the phytoplankton groups using their optical properties, spectral shape of light absorption and scattering coefficient, in the Southern Ocean to apply it to satellite ocean color data. Relationship between DMSP and chlorophyll *a* concentrations of each dominant phytoplankton group was also investigated for future application to remote estimation of DMSP from space.

MATERIALS AND METHODS

Oceanographic investigations and water sampling from several layers or sea surface were carried out in the Indian sector of Southern Ocean (Fig. 1) during the cruises of icebreaker Shirase, R/V Hakuho Maru, R/V Tangaroa and TR/V Umitaka Maru in austral summer of several years (1999-2008). Spectral radiation (radiance and irradiance), absorption coefficients as optical properties, phytoplankton pigments concentration with HPLC (Hashihama et al., 2008) and total DMSP concentration (Kasamatsu et al., 2004) were analyzed.

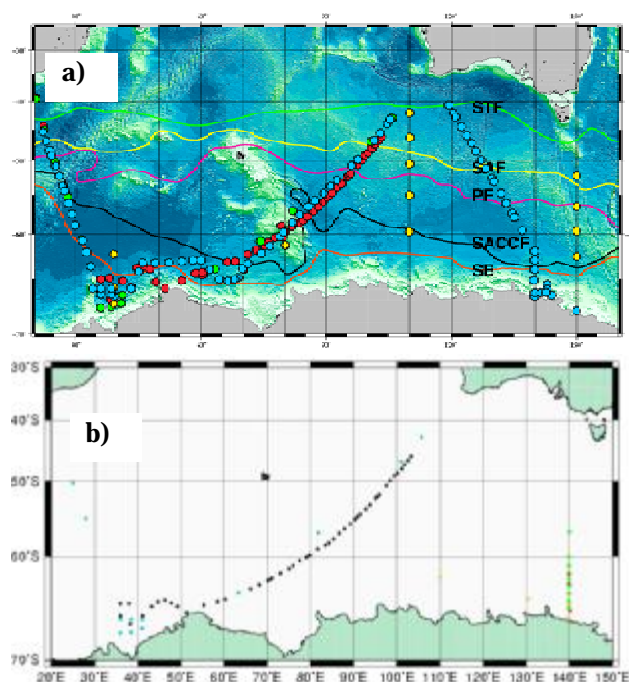


Fig. 1. Sampling stations for (a) optical properties and phytoplankton pigments and (b) DMSP concentration.

Absorption coefficient of accessory pigments, a_{ap} , was determined by eliminating absorption of chl-*a* (Bidigare et al., 1990) from total absorption of phytoplankton, a_{ph} . Spectral slope of back scattering coefficient, γ_{bbp} , was empirically calculated from spectral radiation (Reynolds et al., 2001). Phytoplankton groups were determined according to the pigments composition with CHEMTAX (Mackey et al., 1996).

OPTICAL DISCRIMINATION OF PHYTOPLANKTON GROUPS

Haptophytes, diatoms and chrysophytes were dominant groups in the Southern Ocean. Haptophytes and chrysophytes (H+C) are processed as a group with much higher content of DMSP inside their cell compared with diatoms (D). Either light absorption of accessory pigments (a_{ap}) or spectral slope of back scattering coefficient (γ_{bbp}) alone was difficult to represent the abundance of H+C and D sufficiently. Multi-regression analysis using combinations of these optical properties and sea surface temperature showed better results to estimate H+C abundance with $R^2=0.56$ (Fig. 2).

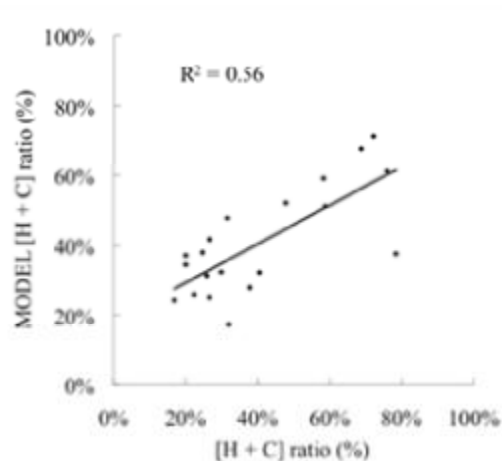


Fig. 2. Relationship between observed and modeled H+C abundances.

CHL-A VS. DMSP FOR EACH PHYTOPLANKTON GROUP

Data was classified phytoplankton groups to H+C, D dominated (> 70%) and Mixed according to CHEMTAX results. Moreover, H+C dominated and Mixed data were separated to 0-30 m and 30-200 m. DMSP concentration of each group (and/or depth) had high correlation with chlorophyll *a* concentration ($r = 0.61-0.87$), except low correlation on the surface Mixed samples probably due to salinity temperature and growing phase of phytoplankton. DMSP/chl-*a* ratio of each phytoplankton group was almost same level as the results of isolated culture samples (Keller and Bellows, 1996). As shown in Fig. 3, Using of these classification and DMSP/chl-*a* values accounted for 56% of observed variability (18% without classification). However, irregularly elevated values (not used in this analysis) were also found especially near sea ice edge. Further research to know factors and mechanism affecting DMSP dynamics in the sea ice area are required.

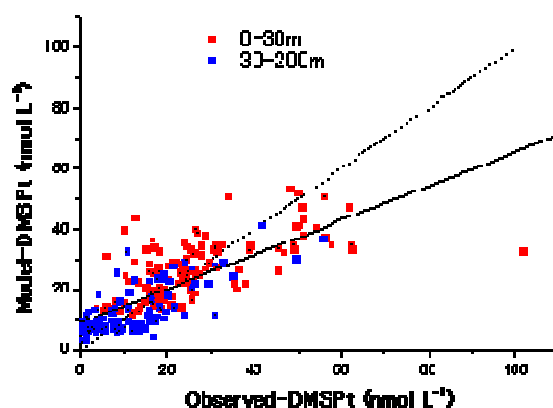


Fig. 3. Relationship between observed and modeled DMPS concentrations

REFERENCES

- Alvain, S., Moulin, C., Dandonneau, Y., Bréon, F.M., 2005. Remote sensing of phytoplankton groups in case 1 waters from global SeaWiFS imagery. *Deep-Sea Research I* 52, 1989-2004.
- Belviso, S., Moulin, C., Bopp, L., Stefels, J., 2004. Assessment of a global climatology of oceanic dimethylsulfide (DMS) concentration based on SeaWiFS imagery (1998-2001). *Canadian Journal of Fisheries and Aquatic Sciences* 61, 804-816.
- Bidigare, R.R., Ondrusek, M.E., Morrow, J.H., Kiefer, D.A., (1990). In vivo absorption properties of algal pigments. In R.W. Spinrad (Ed.), *Ocean Optics X* (pp. 290-302). SPIE 1302.
- Charlson, R.J., Lovelock, J.E., Andreae, M.O., Warren, S.G., 1987. Oceanic phytoplankton, atmospheric sulphur, cloud albedo and climate. *Nature* 326, 655-661.
- Hashihama, F., Hirawake, T., Kudoh, S., Kanda, J., Furuya, K., Yamaguchi, Y., Ishimaru, T., 2008. Size fraction and class composition of phytoplankton in the Antarctic marginal ice zone along the 140-E meridian during February-March 2003. *Polar Science* 2, 109-120.
- Kasamatsu, N., Kawaguchi, S., Watanabe, S., Odate, T., Fukuchi, M., 2004. Possible impacts of zooplankton grazing on dimethylsulfide production in the Antarctic Ocean. *Canadian Journal of Fisheries and Aquatic Sciences* 61, 736-743.
- Keller, M.D., Bellows, W.K., (1996). Physiological aspects of the production of dimethylsulfoniopropionate (DMSP) by marine phytoplankton. In R.P. Kiene, P.T. Visscher, M.D. Keller & G.O. Kirst (Eds.), *Biological and environmental chemistry of DMSP and related sulfonium compounds* (pp. 131-142). New York: Plenum Press.
- Mackey, M.D., Mackey, D.J., Higgins, H.W., Wright, S.W., 1996. CHEMTAX - a program for estimating class abundances from chemical markers: application to HPLC measurements of phytoplankton. *Marine Ecology Progress Series* 144, 265-283.
- Reynolds, R.A., Stramski, D., Mitchell, B.G., 2001. A chlorophyll-dependent semianalytical reflectance model derived from field measurements of absorption and backscattering coefficients within the Southern Ocean. *Journal of Geophysical Research* 106, 7125-7138.

**DEVELOPMENT OF A NEW SHIP-BOARD SKY-RADIOMETER FOR
REMOTE-SENSING OF COLUMN AEROSOL OPTICAL PROPERTIES OVER
THE OCEAN FROM JAPANESE NEW ANTARCTIC R/V SHIRASE**

Masataka Shiobara¹, and the POM-01 MK III Skyradiometer Development Team

¹National Institute of Polar Research, Tachikawa, Japan
shio@nipr.ac.jp

Sky-radiometers measure spectral solar attenuation and scattered radiance, and are useful for investigating column aerosol optical properties by a passive remote sensing technique. Ground-based measurements using sky-radiometers are coming popular after deployed for the SKYNET Project in Asia. Ship-board sky-radiometers are also useful for observing aerosols over the ocean. A Prede POM-01 MK II is commercially available for ship-board measurement, and has been used aboard the Antarctic Research Vessel Shirase for measurement during cruises between Japan and Antarctica. Unfortunately, we have known that the performance of the existing instrument is not sufficient for accurately tracking the sun against large rolling of the ship. And thus, data available for analysis are quite limited.

Recently a new ship-board sky-radiometer was developed by collaboration of National Institute of Polar Research and Prede Co., Ltd. The newly developed sky-radiometer, POM-01 MK III, has attained sun tracking and sky scanning measurements faster and more accurate than the former MK II. The new instrument is planned to be aboard the new Antarctic R/V Shirase that will follow the former R/V Shirase to be engaged in the Japanese Antarctic Research Expedition activities beyond 2009. In this paper, the performance of the POM-01 MK III sky-radiometer is shown and compared with that of the former one, based on results from ground and ship-based experiments. Including the new sky-radiometer, an onboard aerosol measurement system planned for the air-sea interaction research in the Antarctic will be presented.

* The POM-01 MK III Skyradiometer Development Team: M. Shiobara (PI, NIPR), T. Abe (Prede), K. Aoki (U. Toyama), K. Inei (Prede), K. Kawai (Prede), H. Kobayashi (U. Yamanashi), Y. Muraji (ESCoT), T. Murayama (TUMST), T. Nakajima (U. Tokyo), K. Sasamoto (Prede), A. Uchiyama (MRI), M. Yabuki (Chiba U.), M. Yamano (ESCoT)

**FINDINGS FROM THE ATLANTIC MERIDIONAL TRANSECT (AMT)
PROGRAM, IMPLICATIONS TO THE PACIFIC OCEAN**

Youngnam Kim

Korea Polar Research Institute, Incheon 406-840, Republic of Korea
ynk@kopri.re.kr

The AMT program undertakes biological, chemical and physicaloceanographic research during the annual return passage of the RRS James Clark Ross (ice breaker) between the UK and the Falkland Islands, a distance of up to 13,500 km. The track cover a range of ecosystems from sub-polar to tropical and from eutrophitic shelf seas and upwelling systems to oligotrophic mid-ocean gyres. Scientific aims of AMT are to quantify the nature and the causes of ecological and biogeochemical variabilities in the planktonic ecosystems of the Atlantic Ocean, and to assess the effects of these variabilities on biological carbon flux and air-sea exchange of radiatively active trace gases and aerosol.

A wide range of measurements of both the phytoplankton community and hydrographic situation were made during the Atlantic Meridional Transect (AMT) cruises 13, 14 and 15 (2003-2004). Additionally, use of fast repetition rate (FRR) fluorescence technique to provide high-resolution vertical profiles of physiological properties of phytoplankton is explored. Vertical distributions of chlorophyll, light, nitrate, dissolved oxygen and photosynthetic parameters varied across the thermocline. These variations are interpreted in a regional context and compared with estimates of population size structure and the C/Chl a ratio. The community found in the chlorophyll maximum was physiologically distinct from the surface community and optimized for light harvesting and photosynthesis at low light levels. The physiological and biological environment in the nutrient-rich equatorial upwelling region and in the oligotrophic subtropical gyre is also compared.

In the presentation, I will describe the rationale, methodology, and some of key findings of the AMT program and introduce briefly a general idea of studying the Pacific Ocean with similar sailing opportunities using a new ice breker, Araon, along the meridional transects.

SEASONALITY OF PHYTOPLANKTON ABUNDANCE IN THE SOUTHWEST ATLANTIC SECTOR OF THE SOUTHERN OCEAN

Jisoo Park^{1,2}, Im-Sang Oh², Hyun-Cheol Kim³, Hyoung-Chul Shin³, and Sinjae Yoo¹

¹Korea Ocean Research and Development Institute (425-170) Sa-dong 1270, Ansan,
Republic of Korea
jspark@kordi.re.kr

²Seoul National University, Korea

³Korea Polar Research Institute

INTRODUCTION

Antarctic waters are peculiar to the condition of low phytoplankton standing stocks and rates of primary productivity in spite of high concentrations of inorganic nutrients (Mitchell and Holm-Hansen, 1991a; Chisholm and Morel, 1991). This has often been referred to as a major "paradox" of the Southern Ocean (SO) (El-Sayed, 1987; Levitus et al., 1993). Typical chlorophyll-a concentrations in the SO range between 0.05 and 1.5 mg m⁻³ (Arrigo et al., 1998; El-Sayed, 2005; Marrari et al., 2006), and according to Marrari et al. (2006), 96% of the satellite chlorophyll-a in the surface waters fall within this range. Meanwhile, high chlorophyll-a concentrations are shown in the marginal ice zone and downstream area of islands and coast.

Difficulties in assessing the primary productivity as well as phytoplankton biomass in the SO are primarily attributed to the temporal and spatial variability of those, while measurements are sparse due to its geographical limitation of access (Strass et al., 2002). Satellite data can be an important source of ocean basin-scale pigment distributions at high latitudes, and high resolution remotely sensed observational data have overcome the issue of geographical remoteness (Mitchell, 1992; Sullivan et al., 1993). Historically, Comiso et al. (1993) made first attempt to evaluate the large-scale spatial, seasonal and interannual distributions of pigment concentrations in the SO using CZCS (Coastal Zone Color Scanner) satellite data (1978-1986). At present, it has been more than ten years after launching SeaWiFS ocean color sensor (from September, 1997 to present), so the time is ripe we can explain somewhat long term and consecutive trend of variability of pigment biomass by remote sensing utility.

More than half of the SO krill stocks concentrated in the southwest Atlantic sector of the Southern Ocean (SASSO), and summer krill density correlated positively with chlorophyll-a concentration in that region (Atkinson et al., 2004, 2008; see also Siegel, 2005). The potential biomass of krill in the SO range from 67 to 297 million tons (reviewed in Siegel, 2005), and krill stock biomass in a given area can vary by one order of magnitude between consecutive years (Brierley et al., 1999). However, to date, there is no adequate explanation about this regional distribution of krill (Murphy et al., 1998). The SASSO thus provides a case study for understanding of fluctuation and relationship between phytoplankton and krill biomass. Our major objectives of this study are (1) utilize satellite chlorophyll-a data to classify biological domain over an extended region

which include the Antarctic Peninsula, the Scotia Sea, and downstream area of South Georgia; (2) evaluate spatial patterns and seasonal-to-interannual variability of chlorophyll-a of the study area; and (3) identify possible mechanisms that could control the seasonal pattern of phytoplankton dynamics at each classified region.

1. Data and materials

Remotely sensed chlorophyll-a, sea-ice extent & concentration, and wind speed data were extracted and analyzed. Firstly, SeaWiFS (Sea-viewing Wide Field-of-view Sensor)-derived estimates of surface chlorophyll-a concentrations for the period September 1997 through December 2007 were obtained from the Goddard Space Flight Center (McClain et al., 1998). MODIS (Moderate Resolution Imaging Spectroradiometer) Aqua data were also obtained for the period January 2008 to August 2008 because SeaWiFS has missed data due to its board (satellite) was out of order quite a while. Monthly mean sea ice concentrations are from NASA's Scanning Multichannel Microwave Radiometer (SMMR) and the Defense Meteorological Satellite Program's (DMSP) Spectral Sensor Microwave/Imager (SSM/I). Ice concentrations of <15% were considered to be open water in our analysis (Gloersen et al., 1992; Smith et al., 1998; Stammerjohn et al., 2008). Climatological mixed layer depth (MLD) for the World Ocean was used (de Boyer Montegut et al., 2004). The Southern Oscillation Index (SOI) is calculated from the monthly or seasonal fluctuation in the air pressure difference Tahiti and Darwin. Positive values of the SOI are associated with stronger Pacific trade winds and warmer sea temperatures to the north of Australia, popularly known as a La Niña episode. The Southern Hemisphere Annular Mode (SAM) is an expression of the meridional pressure gradient between the sub-Antarctic and middle latitudes. Here we use an observation-based SAM index (Marshall, 2003).

2. Results

Classification of biological domain

We used classical Principle Component Analysis (PCA) to compute the EOFs (empirical orthogonal function) decomposition and PCs from the eleven year monthly time-series of SeaWiFS/MODIS chlorophyll-a data to examine the dominant temporal patterns on geographically. As a consequence, we divide eight regions for time-series analysis by using K-means. Pretreatment removed, from the analysis, region of less than 50% of valid chlorophyll-a data per grid cell with Patagonia basin and west of South America. The first mode described phytoplankton bloom in December in northern region of the Drake Passage explaining 19.1% of the variability in space and time; second mode described early phytoplankton bloom in November in southern region of the Drake Passage explaining 11.1% of the variability. The first eight modes explained approximately 60 percent of the variability, and by these we clustered eight regions using by k-means algorithm (Fig. 1a). Here northern and southern region of Drake Passage were well classified across the approximate location of Polar Front. And, the shelf region of Antarctic Peninsula was also well divided by SACCF. Consequently, western Scotia Sea region was classified by Shackleton Fracture Zone. Two downstream area of South Georgia were also classified to northern and eastern Scotia Sea region. It was clear that the sub-regions by our method well represent the biological geography at least from the point of chlorophyll maximum timing of view (Fig. 1b). Climatologically, chlorophyll-a early peaked (in November) in the southern Drake Passage (sDP) and eastern Scotia Sea region (eSC). Chlorophyll-a peaked at the middle of summertime in the northern Drake Passage (nDP), northern South Georgia (nSG; in December) and the northern Scotia Sea region (nSC; in January). Late timing of maximum chlorophyll-a was shown in the southern South Georgia (sSG) and eastern part of the Antarctic

Peninsula region (AP; in February). The magnitude of chlorophyll-a concentrations at peak-time was high in shelf regions and across the fronts especially the SACCF region. The peak concentration was remarkably high in the northwest of South Georgia where high chlorophyll-a value was clearly distinguished from that of other regions by PF and SACCF. This high chlorophyll-a concentration ($>3 \text{ mg m}^{-3}$ in the Georgia Basin) was good contrast to low concentration in the DP and nSC regions ($\sim 0.3 \text{ mg m}^{-3}$ in DP and nSC) with an order of magnitude. In these eight regions, we extracted time-series data for further analysis.

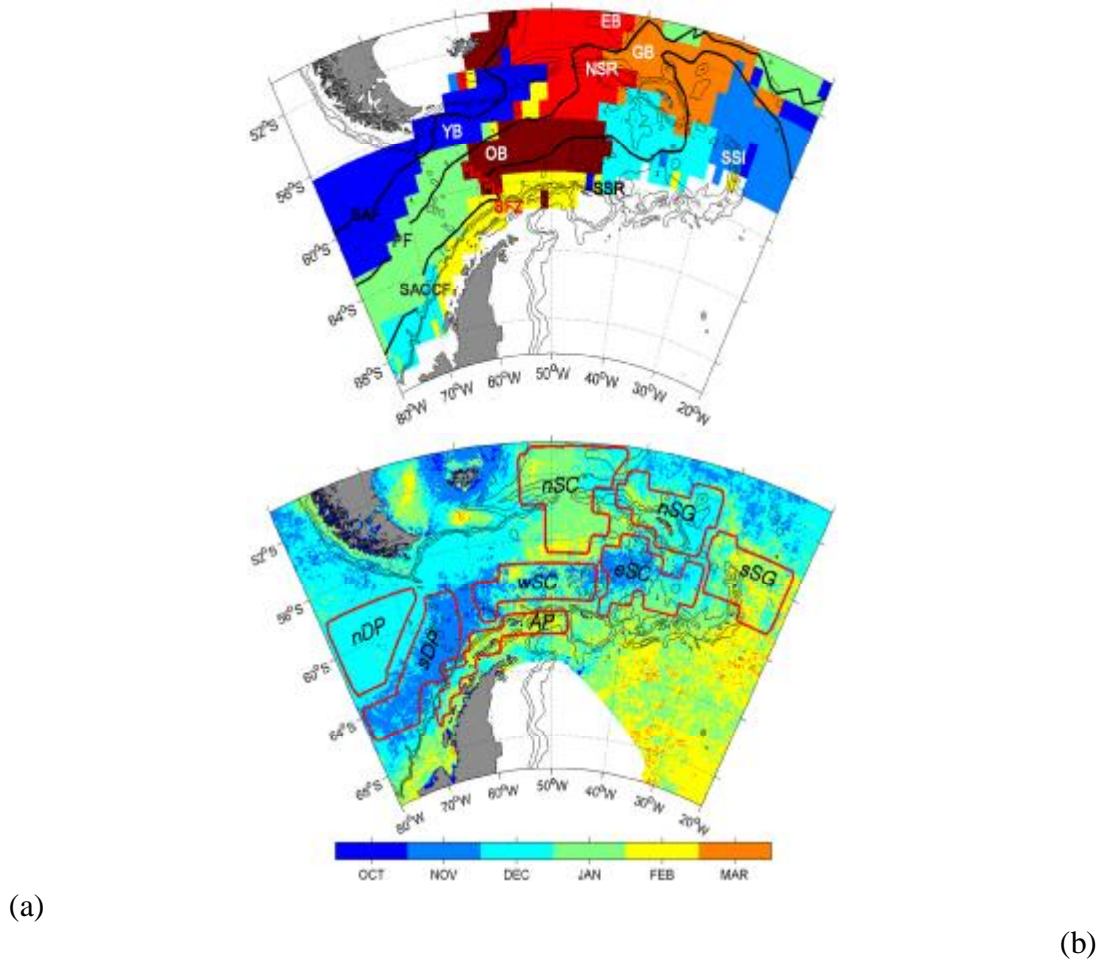


Fig. 1. a) Eight regional classification of the largest eight PCs from the decomposition of monthly chlorophyll-a concentration by K-means algorithm. Lines indicate 1000, 2000 and 3000 m isobaths. Three thick lines are the approximate location of the sub-Antarctic Front (SAF), Polar Front (PF) and Southern Antarctic Circumpolar Current Front (SACCF), respectively (after Orsi et al., 1995; Moore et al., 1997). Basins and topographical barriers are also depicted (YB-Yaghan Basin; OB-Ona Basin; SFZ-Shackleton Fracture Zone; EB-Ewing Bank; NSR-northern Scotia Ridge; SSR-southern Scotia Ridge; GB-Georgia Basin; SSI-South Sandwich Islands). b) Eight regions of interest for time-series data analysis (denoted by red polygons). nDP: northern Drake Passage region; sDP: southern Drake Passage region; AP: northern Antarctic Peninsula region; wSC: western Scotia Sea region; nSC: northern Scotia Sea region; eSC: eastern Scotia Sea region; nSG: northern downstream region of South Georgia; and sSG: southern downstream region of South Georgia. Base map is a timing of the annual maximum in chlorophyll-a.

Seasonal and interannual variation

By the regionally median value of chlorophyll-a concentration (8-days composite) we generated a time-series chlorophyll-a data for each region (Fig. 2). Seasonal variation of chlorophyll-a in the eight regions was highly variable. It is of interest that the seasonality of phytoplankton bloom was appeared only in the nDP, sDP, and nSC regions though MLD decreased in all regions in austral spring time. Earliest spring blooms begin in the sDP, wSC, eSC, and nSG. A common point was that these four regions are located across the SACCF. And, elevated chlorophyll concentrations reform in the late summer in these regions except sDP. Subsequently, from December to March, perennial bloom was shown in the sSG though interannual variation was also high. These downstream blooms may be of both gradually ageing populations (Fryxell et al., 1979) and of actively growing cells (Whitehouse et al., 1996, 2000). According to the result of Ward et al. (2002), the duration of phytoplankton bloom was about 82 ~ 122 days in the ACC and South Georgia Island. In the AP, an intense bloom with chlorophyll-a value 1.989 mg m⁻³ (second largest value was 0.588 mg m⁻³ in other years) appeared in January 2006.

Decadal scaled seasonal-to-interannual variability of chlorophyll-a showed different patterns at each region. The early and/or consistent pattern of bloom in the Drake Passage regions with weak pattern of that in the nSC region were good contrast to the irregular pattern of that in other regions. Generally, in the most regions, 2001/2002 and 2002/2003 years were low productive season except downstream region of South Georgia. Consequently, chlorophyll-a was high in the nDP during two El niño years (1997/1998 and 2004/2005 years). And, in the AP region, there was one prominent (in 2005/2006), and not any more repeated in the last decade, bloom. Seasonal-to-interannual variation of chlorophyll-a in the Scotia Sea and South Georgia regions have own characteristics and this advocate that our regional classification of the SASSO is reasonable for biological aspect. Summertime averaged chlorophyll-a concentration also showing high variability both in magnitude and peak timing but relatively low in the northern regions of PF. An intriguing point was that decadal scaled interannual variation of chlorophyll-a have mostly periodicity (five to more than nine years).

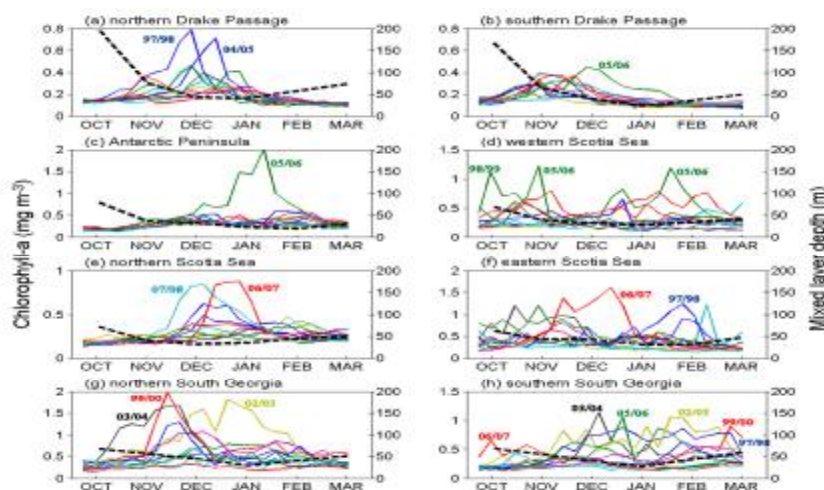


Fig. 2. Seasonal variation of chlorophyll-a concentration and mixed layer depth (black dots) at each region during austral summer time. Here 8-days composite chlorophyll-a data (median value of each region) were used. Eleven year chlorophyll-a

concentration were overlaid by different color. Note that the vertical axes of chlorophyll-a have different scales.

3. Discussion

Longhurst (2007) divided global ocean to several provinces by ecological geography of the sea. In his book, the SO (south of sub-Antarctic Front) is represented by strong seasonality of surface chlorophyll-a which has peak in austral summer. However, in our results, we could find a strong and/or regular seasonality of phytoplankton bloom only in the Drake Passage region. In other regions of the SASSO, weak (in the nSC) or no seasonality (in the AP, wSC, eSC, nSG, and sSG) of phytoplankton bloom was shown. After Martin et al. (1990), many research have suggested that low productivity in the nutrient-rich waters of the SO may result from a deficiency of iron. However, owing to difficulties of handling of iron samples on ship-board, there are few results about vertical distribution of dissolved Fe. Nonetheless, according to limited study, ferrocline in the study area formed around 200 m depth (Loscher et al., 1997), and the highest average Fe concentrations in upper mixed layer (UML) was only observed in the PF and SACCF (Measures and Vink, 2001). In the Drake Passage region, formation of deep mixed layers during winter could entail entrainment of sub-surface waters enriched in Fe (Measures and Vink, 2001), and hence consistent bloom might be occurred when the light condition is favorable in spring. Namely, micronutrient-light co-limitation might be particularly relevant to the UML depths of these regions (Sunda and Huntsman, 1997). On the other hand, in the Scotia Sea and South Georgia regions, although mean light condition in the UML exceed the saturating light value for photosynthesis (I_k) in austral summer (Holm-Hansen et al., 2004), phytoplankton bloom did not show seasonality. This non-seasonality, in these regions, was likely to be due to the maximum UML depth does not deepened below the ferrocline. The climatology of winter maximum of MLD does not exceed 150 m in the Scotia Sea and South Georgia region, whereas it reaches 300 m in the Drake Passage region. Moreover, even though in summer, the evident feature of the lack of a significant relationship between chlorophyll-a concentration and UML depth in these regions (Holm-Hansen et al., 2004) could induce phytoplankton bloom happened irregularly.

Why the interannual variations of chlorophyll-a are so high in the SASSO may has been explained already by some previous studies. We endeavor to explain about high peak of blooms in our result by some aspects. Firstly, Kahru et al. (2007) mentioned that the variability around South Georgia and Scotia Sea may be induced by the cyclonic/anticyclonic eddies activity in the SACCF zone. They emphasized the role of cross-frontal mixing mediated by eddies for the increased productivity and chlorophyll-a concentration in the frontal zone. In the nDP, the high concentration of chlorophyll-a coincided with eddy formation where anticyclonic eddies have low chlorophyll-a in the core but increased chlorophyll-a in the surroundings on December 2004. Secondly, because the study region hosts a wide range of bathymetric and oceanographic conditions, there are some topographic barriers of currents which may induce the vertical mixing. For example, in the east of the SFZ, phytoplankton bloom happened in early spring and this bloom spread out to the east in 1988.

In the Antarctic Peninsula region, there was a conspicuous large bloom in 2005/2006 year. This may be related to the sea-ice retreat. In 2005/2006 year, sea-ice retreat quickly, and phytoplankton bloom was happened within the area of sea-ice retreated. Many reports said that ice-edge blooms are quite related to spring ice-edge retreat in Antarctic waters (e.g. Sullivan et al., 1993; Siegel and Loeb, 1995; Arrigo and McClain, 1994; Smith et al., 1998; Garibotti et al., 2005; Williams et al., 2008; Vernet et al., 2008), where blooms develop within about 2 weeks after the ice recedes (Marrari et al., 2008). According to previous study, when La niña year, strong and warm northerly winds promote sea-ice retreat in the western Antarctic Peninsula region in spring time

(Stammerjohn et al., 2008), and this leads to relatively high pigment (Smith et al., 2008). However, because sea-ice retreat relatively fast in other La niña seasons (1998-2000 and 2007/2008 year) as well as in 2005/2006 year, it is hard to recognize the exceptional year to this. We also examined about interannual variation of irradiance, sea surface temperature as well as wind speed/direction in the AP region. However, no single environmental factor has been found that shows a predictable relationship with the bloom. It is feasible that, as we know up to the present, favorable bloom condition is buttressed by the stratification and shoaling of the UML by horizontal mixing of nutrient rich water from the Weddell origin with iron-poor but well-stratified Antarctic Surface Water rather than vertical processes (Holm-Hansen et al., 1997; Hewes et al., 2008). Namely light condition may be a dominant limiting-factor of the productivity in the AP region.

More recently, the high-latitude atmospheric ENSO response appeared to have intensified (Smith et al., 2008; Meredith et al., 2008). And, SAM play an important role in determining SST variability at South Georgia (Marshall and Connolley, 2006; Meredith et al., 2008), and also shows a connections with negative and positive anomalies of sea level pressure of the AP (Stammerjohn et al., 2008), oceanic transport (Meredith et al., 2004; Yang et al., 2007), CO₂ uptake (Lenton and Matear, 2007), and sea-ice variability (Gupta and England, 2006). The second component (PC2) of EOFs was significantly correlated with SOI and SAM (Fig. 3). PC2 was dominant in the DP and wSC region, there was no significant or negative correlation in the north of PF and sSG region. This infers that ENSO and SAM signals primarily propagate through the ACC and may affect sea-ice dynamics particularly in the south of PF. Data discussed herein do not cover a long enough time period to establish co-relationship between SOI/SAM and interannual variability of chlorophyll-a, however on-going research will continue to address this subject as more data become available. Global warming will reduce vertical mixing in the water column (Huisman et al., 2006), and that will make more variability both in nutrient supply and vertical distribution of phytoplankton. By that means, future study should also strive for more understanding about long term variation as these.

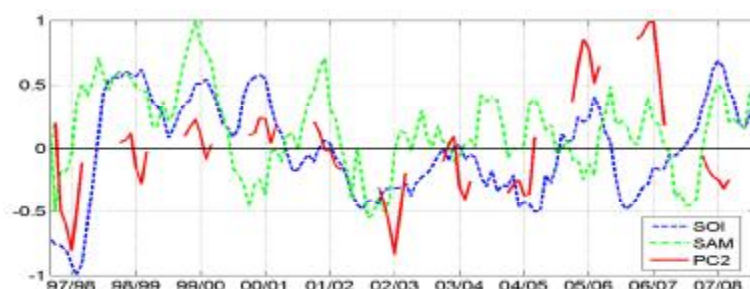


Fig. 3. The PC2 of EOFs (red), SOI (blue) and SAM (green) versus time (September 1997 ~ August 2008). The SOI and SAM values are normalized by their minimum and maximum values for ease of comparison with PC2, respectively. Note that all indices were smoothed with a six-month running mean.

values for ease of comparison with PC2, respectively. Note that all indices were smoothed with a six-month running mean.

REFERENCES

- Arrigo, K.R., McClain, C.R., 1994. Spring phytoplankton production in the Western Ross Sea. *Science* 266, 261-263.
- Arrigo, K.R., Worthen, D., Schnell, A., Lizotte, M.P., 1998. Primary production in Southern Ocean waters. *J Geophys. Res.* 103, 15587-15600.
- Atkinson, A., Siegel, V., Pakhomov, E., Rothery, P., 2004. Long-term decline in krill stock and increase in salps within the Southern Ocean. *Nature* 432, 100-103.

- Chisholm, S.W., Morel, F.M.M., 1991. What controls phytoplankton production in nutrient-rich areas of the open sea? *Limnol. Oceanogr.* 36, 1507-1570.
- Comiso, J.C., McClain, C.R., Sullivan, C.W., Ryan, J.P., Leonard, C.L., 1993. Coastal Zone Color Scanner pigment concentrations in the Southern Ocean and relationships to geophysical surface features. *J Geophys. Res.* 98 (c2), 2419-2451.
- De Boyer Montegut, C., Mignot, J., Lazar, A., Cravatte, S., 2007. Control of salinity on the mixed layer depth in the world ocean 1 General description. *J Geophys. Res.* Doi:10.1029/2006JC003953.
- El-Sayed, S.Z., 1987. Biological productivity of Antarctic waters: present paradoxes and emerging paradigms. In: El-Sayed, S.Z., Tomo AP (eds) *Antarctic aquatic biology BIOMASS Sci Ser SCAR*, Cambridge.
- El-Sayed, S.Z., 2005. History and evolution of primary productivity studies of the Southern Ocean. *Pol. Biol.* 28, 423-438.
- Fryxell, G.A., Villareal, T.A., Hoban, M.A., 1979. *Thalassiosira scotia*, sp. nov.: observations on a phytoplankton increase in early austral spring north of the Scotia Ridge. *J Plankt. Res.* 1, 355-370.
- Garibotti, I.A., Vernet, M., Smith, R.C., Ferrario, M.E., 2005. Interannual variability in the distribution of the phytoplankton standing stock across the seasonal sea-ice zone west of the Antarctic Peninsula. *J Plankt. Res.* 27 (8), 825-843.
- Gloersen, P., Campbell, W.J., Cavalieri, D.J., Comiso, J.C., Parkinson, C.L., Zwally, H.J., 1992. Arctic and Antarctic Sea ice, 1978-1987: Satellite Passive Microwave Observations and Analysis. NASA SP 511.
- Gupta, A.S., England, M.H., 2006. Coupled ocean-atmosphere-ice response to variations in the Southern Annular Mode. *J Clim.* 19, 4457-4486.
- Hewes, C.D., Reiss, C.S., Kahru, M., Mitchell, B.G., Holm-Hansen, O., 2008. Control of phytoplankton mixed layer depth in the western Weddell-Scotia Confluence. *Marine Ecology Progress Series* 366, 15-29.
- Holm-Hansen, O., Hewes, C.D., Villafane, V.E., Helbling, E.W., Silva, N., Amos, T., 1997. Distribution of phytoplankton and nutrients in relation to different water masses in the area around Elephant Islands, Antarctica. *Pol. Biol.* 18, 145-153.
- Holm-Hansen, O., Naganobu, M., Kawaguchi, S., et al., 2004b. Factors influencing the distribution, biomass, and productivity of phytoplankton in the Scotia Sea and adjoining waters. *Deep-Sea Res. II* 51, 1333-1350.
- Huisman, J., Pham Thi, N.N., Karl, D.M., Sommeijer, B., 2006. Reduced mixing generates oscillations and chaos in the oceanic deep chlorophyll maximum. *Nature* 439, 322-325.
- Kahru, M., Mitchell, B.G., Gille, S.T., Hewes, C.D., Holm-Hansen, O., 2007. Eddies enhance biological production in the Weddell-Scotia Confluence of the Southern Ocean. *Geophys. Res. Lett.* 34, L14603, Doi:10.1029/2007GL030430.
- Lenton, A., Matear, R.J., 2007. Role of the Southern Annular Mode (SAM) in Southern Ocean CO₂ uptake. *Global Biogeochem Cycles* Doi:10.1029/2006GB002714.
- Levitus, S., Conkright, M.E., Reid, J.L., Najjar, R.G., Mantyla, A., 1993. Distribution of nitrate, phosphate and silicate in the world ocean. *Progress in Oceanography* 31, 245-273.
- Longhurst, A.R., 2007. *Ecological geography of the sea*, 2nd edn. Academic Press
- Loscher, B.M., de Baar, H.J.W., de Jong, J.T.M., Veth, C., Dehairs, F., 1997. The distribution of Fe in the Antarctic Circumpolar Current. *Deep-Sea Res. II* 44 (1-2), 143-187.
- Marrari, M., Hu, C., Daly, K., 2006. Validation of SeaWiFS chlorophyll a concentrations in the Southern Ocean: A revisit. *Remote Sensing of Environment* 105, 367-375.

- Marrari, M., Daly, K.L., Hu, C., 2008. Spatial and temporal variability of SeaWiFS chlorophyll a distributions west of the Antarctic Peninsula: Implications for krill production. *Deep-Sea Res. II* 55, 377-392.
- Marshall, G.J., 2003. Trends in the Southern Annular Mode from observations and reanalyses. *J Clim.* 16, 4134-4143.
- Marshall, G.J., Connolley, W.M., 2006. Effect of changing Southern Hemisphere winter sea surface temperatures on Southern Annular Mode strength. *Geophys. Res. Lett.* Doi:10.1029/2006GL026627.
- Martin, J.H., Gordon, R.M., Fitzwater, S.E., 1990. Iron in Antarctic waters. *Nature* 345, 156-158.
- McClain, C.R., Cleave, M.L., Feldman, G.C., Gregg, W.W., Hooker, S.B., Kuring, N., 1998. Science quality SeaWiFS data for global biosphere research. *Sea Technology* 39 (9), 10-16.
- Measures, C.I., Vink, S., 2001. Dissolved Fe in the upper waters of the Pacific sector of the Southern Ocean. *Deep-Sea Res II* 48, 3913-3941.
- Meredith, M.P., Woodworth, P.L., Hughes, C.W., Stepanov, V., 2004. Changes in the ocean transport through Drake Passage during the 1980s and 1990s, forced by changes in the Southern Annular Mode. *Geophys. Res. Lett.* Doi:10.1029/2004GL021169.
- Meredith, M.P., Murphy, E.J., Hawker, E.J., King, J.C., Wallace, M.I., 2008. On the interannual variability of ocean temperatures around South Georgia, Southern Ocean: Forcing by El Nino/Southern Oscillation and the Southern Annular Mode. *Deep-Sea Res. II* 55, 2007-2022.
- Mitchell, B.G., Holm-Hansen, O., 1991a. Observations and modelling of the Antarctic phytoplankton crop in relation to mixing depth. *Deep-Sea Res. I* 38 (8/9), 981-1007.
- Mitchell, B.G., 1992. Predictive bio-optical relationships for polar oceans and marginal ice zones. *J Mar. Syst.* 3, 91-105.
- Moore, J.K., Abbott, M.R., Richman, J.G., 1997. Variability in the location of the Antarctic Polar Front (90°-20°W) from satellite sea surface temperature data. *J Geophys. Res.* 102 (c13), 27825-27833.
- Murphy, E.J., Watkins, J.L., Reid, K., Trathan, P.N., Everson, I., Croxall, J.P., Priddle, J., Brandon, M.A., Brierley, A.S., Hofmann, E., 1998. Interannual variability of the South Georgia marine ecosystem: biological and physical sources of variation in the abundance of krill. *Fish. Oceanogr.* 7, 381-390.
- Orsi, A.H., Whitworth III, T., Nowlin, W.D., 1995. On the meridional extent and fronts of the Antarctic Circumpolar Current. *Deep-Sea Res. I* 42 (5), 641-673.
- Siegel, V., Loeb, V., 1995. Recruitment of Antarctic krill *Euphausia superba* and possible causes for its variability. *Mar. Ecol. Prog. Ser.* 123, 45-56.
- Siegel, V., 2005. Distribution and population dynamics of *Euphausia superba*: summary of recent findings. *Pol. Biol.* 29, 1-22.
- Smith, R.C., Baker, K.S., Vernet, M., 1998. Seasonal and interannual variability of phytoplankton biomass west of the Antarctic Peninsula. *J Mar. Syst.* 17, 229-243.
- Smith, R.C., Martinson, D.G., Stammerjohn, S.E., Iannuzzi, R.A., Ireson, K., 2008. Bellingshausen and western Antarctic Peninsular region: Pigment biomass and sea-ice spatial/temporal distributions and interannual variability. *Deep-Sea Res. II* 55, 1949-1963.
- Stammerjohn, S.E., Martinson, D.G., Smith, R.C., Iannuzzi, R.A., 2008. Sea ice in the western Antarctic Peninsula region: Spatio-temporal variability from ecological and climate change perspectives. *Deep-Sea Res. II* 55, 2041-2058.

- Strass, V.H., Naveira Garabato, A.C., Pollard, R.T., Fischer, H.I., Hense, I., Allen, J.T., Read, J.F., Leach, H., Smetacek, V., 2002. Mesoscale frontal dynamics: shaping the environment of primary production in the Antarctic Circumpolar Current. *Deep-Sea Res. II* 49, 3735-3769.
- Sullivan, C.W., Arrigo, K.R., McClain, C.R., Comiso, J.C., Firestone, J., 1993. Distributions of phytoplankton blooms in the Southern Ocean. *Science* 262, 1832-1837.
- Sunda, W.G., Huntsman, S.A., 1997. Interrelated influence of iron, light and cell size on marine phytoplankton growth. *Nature* 390, 389-392.
- Vernet, M., Martinson, D., Iannuzzi, R., Stammerjohn, S., Kozłowski, W., Sines, K., Smith, R., Garibotti, I., 2008. Primary production within the sea-ice zone west of the Antarctic Peninsula: I-Sea ice, summer mixed layer, and irradiance. *Deep-Sea Res. II* 55, 2068-2085.
- Ward, P., Whitehouse, M., Meredith, M., Murphy, E., Shreeve, R., Korb, R., Watkins, J., Thorpe, S., Woodd-Walker, R., Brierley, A., Cunningham, N., Grant, S., Bone, D., 2002. The Southern Antarctic Circumpolar Current Front: physical and biological coupling at South Georgia. *Deep-Sea Res. I* 49, 2183-2202.
- Whitehouse, M.J., Priddle, J., Trathan, P.N., Brandon, M.A., 1996. Substantial open-ocean phytoplankton blooms to the north of South Georgia, South Atlantic, during summer 1994. *Mar. Ecol. Prog. Ser.* 140, 187-197.
- Whitehouse, M.J., Priddle, J., Brandon, M.A., 2000. Chlorophyll/nutrient characteristics in the water masses to the north of South Georgia, Southern Ocean. *Pol. Biol.* 23, 373-382.
- Williams, G.D., Nicol, S., Raymond, B., Meiners, K., 2008. Summertime mixed layer development in the marginal sea ice zone off the Mawson coast, East Antarctica. *Deep-Sea Res. II* 55, 365-376.
- Yang, X.Y., Wang, D., Wang, J., Huang, R.X., 2007. Connection between the decadal variability in the Southern Ocean circulation and the Southern Annular Mode. *Geophys. Res. Lett.* Doi:10.1029/2007GL030526.

**SEA ICE, BIOGEOCHEMISTRY AND ECOSYSTEM PROCESSES IN THE
MOST RAPIDLY WARMING PART OF THE SOUTHERN OCEAN**

Hyoung Chul Shin

Korea Polar Research Institute, Incheon 406-840, Republic of Korea
hcshin@kopri.re.kr

Southern Ocean is known to be a significant component of global carbon cycle and play a role in climate change at the planetary scale. The west Antarctic, in particular, is experiencing a warming at an unprecedented rate and offers an opportunity to examine the role of Southern Ocean as a driver and detector of global changes. A multi-disciplinary study focusing on the interaction between sea ice dynamics, biogeochemical cycles, and ecosystem process on board the new research ice breaker will be one of the major thrusts in Korea Polar Program's research for the next several years. A preliminary implementation plan including study sites and field activities will be introduced. Contribution from the international expertise will be sought with discussion on possible collaboration.

**WORKSHOP ON
CLIMATE CHANGE
AND
POLAR OCEAN SYSTEM**

SESSION 2

THE ARCTIC OCEAN

MARINE GEOLOGICAL AND GEOPHYSICAL SCIENCE IN A RAPIDLY CHANGING ARCTIC

Julian A. Dowdeswell¹

¹Scott Polar Research Institute, University of Cambridge, Cambridge CB2 1ER, UK
jd16@cam.ac.uk

The Arctic is predicted to be the most sensitive part of the global climate system in the coming century. Environmental change is already affecting the Arctic cryosphere in terms of summer sea-ice cover and the shifting dynamics of fast-flowing outlet glaciers draining the Greenland Ice Sheet. Although likely to be variable from year to year, less severe summer sea-ice allows geophysical research vessels to collect high-quality data in locations that were previously very difficult to reach. In addition, the fjords and continental shelves of the Arctic seas continue to provide an archive of past environmental and cryospheric change, which is a baseline against which modern changes can be compared. Many parts of the seas fringing the Arctic Ocean are little known in terms of their environmental and glacial history. Examples include the following. There are large fan systems, fed by full-glacial ice streams draining the Eurasian and northernmost Laurentide ice sheets that are largely uninvestigated. Little is known about the past extent and dynamics of ice in the Sea of Okhotsk and east of Kamchatka. The puzzle around the question of whether there was a huge floating Arctic ice shelf at some time in the Quaternary also remains. In each of these areas, marine geological and geophysical investigations can help us to provide greater understanding.

A PERSPECTIVE ON FUTURE OBSERVATIONAL RESEARCH TO UNDERSTAND THE FATE OF ARCTIC OCEAN AND GLOBAL CLIMATE

Koji Shimada

Faculty of Marine Science, Department of Ocean Sciences,
Tokyo University of Marine Science and Technology
koji@kaiyodai.ac.jp

INTRODUCTION

The rate of recent sea ice reduction is beyond any projections of global climate model. Model results show spatially symmetric reduction pattern of sea ice cover from the low latitude toward the pole. However, the actual sea ice reduction occurs from the Pacific sector as mentioned in the first day of this symposium. This difference is crucial to predict the fate of Arctic climate.

CHANGES IN CLIMATE PATTERN (MERIDIONAL PATTERN)

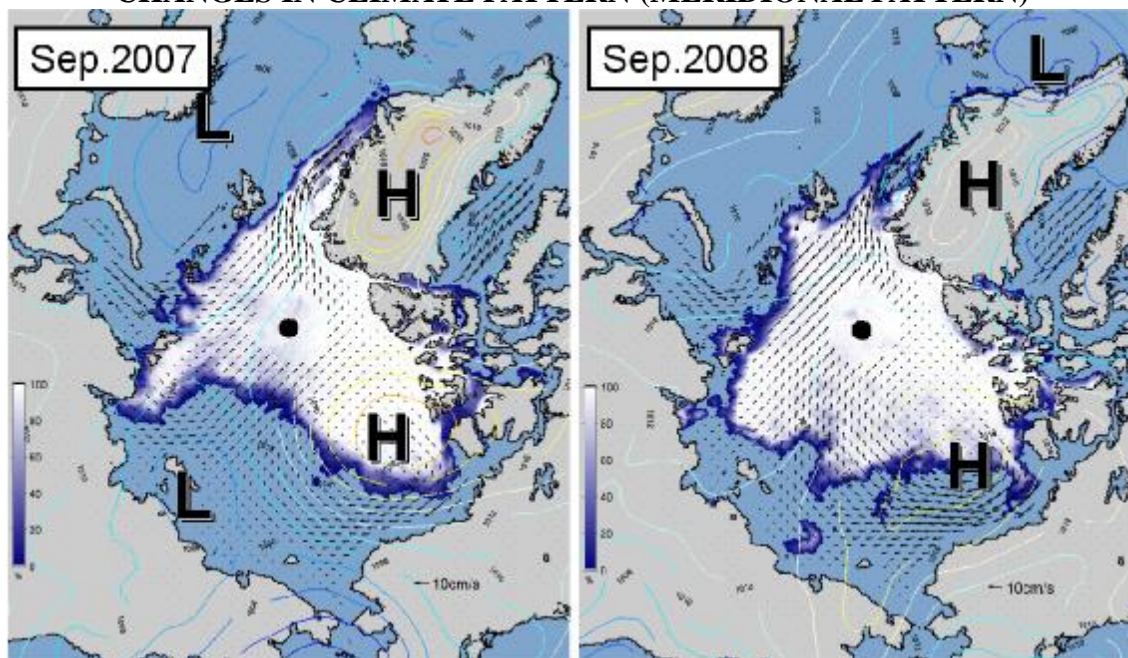


Figure 1. Sea ice cover with sea level atmospheric pressure field in September, 2007 (left) and 2008 (right). In 2007, asymmetric sea ice cover in zonal direction establishes meridional atmospheric circulation pattern (dipole pattern in SLP) north of the Bering Strait. This enhances further retreat of sea ice cover in the Pacific sector of the Arctic Ocean. In 2008, however, the meridional pattern was not settled.

We have mentioned the importance of zonally asymmetric sea ice distribution to understand the acceleration of sea ice retreat in the summer of 2007. This sea ice distribution easily set up a dipole pattern of atmospheric circulation that brought southerly wind from the Pacific toward the Arctic. This meridional circulation pattern of atmosphere enhanced the melt of first year ice in the Pacific Sector (Figure 1). It means that heat exchange between high latitude and mid-latitude is enhanced. The sea ice changes in the Arctic Ocean are important not only for Arctic regional climate but also for global climate. In 2008, such asymmetry was not settled (Figure 1) due to rapid and huge deliveries of heavy multiyear ice from near Canadian Archipelago to the north of East Siberian Sea (Figure 2). In the Pacific sector, zonal contrast of sea ice cover was not apparent. High SLP (Sea Level Pressure) field was extended from the Canadian side toward the Siberian side (Figure 1). Consequently, the dipole pattern observed in 2007 was not established. The meridional atmospheric circulation pattern was considerably weaker than that in 2007. As the result, some part of thin first year ice could survive the summer season.

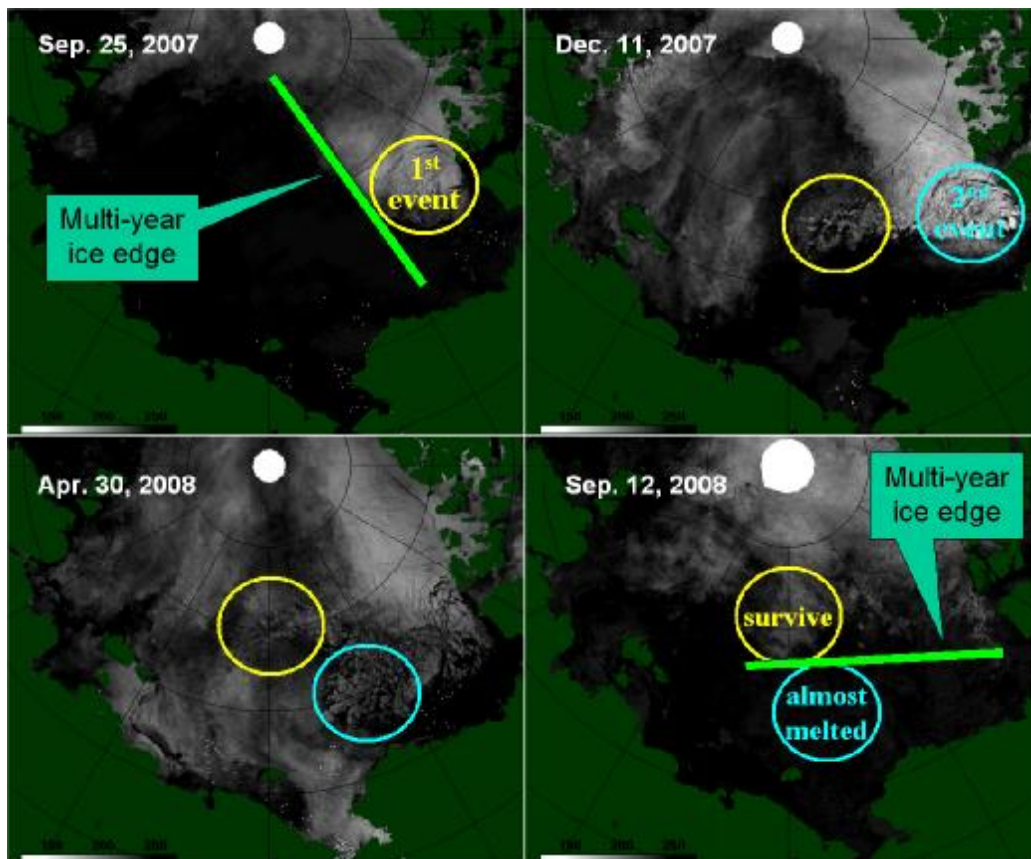


Figure 2. Sequences of brightness temperature of AMSR-E 89GHz vertical channel. Crash of multiyear ice (white color) occurred near the Banks Island. Multi year ice stored near the coast of Canadian Archipelago was crashed. The fragmental multi year ice was rapidly carried to western Canada basin north of Bering Strait / East Siberian Sea.

WHAT IS GOING ON THIS YEAR? (A PERSPECTIVE OF 2009 SUMMER)

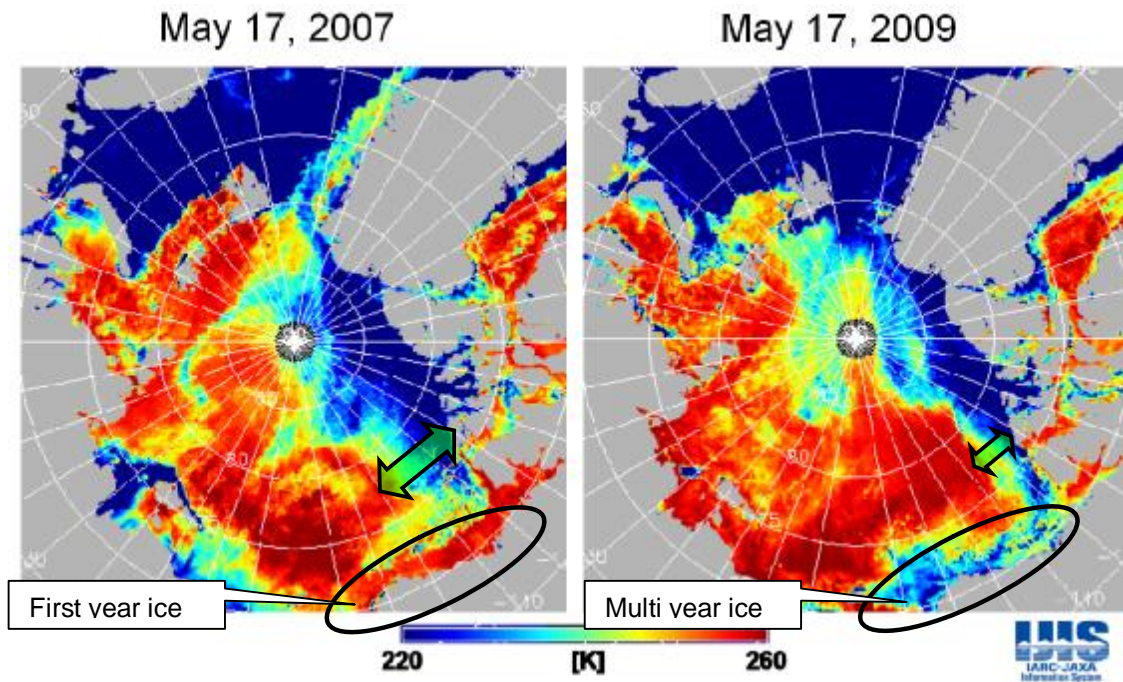


Figure 3. Brightness temperature of AMSR-E 36.5GHz vertical channel for May 17, 2007 (left) and 2009 (right).

Figure 3 shows the brightness temperature of 36GHz vertical channel for May 17, 2007 and 2009. The multiyear ice tongue near the Canadian Archipelago, where the warm Pacific Summer Water spreads toward east, is now getting smaller its area and width. This suggests that sea ice growth was not so effective along the circulation pathway of the warm Pacific Summer Water. As the result, the thinner multi year ice near the coast off Canadian Archipelago was not so strong against the internal stress. In a condition beyond the critical value of the internal stress, large but thin multi year ice floe was easily broken into fragmental pieces of small ice floe. The fragmented feature of sea ice set up more slip condition near the coast. As the result, sea ice motion was further activated there even if the wind forcing was not changed. During the winter season of 2008/2009, the sea ice motion was not parallel to the Alaskan coast due to slight change in wind angle in the southern Canada Basin. The delivered ice near the Alaskan coast was piled up. Consequently, ice property near the Alaskan coast in the spring of 2009 was quite different from that in 2007 (Figure 3). This summer, the heavy ice band will remain until the late summer or survive the summer season. This ice band would affect the climate pattern of forthcoming summer. In addition, the ice band would also affect the ecosystem of the Pacific Sector of the Arctic Ocean.

RECOMMENDATION

In order to understand the sequential changes among ice-ocean-atmosphere system in the Arctic, we should monitor the first domino that initiates the sequential changes (positive feedback). The physical environmental changes also affect the biogeochemical environment, e.g. nutrient rich water circulation, light condition, summer time ice covers for the ecosystem. We should establish sustaining observing networks not only by integration of existing observations, but also by the systematic linkages of observations to quantitatively evaluate the mechanism of the feedback loop and associated environmental changes. The current climate model is not sufficient to demonstrate the key features that were observed in the real Arctic. We often see the following sentence; “The rate of recent sea ice reduction is beyond any projections of global climate model.” This means the current climate model is insufficient to predict the fate of the Arctic climate. Now we need to look carefully real Arctic Ocean with scientific perspective.

SEA ICE VARIABILITY IN THE CHUKCHI BORDERLAND OF THE ARCTIC OCEAN

B.J. (Phil) Hwang¹ and Jeremy Wilkinson¹

¹The Scottish Association for Marine Science, Dunstaffnage Marine Laboratory,
Oban, Argyll, United Kingdom, PA37 1QA
Phil.Hwang@sams.ac.uk

Over the past two decades, the Arctic sea ice has been significantly declined in its horizontal extent (Stroeve et al. 2007), and likely its thickness (Rothrock et al., 2003). Until 1995 the strongest negative trend in sea ice concentration mostly occurred in the East Siberian Sea. This was attributed to dominant positive phase of winter Arctic Oscillation (AO) index during 1989-1995 and the associated changes in sea ice dynamics (Rigor and Wallace, 2004). Since 1995, the centre of strong negative trend in September sea ice concentration has been shifted from the East Siberian Sea to the Chukchi Borderland (CBL) region. The possible causes for this shift are i) changes in atmospheric circulation (Maslanik et al. 2007), ii) advection of ocean heat flux from Pacific (Shimada et al. 2006) and North Atlantic (Polyakov et al. 2007) waters, iii) enhanced solar heating of the upper ocean (Perovich et al. 2008), vi) and low-level clouds (Francis and Hunter, 2006). It appears all these factors contribute the negative sea ice trend in the CBL region, but it is still in debate which mechanism is most dominant or how these mechanisms are interacted with one another in the complex atmosphere-sea ice-ocean system.

Here we briefly present the year-to-year variability of sea ice parameters (concentration, breakup/freeze dates and ice motion) and how the sea ice variability can be interpreted in the context of atmospheric/oceanic variability in the CBL region, which can provide an insight on further understanding of possible forcing mechanisms. We introduce innovative in-situ and satellite observation technologies that can be used to address questions about forcing mechanisms and changing ice type: self-floating ice mass balance buoy and high resolution ice motion/the age of sea ice. We propose a discussion of how the reduction of sea ice is translated to changing ice type in that region, i.e., from multiyear ice to seasonal ice and more frazil/pancake/ice sheet cycle, and how this transition affect ice growth rate, brine drainage and bio-geo-chemical processes.

A BRIEF VIEW OF SEA ICE VARIABILITY

The variability of sea ice variables (e.g. concentration, breakup/freezeup dates, ice motion) contains a “visible” clue for how those mechanisms interact with one another and affect sea ice condition. Here we present a preliminary analysis. It clearly shows the strong negative trend in September sea ice

Concentration from 1979 to 2007 in the CBL region (Figure 1). Within the negative trend, there is significant interannual variation (Figure 2). As 2007 anomaly clearly stands out, it shows less ice condition (early breakup and late freezeup) during 1997-1999 and 2002-2004 summers and more sea ice condition (late breakup and early freezeup) during 2000-2001 and 2005-2006 summers (Figure 2). What makes such contrasting sea ice conditions between these two periods? One of contrasting feature between high and low ice conditions can be found in the ice dynamics. For example, during 1997-1998 the ice motion was consistently westward from November to June, and this continuously brought the ice flux from the Southern Beaufort Sea to the CBL region (not shown here). Similar consistent westward ice motion occurred during December 2006 to February 2007. This consistent ice motion could efficiently have brought thinner first-year ice formed in the Southern Beaufort Sea region (Figure 3), which could quickly melt by increasing oceanic heat flux (from Pacific water or solar heating). In 2000 the westward ice motion was not consistent and tended to bring the ice flux from the central Beaufort Sea or the East Siberian Sea (Figure 3). This would cause the influx of thicker ice and less intrusion of Pacific waters. Ice motion data with multiyear ice area can provide us an insight for possible causes associated with sea ice variability in the CBL region, but it does not give us the complete picture. More in-depth studies are further required.

IN-SITU AND SATELLITE OBSERVATION

Here we briefly introduce some of techniques to assist us for more accurate in-depth analysis of sea ice variability and associated forcing mechanisms.

Higher resolution ice motion and age algorithm: As shown above, it is a great deal to know the thickness (or type) of ice and where the ice is originated. Now high-resolution ice motion data is available from ASAR/Envisat and an algorithm to calculate the age of sea ice using the ASAR ice motion data is underway. This algorithm allows us to calculate the age distribution (a proxy of thickness) and trace back the origin of the ice in higher resolution and more reliable way.

Self-floating ice-mass-balance buoy: The buoy can be deployed in open water during summer season, and it can be frozen in as ice is formed around it. This allows us to record the evolution of air, ice and water temperature and ice thickness throughout complete freezeup/breakup cycle.

CHANGING ICE TYPE

It should be noted that the reduction of sea ice does not mean total disappear of sea ice in that region, but changing ice type: from multiyear ice to seasonal ice and longer duration of open water. Prolonged open water duration would be in favor of rough sea state and pancake ice formation. This ice formation cycle, different from the ice formation in calm water, can affect the amount of brine input to the upper ocean, the mechanical strength of the ice and the freezeup/breakup rate of ice. This changing ice type would have significant impact on bio-geo-chemical process in that region.

REFERENCES

- Francis, J.A., and E. Hunter, (2006), New insight into the disappearing Arctic sea ice cover, *Eos Trans.*, AGU, 67, 509-511.
- Perovich, D.K., J.A. Richter-Menge, K.F. Jones, and B. Light, (2008), Sunlight, water, and ice: Extreme Arctic sea ice melt during the summer of 2007, *Geophys. Res.*

Let., 35, L11501, doi:10.1029/2008GL034007.

Rigor, I.G., and J.M. Wallace (2004), Variations in the age of Arctic sea-ice and summer sea-ice extent, *Geophys. Res. Lett.*, 31, L09401, doi:10.1029/2004GL019492.

Rothrock, D.A. et al. (2003), The Arctic ice thickness anomaly of the 1990s, *J. Geophys. Res.*, 108(C3), 3083, doi:10.1029/2001JC001208.

Rigor, I.G., and J.M. Wallace, (2004), Variations in the age of Arctic sea ice and summer sea-ice extent, *Geophys. Res. Lett.*, 31, L09401, doi:10.1029/2004GL019492.

Shimada et al (2006), Pacific Ocean inflow : Influence on catastrophic reduction of sea ice cover in the Arctic Ocean, *Geophys. Res. Lett.*, 33, L08605, doi:10.1029/2005GL025624.

Stroeve J., et al. (2007), Arctic sea ice decline: Faster than forecast, *Geophys. Res. Lett.*, vol. 34, L09501, doi: 10.1029/2007GL029703.

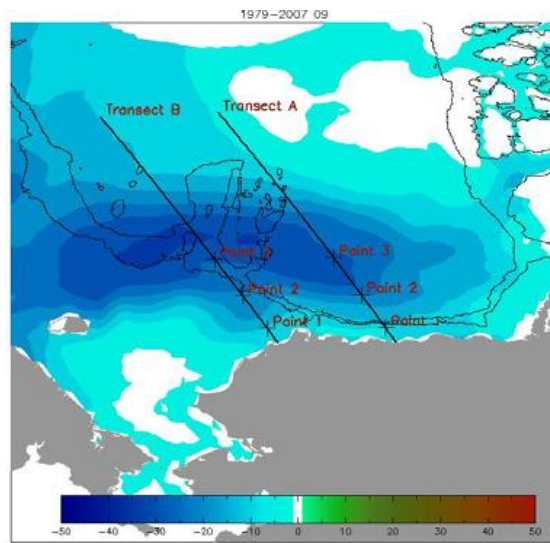


Figure 1 Linear trend of September sea ice concentration from 1979 to 2007. (note: ice concentration data from NSIDC).

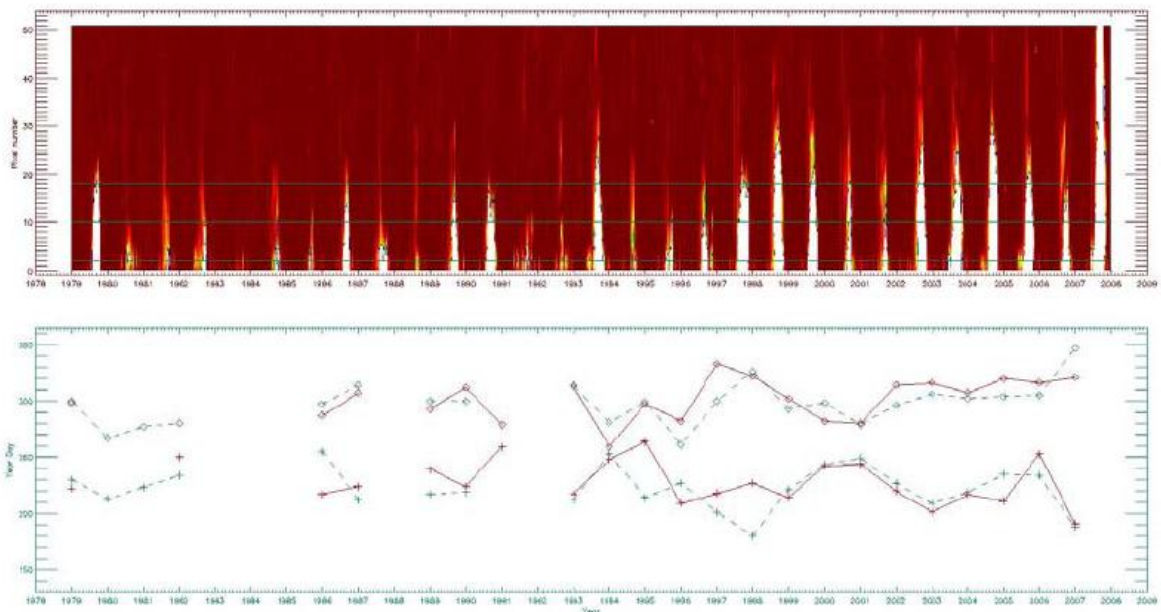


Figure 2 a) Interannual variations of sea ice concentration along the transect line B. b) breakup (+) and freezeup (diamond) dates at Point 1 in transect line A (dotted green)

line) and B (solid red line). (note: ice concentration data from NSIDC).

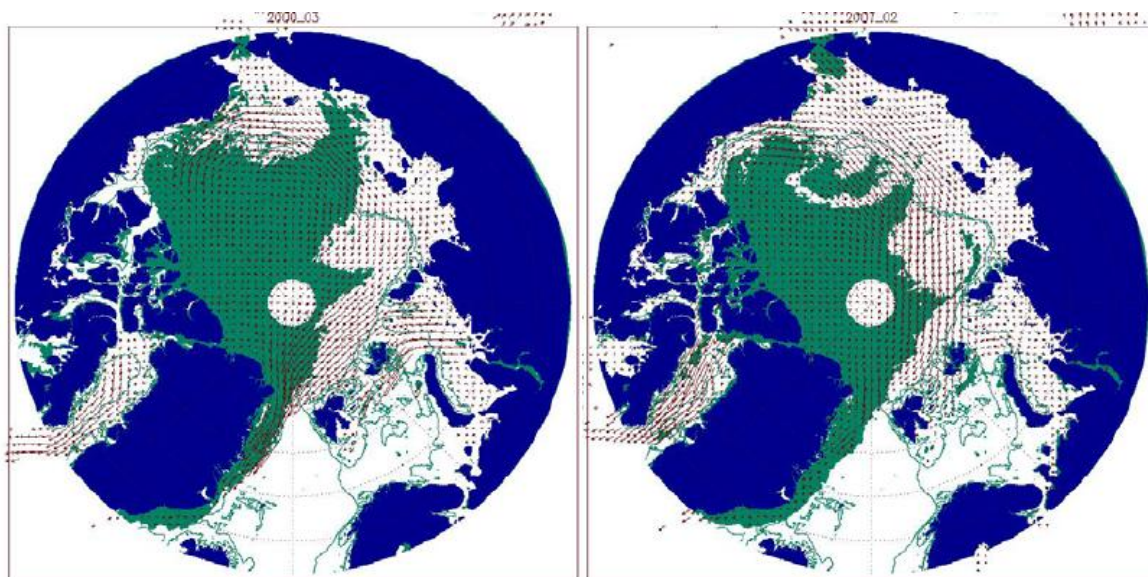


Figure 3 Monthly ice motion (red arrow) overlaid with multiyear area (green colored area) for March 2000 (left) and February 2007 (right). The multiyear ice area was estimated from QuikSCAT images by using a simple threshold technique (note: ice motion data from NSIDC and QuikSCAT data from BYU)

SEA ICE MASS BALANCE

Jeremy Wilkinson¹, Phil Hwang¹ and Ted Maksym²

¹ Scottish association for Marine science, Scotland, UK
jeremy.wilkinson@sams.ac.uk

² British Antarctic Survey, Cambridge, UK

Understanding the mass balance of sea ice, i.e. its growth and melt, is key to elucidating the reasons behind the dramatic changes we have recently witnessed in the Arctic sea ice cover as well as possible changes in the Antarctic sea ice cover. At present no satellite sensor is able to directly monitor the thickness of sea ice. We have therefore had to rely on in situ measurement campaigns to gather mass balance data. Recently two novel instruments have been developed to autonomously monitor sea ice thickness; the Autonomous Underwater Vehicle and the Ice mass Balance buoy. In this presentation we will discuss results from these technologies as well as collaborative possibilities for joint research in the Bellingshausen Sea in November 2010.

PARTICULATE ORGANIC CARBON CYCLE IN THE DEEP CANADA BASIN

Jeomshik Hwang^{1,2}, Timothy I. Eglinton², Steven J. Manganini²

¹. Pohang University of Science and Technology (POSTECH), Pohang, Korea

². Woods Hole Oceanographic Institution, Woods Hole, MA 02543, USA

Understanding the carbon cycling and its sensitivity to perturbation is an important basis for assessing the impact of anthropogenically-driven climate change in the Arctic Ocean. However, our knowledge of the operation of the carbon cycle in the Arctic Ocean, especially under the ice-covered central Arctic basins, is severely hampered by the paucity of information on fluxes and fate of biogenic materials exported from the surface waters to the ocean interior.

We analyzed sinking particles intercepted by a sediment trap deployed at shallow depth (120m) via an ice tethered mooring during the SHEBA (Surface HEat Budget of the Arctic Ocean) in 1997/1998, and by a sediment trap moored at 3000m depth in the southwest Canada Basin under the marginal ice zone (MIZ) in 2004/2005 and 2007/2008. Primary production and mixing with resuspended sediment laterally transported from local or distant sources appear to be major processes that are responsible for the observed fluxes and composition of the particles, and radiocarbon isotopes. In particular, aluminum concentrations were negatively correlated with $\Delta^{14}\text{C}$ values implying that pre-aged organic matter was associated with lithogenic debris. In the deep Canada Basin, the low average $\Delta^{14}\text{C}$ value (-217 per mil), and high abundances of lithogenic debris ($\sim 80\%$) imply that the majority of the particles derive from lateral advection. The contribution of primary production to POC in the deep Canada Basin estimated by radioisotope mass balance was less than 20%. Taken together, these findings indicate the operation of lateral carbon pump in the present-day Canada Basin. How organic carbon dynamics will change in the face of decreasing ice cover and increasing terrestrial organic carbon fluxes is the subject of on-going studies.

THE MALINA PROJECT: CARBON CYCLING AND RETROSPECTIVE PALEOCLIMATIC APPROACH IN THE MACKENZIE BAY, ARCTIC OCEAN.

I.Tolosa¹, J.C. Miquel¹, J. R. Oh¹, M. Babin²

¹Marine Environmental Laboratories, International Atomic Energy Agency, 4 Quai
Antoine 1^{er}, MC-98000 Monaco
I.Tolosa@iaea.org

²Laboratoire d'Océanographie de Villefranche, Observatoire Océanologique,
INSU/CNRS/UPMC, UMR 7093, BP 08, F 06230 Villefranche-sur-Mer, France

INTRODUCTION

We currently witness in the Arctic a decrease in summer ice cover that exposes sea surface to solar radiation and physical forcings. Organic carbon previously sequestered in the Tundra is, possibly, increasingly exported to the ocean because of combined permafrost thawing and enhanced river runoff. These phenomena may favour the mineralization of organic carbon through photo-oxidation and bacterial activity, and thus amplify the atmospheric CO₂ concentration. At the same time, the exposure of a larger fraction of ocean surface to sunlight and the increase in nutrients imported by rivers may lead to a larger autotrophic production and thus to a sequestration of atmospheric CO₂. Will the Arctic Ocean become a new net source or net sink of CO₂? To predict the balance between source and sink processes, an extensive field study in the Mackenzie River/Beaufort Sea system will take place in July-August 2009 on board of the Canadian research icebreaker CCGS Amundsen. This oceanographic cruise is a major stage of the Malina project, which is funded in France by CNRS, ANR, CNES and ESA, in Canada by NSERC, and in USA by Nasa and NSF (see also the website www.obs-vlfr.fr/Malina). The project, running from 2009 to 2012, is also tightly coordinated with a major Canadian project, the Network of Centres of Excellence of Canada ArcticNet. The consortium of partners includes cutting-edge expertise on every aspect of the Project (processes, modelling and remote sensing) and specialists of the Arctic Ocean. Some 66 scientists, technicians and postdocs from 17 different laboratories will contribute to the Project.

The general objective of the MALINA project is to determine the impact of climate change on 1) the fate of terrestrial carbon exported to the Arctic Ocean, 2) on the photosynthetic production of organic carbon, and 3) on microbial diversity. In the framework of the Project, IAEA-MEL (Marine Environment Laboratories of the International Atomic Energy Agency) will participate in the scientific expedition and will contribute to the marine biogeochemical studies of the particulate matter and to the

reconstruction of the past climate.

STUDY AREA, SAMPLING AND METHODS

The geographic region of the Arctic Ocean that will be more specifically studied in this project is the continental shelf off the Mackenzie River delta in the Beaufort Sea. The Mackenzie river is the major contributor of particulate organic matter to the Arctic, and the third most important for the export of total (dissolved and particulate) organic carbon of terrestrial origin (Rachold et al. 2004). Figure 1 shows the study area and an schematic presentation of the different sites to be sampled in July-August 2009 on the Canadian research icebreaker CCGS Amundsen.

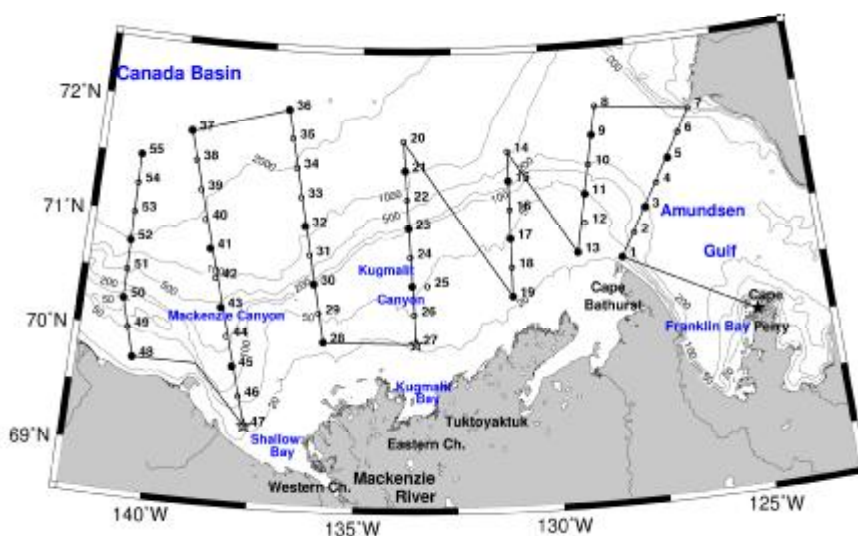


Fig. 1. Study area of the MALINA project and schematic presentation of the different sites to be sampled in July-August 2009. The final cruise track will be adapted to the ice-coverage of the area at the period of the cruise.

In-situ pumps will be used to filter large volumes (100 to 900 liters) of water and to collect particles. These pumps deployed at different depths and together with water samples obtained from Niskin bottles on a Rosette sampler, provide a unique tool to study vertical profiles of radionuclides, organic compounds and inorganic chemical elements. Drifting sediment traps will be deployed in the field during few days to directly assess the vertical flux of particles, radionuclides, carbon and associated elements.

Sediment cores will be collected using box and gravity corers along an inshore-offshore transect extending to the shelf break. Cores will be dated to identify suitable cores for further proxy record reconstructions.

A nuclear technique using the disequilibrium between natural uranium and thorium in sea water will be used to indirectly estimate the removal of biologically produced carbon from the upper ocean through its vertical transport to the depths; data

will be compared with carbon flux measurements using the drifting sediment traps

(Miquel et al., 2006); lipid biomarker analyses and the recently developed Gas Chromatography-Combustion-Isotope Ratio Mass Spectrometry (GC-C-IRMS) will be used for the determination of the $\delta^{13}\text{C}$ of specific lipid biomarkers (Tolosa and de Mora, 2004).

CARBON CYCLING

The evaluation of sources, fluxes and fate of the particulate matter are fundamental for understanding carbon cycling in the ocean. Nuclear techniques based on natural radionuclide measurements will be used for quantifying particle and carbon fluxes. The spatial distribution of organic carbon stocks in the water column and sediments will be determined on the shelf and further offshore. The lipid biomarker composition of the particles and their $\delta^{13}\text{C}$ will be investigated to distinguish the different sources of carbon (e.g., marine, terrestrial, bacterial) and to elucidate the transport and degradation processes of organic material through the water column.

Diagnostic models of the studied processes (primary production, bacterial activity and light-driven mineralization of organic matter) will be combined with a coupled physical-biological ecosystem model. The obtained results together with outputs from global climate models will be applied to predict carbon cycling in the Arctic Ocean during the next decades under different climate change scenarios.

RETROSPECTIVE PALEOCLIMATIC APPROACH

An alternative approach to determine the future impacts of global warming on the processes that are of interest to Malina is to reconstruct high-resolution records of past climatic events and to determine their impact on the study area. We will therefore conduct an additional study using selected organic proxies measured in undisturbed sediment cores spanning over the last millennium to evaluate the changes 1) the Mackenzie river freshwater outflow, 2) the organic carbon export from the Mackenzie river, 3) bacteria abundance, and 4) changes in sea-ice abundance. This time interval encompasses the little ice age (1400-1800 year A.D.) and the medieval climatic optimum (1000-1400 year A.D.), two major climatic episodes of the recent past.

We will measure the concentration of organic carbon, and the contributions of terrigenous and marine organic carbon using a number of proxies (C/N ratio, $\delta^{13}\text{C}$) and lipid biomarkers (n-alkyl compounds, e.g., Pancost and Boot 2004; and marine sterols, e.g. Volkman, 1996). The abundance of bacterially derived organic matter and/or the degree of bacterial reworking will be inferred from analysis of fatty acids and bacteria related hopanoid biomarkers. Other specific lipid biomarkers together with their stable isotope composition will be used as proxy data to reconstruct temperature, sea ice abundance, marine productivity, terrigenous input, as well as to assess basin-wide vegetation on geological timescales.

REFERENCES

- Miquel , J.C., B.Gasser , A. Rodriguez y Baena , S.W. Fowler , J.K. Cochran, 2006. Carbon Export Assessed by Sediment Traps and ^{234}Th : ^{238}U Disequilibrium during the Spring Summer Transition in the open NW Mediterranean. In: *Isotopes in Environmental Studies*, IAEA-CSP-26, IAEA, Vienna, 97-98.
- Pancost, R.D. and Boot, C.S., 2004. The palaeoclimatic utility of terrestrial biomarkers in marine sediments. *Marine Chemistry*, 92(1-4): 239-261.
- Rachold, V., H. Eicken, et al. (2004). Modern Terrigenous Organic Carbon input to the Arctic Ocean. *The organic carbon cycle in the Arctic Ocean*. R. Stein and R. W. MacDonald. Berlin, Springer: 33-41.
- Tolosa, I. and de Mora, S., 2004. Isolation of neutral and acidic lipid biomarker classes for compound-specific-carbon isotope analysis by means of solvent extraction and normal-phase high-performance liquid chromatography. *Journal of Chromatography A*, 1045, 71-84.
- Volkman, J.K., 1986. A review of sterol markers for marine and terrigenous organic matter. *Organic Geochemistry*, 9, 83-99.

THE PICOPLANKTON IN THE ARCTIC OCEAN IN SUMMER 2008

Jianfeng He¹, Ling Lin^{1,2}, Fang Zhang¹, Minghong Cai¹, Wei Luo¹

¹Key Laboratory for Polar Science of State Oceanic Administration, Polar Research
Institute of China, Shanghai 200136, China

²College of Life Science, East China Normal University, Shanghai 200062, China

ABSTRACT

Using a flow cytometer onboard the R/V Xuelong, horizontal and vertical distribution of picoplankton were examined in the subarctic Pacific and Arctic Ocean in summer 2008 during the 3th Chinese Arctic cruise. In the Bering Sea, *Synechococcus*, picoeukaryotes and heterotrophic bacteria constituted major part of picoplankton and reached an abundance of 4.13×10^4 , 3.07×10^4 and 6.11×10^5 cells ml⁻¹, respectively. Major oceanic distribution of *Synechococcus* appeared between latitudes 53°N and 60°N, and most of the high abundance of *Synechococcus* occurred in the upper 100 m water column. In the Arctic Ocean, picoeukaryotes and heterotrophic bacteria constituted major part of picoplankton and could reach an abundance of 1.96×10^4 and 1.09×10^6 cells ml⁻¹, respectively. An exception of *Synechococcus* distribution was examined at Chukchi Sea at Station R05-2. The high abundance of picoeukaryotes of the central Arctic Ocean was observed in the water column between 50 and 75 m depths.

*: The study was financially supported by the National Nature Science Foundation of China (40576002, 40806073), and the Science and Technology Committee of Shanghai, China (052307053).

The 16th International Symposium on Polar Sciences
Incheon, Korea, June 10-12, 2009
Korea Polar Research Institute

**NEW U.S. ICE-CAPABLE RESEARCH VESSEL - NEW OPPORTUNITIES FOR
COLLABORATION**

Terry Whitledge

**COLLABORATION OPPORTUNITIES WITH THE INTERNATIONAL ARCTIC
RESEARCH CENTER (IARC)**

C. Peter McRoy, Larry Hinzman, John Walsh and Elena Sparrow

International Arctic Research Center, University of Alaska Fairbanks, USA

ABSTRACT

IARC's mission is to foster arctic research in an international setting to help the nation and the international community to understand, prepare for and adapt to the pan-arctic impacts of climate change. International collaboration focusing on comprehensive studies of the arctic system is the core of the institute. This collaboration occurs through joint research projects and expeditions, visiting researchers, shared datasets and networks, workshops, model development and public interactions. IARC has access to numerous arctic resources and serves as a gateway and liaison between researchers and institutions in many countries. Promoting and fostering these activities in the pan-arctic scientific community is a constant driving force of the institution. IARC is a source of climate information and has taken a central role in facilitating development of an Arctic System Model. The physical, chemical, biological and social components of the arctic are interrelated and require a holistic perspective from multi-national research efforts to advance predictive capabilities, thereby helping to prepare society for environmental change and its impact on humans, ecosystems, and the global climate. On this occasion celebrating the launch of the new icebreaker in Korea, the R/V Araon, the faculty and staff of IARC wish KOPRI every success and look forward to collaborating with you to meet the challenge of the changing Arctic.

KOREAN LONG-TERM OBSERVATION IN THE WESTERN ARCTIC ECOSYSTEM

Sang H. Lee

Polar Environmental Research Division, Korea Polar Research Institute, Incheon 406-840, Republic of Korea
sanglee@kopri.re.kr

ABSTRACT

Recently, it was found that higher temperatures along with a possible increase in the ice export have decreased the extent and thickness of perennial sea ice in the Arctic Ocean over the past 40 years and produced more open water especially in the western Arctic Ocean (Rothrock et al. 2003; Perovich and Richter-Menge 2009). The changes in climate on many scales influence the ecosystems in different regions of the Arctic Ocean. The study regions for the Korean Long-term Observation will be the Bering Strait/Chukchi Sea and Canada Basin in the western Arctic Ocean. Intensive long-term observation for the ecosystem in these regions is specifically urgent because physical environments, especially ice extent and thickness, are currently changing faster than other regions in the Arctic Ocean. The main goals of the Korean program will be to integrate the effects of climate change across spatial and temporal scales based on a long-term observation in the western Arctic Ocean, lay the groundwork for the future monitoring of ecosystem response to ongoing climate and environmental changes, and consequently predict the impacts of current climate and environmental changes on the marine ecosystems in the western Arctic Ocean.

INTRODUCTION AND RATIONALE

Over the past few decades, the environments in the Arctic have been changing at a very rapid rate. The higher temperatures plus a possible increase in ice export have decreased the ice extent and sea-ice thickness in the Arctic Ocean over the past 40 years contributing to more open water, especially in coastal regions (Rothrock et al. 2003). Laxon et al. (2003) expect additional thinning of Arctic sea ice with the continued increase in melt season length. In addition, the average annual discharge of fresh water from the six largest Eurasian rivers to the Arctic Ocean increased by 7 % from 1936 to 1999 (Peterson et al. 2002). These environmental and climate changes may alter the marine ecosystem in the Arctic Ocean. For examples, these changes may alter the relative contributions of sea ice algae and phytoplankton, with respect to the species and/or size composition of primary producers, and the new and total primary production that is occurring. In fact, Melnikov et al. (2002) found the physical-chemical characteristics of sea ice and the biological structure of ice communities in 1997-1998 were very different from conditions during the 1970s, based on comparisons of SHEBA

results with historical data. Moreover, the current environmental changes in the Arctic Ocean might lead to different compositions in photosynthetic-end products of sea ice algae and phytoplankton, which could affect the nutritional status of higher trophic levels. As a consequence, the seasonal distributions, geographic ranges, and nutritional structure of zooplankton and higher trophic levels such as seals and whales have been projected to be altered in the Arctic Ocean (Tynan and DeMaster 1997). Therefore, in order to understand and assess the marine ecosystem response to ongoing environmental changes in the Arctic Ocean, evaluation for many different variations; geographical/seasonal/interannual variations, should be immediately conducted based on a long-term observation.

MAIN STUDY AREAS AND RESEARCHES IN THE ARCTIC OCEAN

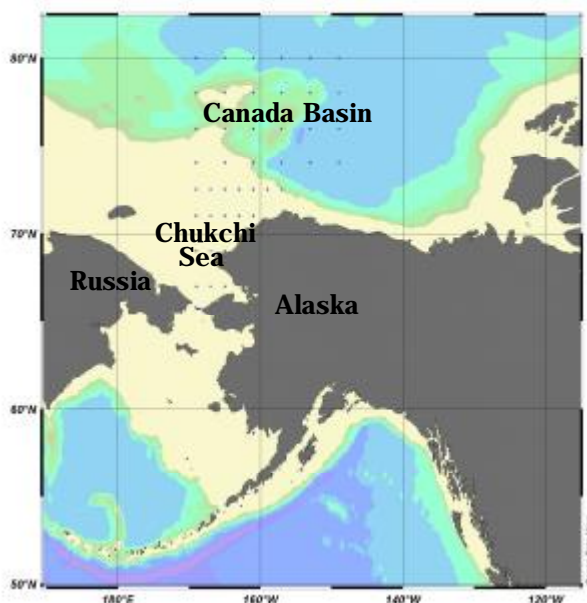


Fig. 1. Proposed main study regions in the western Arctic Ocean

The main study regions for the Korean Arctic Long-term Observation program will be Bering Strait/Chukchi Sea and Canada Basin in the western Arctic Ocean. It is important to understand the ecosystem related to physical and chemical dynamics in the Bering Strait and Chukchi Sea in order to monitor the arctic marine ecosystem, since they are only conduit connecting between the north Pacific and Arctic Oceans. In addition, the understanding of the ecosystem in the Canada Basin, as one of the least known region in the Arctic Ocean which is mostly covered by multi-year or first-year ice, is specifically urgent because of a fast rate of the environment changes in the basin. Thus, the main goal of the Korean program is to understand and predict the impacts of climate and environmental changes on the marine ecosystems of the western Arctic Ocean.

BIOPHYSICAL MECHANISMS OF SEA ICE

The recent reduction of ice-cover is a predominantly spring-summer phenomenon (Chapman and Walsh 1993) and consequently there would be some changes such as the relative amount of primary production, timing of blooms, and physiology of primary producers under the ice cover. However, the underlying mechanisms are not well understood since there have been few recent studies about ice algae or related water column phytoplankton in different locations and different ice

types in the Pacific Arctic Ocean. Therefore, an understanding of how changing sea ice conditions affect phytoplankton production and the importance of sea ice algal production to total primary production will provide insights into the impact of predicted further reductions of sea ice extent and thickness on the primary production and consequently upper trophic levels.

AIMS AND SCOPES

Our specific research objectives are to:

- (1) Keep monitoring and thus storing basic physical-chemical-biological parameters such as S/T profiles, major nutrients, Chl-a concentration, productions and species compositions of phytoplankton, ice algae, zooplankton, and benthos.
- (2) Quantify seasonal, regional, annual variations of the basic parameters
- (3) Assess the marine ecosystem responding to the current and ongoing environmental changes in the Chukchi Sea and Canada basin of the Western Arctic Ocean.
- (4) Develop a 3-D coupled ice-ocean-biological model in the Western Arctic Ocean.

REFERENCES

- Chapman WL, Walsh JE (1993) Recent variations of sea ice and air temperature in high latitudes. *Bull Am Meteorol Soc* 74(1):33-47
- Laxon S, Peacock N, Smith D (2003) High interannual variability of sea ice thickness in the Arctic region. *Nature* 425:947-950
- Melnikov IA, Kolosova EG, Welch HE, Zhitina LS (2002) Sea ice biological communities and nutrient dynamics in the Canada Basin of the Arctic Ocean. *Deep Sea Res I* 49:1623-1649.
- Perovich DK, Richter-Menge JA (2009) Loss of sea ice in the Arctic. *Annu. Rev. Marine. Sci.* 1: 417-441.
- Peterson BJ, Holmes RM, McClelland JW, Vörösmarty CJ, Lammers RB, Shiklomanov AI, Shiklomanov IA, Rahmstorf S (2002) Increasing river discharge to the Arctic Ocean. *Science* 298:2171-2173.
- Rothrock DA, Zhang J, Yu Y (2003) The arctic ice thickness anomaly of the 1990s: A consistent view from observations and models. *J Geophys Res* 108 (C3):28-1-28-10
- Tynan CT, DeMaster DP (1997) Observations and predictions of Arctic climatic change: Potential effects on marine mammals. *Arctic* 50:308-322

POSTER SESSION 1

GEOLOGY & GEOPHYSICS

HYDROTHERMAL ALTERATION AND ISOTOPIC VARIATIONS OF IGNEOUS ROCKS IN BARTON PENINSULA, KING GEORGE ISLAND, ANTARCTICA

Dongbok Shin¹, Jong-Ik Lee², Jeong Hwang³, and Soon-Do Hur²

¹Dept. of Geoenvironmental Sciences, Kongju Nat'l University, Kongju, Korea
shin@kongju.ac.kr

²Korea Polar Research Institute, Korea Ocean Research & Development Institute,
Incheon, Korea

³Dept. of Geological Engineering, Daejeon University, Daejeon, Korea

INTRODUCTION

Though the characteristics of hydrothermal fluids in Barton peninsula, King George Island, has been discussed so far, it still remains unclear what types of igneous activities were related to hydrothermal fluids, and how the fluids evolved through fluid-rock interaction during hydrothermal processes. Thus, O, H, S and Sr isotopes were investigated to characterize the nature of hydrothermal fluids and alteration processes in volcanic and intrusive rocks in Barton Peninsula.

ISOTOPIC COMPOSITIONS

Five kinds of rock types were classified and analyzed; less altered basaltic andesite, altered basaltic andesite, quartz-veined volcanoclastic rock, altered dyke and granodiorite.

Oxygen isotope compositions vary from 4.1 to 9.8‰ in basaltic andesite. Quartz-veined volcanoclastic rocks show large range from 1.6 to 13.6‰. In contrast, altered dykes are relatively depleted in $\delta^{18}\text{O}$ ranging from 1.1 to 2.5‰. Two fresh granodiorite samples show 4.9 and 5.8‰, while one altered granodiorite in contact with basaltic andesite has a relatively high $\delta^{18}\text{O}$ value of 10.9‰. The δD values of less altered basaltic andesite span narrow range from -86 to -82‰, while those of altered basaltic andesite became heavier and scattered from -82 to -71‰. The latter is similar to those of granodiorite, -79 to -74‰. The δD values of quartz-veined volcanoclastic rock, -88 to -79‰, and altered dyke, -91 to -83‰, are generally lower than those of altered basaltic andesite.

The $\delta^{34}\text{S}$ values of various rock types differ from each other according to their localities. Most $\delta^{34}\text{S}$ values of altered basaltic andesites range from -7.9 to +1.2‰. Some samples in contact with granodiorite are concentrated in heavy isotopes ranging from -2.4 to 1.2‰. The $\delta^{34}\text{S}$ values of the samples from the southern coast of the peninsula are typically low, -10.4 to -6.1‰ in quartz-veined volcanoclastic rock and -7.6

to -7.0‰ in altered dyke. These are lower than those of altered basaltic andesite. The amounts of sulfur present in less altered basaltic andesite and granodiorite were below the detection limit for isotope measurement, but one altered granodiorite produced a $\delta^{34}\text{S}$ value of -0.9‰.

Initial Sr isotopic compositions of less altered basaltic andesite span relatively a narrow range from 0.703215 to 0.703483. In other rock types, $(^{87}\text{Sr}/^{86}\text{Sr})_i$ ratios are generally higher than those of less altered basaltic andesite. The $(^{87}\text{Sr}/^{86}\text{Sr})_i$ ratio of granodiorite ranges from 0.703387 to 0.703443, and in altered basaltic andesite from 0.703397 to 0.704527. In quartz-veined volcanoclastic rock, $(^{87}\text{Sr}/^{86}\text{Sr})_i$ ratios range from 0.703482 to 0.703841, and in altered dyke from 0.703483 to 0.703549, which are similar to those of granodiorite.

EVOLUTION OF HYDROTHERMAL FLUIDS

The oxygen and hydrogen isotope compositions of altered basaltic andesite and granodiorite are similar to each other. The $\delta^{18}\text{O}$ and δD values gradually decrease from altered basaltic andesite to altered dyke and quartz-veined volcanoclastic rock. The genetic linkage between hydrothermal fluid and granodiorite intrusion accounts for similar $\delta^{34}\text{S}$ values among sulfide minerals, both in the granodiorite stock and in nearby altered basaltic andesite.

Broadly positive correlations of $\delta^{18}\text{O}\text{-SiO}_2$, $\delta^{18}\text{O}\text{-}(^{87}\text{Sr}/^{86}\text{Sr})_i$, and $^{87}\text{Sr}/^{86}\text{Sr}\text{-SiO}_2$ can be established by siliceous fluids enriched in ^{18}O as well as ^{87}Sr . In addition, a positive relationship between $(^{87}\text{Sr}/^{86}\text{Sr})_i$ values and $1/\text{Sr}$ contents in basaltic andesites can result from mixing between fresh rocks and infiltrating fluids with different endmember $^{87}\text{Sr}/^{86}\text{Sr}$ values and Sr contents. The hyperbolic variation of $(^{87}\text{Sr}/^{86}\text{Sr})_i\text{-K/Rb}$ suggests that meteoric water participated in hydrothermal activities via mixing with magmatic water, and the contribution of seawater was insignificant.

All of the above results indicate that hydrothermal alteration was influenced by fluids related to granodiorite intrusion, and ^{18}O - and ^{87}Sr -rich meteoric water circulating in the upper crust significantly contributed to hydrothermal activities in Barton Peninsula.

REFERENCES

- Hur, S.D., Lee, J.I., Hwang, J. and Choe, M.Y., 2001, K-Ar age and geochemistry of hydrothermal alteration in the Barton Peninsula, King George Island, Antarctica. *Ocean Polar Research*, 23, 11-21.
- Hwang, J. and Lee, J.I., 1998, Hydrothermal alteration and mineralization in the granodioritic stock of the Barton Peninsula, King George Island, Antarctica. *Economic and Environmental Geology*, 31, 171-183.
- Smellie, J.L., Pankhurst, R.J., Thomson, M.R.A. and Davis, R.E.S., 1984, The geology of the South Shetland Islands: VI. Stratigraphy, geochemistry and evolution. *British Antarctic Survey Science Report*, 87, Cambridge, 85 p.
- Willan, R.C.R. and Armstrong, D.C., 2002, Successive geothermal, volcanic-hydrothermal and contact-metasomatic events in Cenozoic volcanic-arc basalts, South Shetland Islands, Antarctica. *Geological Magazine*, 139, 209-231.

PHOTOGRAPHIC IDENTIFICATION GUIDE TO LARVAE AT HYDROTHERMAL VENTS

Susan W. Mills, Stace E. Beaulieu, and Lauren S. Mullineaux

Biology Department, Woods Hole Oceanographic Institution, Woods Hole, MA 02543,
USA
stace@whoi.edu

We would like to announce our “Photographic Identification Guide to Larvae at Hydrothermal Vents,” available online at: <http://www.whoi.edu/vent-larval-id/>, or by request as a CD or hard copy. The purpose of this guide is to assist researchers in the identification of larvae of benthic invertebrates at hydrothermal vents. Our work is based mainly on plankton sampling at the East Pacific Rise (EPR) 9-10°N vent field from 1991 - present. In this first version of the guide, we have included frequency data from large-volume plankton pump samples and time-series sediment trap samples collected prior to the eruption at this site in 2005/2006. The guide includes an “Introduction and Methods” section that details the collection of larvae, a section on “Terminology” for gastropod and polychaete larvae, and “Literature Cited” for descriptions of species. Gastropod, bivalve, polychaete, arthropod, and other larval types are sorted alphabetically, and gastropod larvae may also be sorted by size. Each species information page also includes thumbnail images of species that are similar in appearance. While our sampling was limited to EPR 9-10°N, the guide is useful to researchers working in other areas, since a number of the species range from 21°N to the southern EPR, and some have congeners in other chemosynthetic environments, e.g., *Lepetodrilus* (Juan de Fuca Ridge, Mid-Atlantic Ridge, wood falls), and *Bathymodiolus* (Mid-Atlantic Ridge, seeps). We would like to expand the guide by including additional species from other areas. We welcome contributions from the ChEss and InterRidge community.

**EXPLORATION STRATEGIES FOR POLAR ENVIRONMENTS:
HIGH-RESOLUTION MAPPING OF HYDROTHERMAL DISCHARGE USING
AN AUTONOMOUS UNDERWATER VEHICLE**

E.T. Baker¹, S.L. Walker¹, C.E. de Ronde², J.A. Resing³, R.E. Embley⁴, D. Yoerger⁵

¹NOAA/Pacific Marine Environmental Lab, 7600 Sand Point Way NE, Seattle, WA
98115, USA

edward.baker@noaa.gov

²GNS Science, PO Box 30368, Lower Hutt, 5040, New Zealand

³JISAO/PMEL/NOAA Univ. Washington, 7600 Sand Point Way NE, Seattle, WA 98115,
USA

⁴NOAA/Pacific Marine Environmental Lab, 2115 SE OSU Dr, Newport, OR 97365,
USA

⁵Woods Hole Oceanographic Institution, Blake 221, MS#7, Woods Hole, MA 02543,
USA

Efficient use of ship time is increasingly urgent, and nowhere more so than in the remote polar seas. Autonomous Underwater Vehicles (AUVs) offer the possibility of enhancing the exploration capability of a research vessel by enabling simultaneous operations, as well as by expanding exploration in waters where ice conditions might restrict the operations of a surface ship. To make full use of AUVs, however, a broad suite of compatible sensors are needed. Here we describe a high-resolution survey in which the WHOI Autonomous Benthic Explorer (ABE) mapped the seafloor and the distribution of hydrothermal indicators in the near-bottom waters blanketing the walls and summits of Brothers volcano, a hydrothermally active submarine caldera located on the Kermadec arc northwest of New Zealand. Brothers caldera is ~3 km in diameter with a floor depth of 1850 m and walls that rise 290-530 m above the caldera floor. A dacite cone with a summit depth of ~1200 m sits within the caldera, partially merging with the southern caldera wall. During our 2007 expedition, the caldera walls and dacite cone (~7 km²) were completely surveyed by ABE with 50-60 m trackline spacing at an altitude of 50 m above the seafloor. Seafloor data included bathymetry at a 2-m grid resolution, and continuous magnetics. Simultaneously, the distribution of hydrothermal discharge was mapped using several indicators. ABE's integrated CTD (conductivity-temperature-depth) measured hydrothermal temperature anomalies. An optical backscatter sensor detected suspended hydrothermal precipitates. A new oxidation-reduction potential (ORP) sensor developed at PMEL indicated the presence of reduced chemical species (e.g., Fe⁺², H₂S). ORP signals are rapidly oxidized in the water column and are thus found only close to their seafloor hydrothermal sources.

The AUV survey found robust hydrothermal indicators in several areas. Along the northwest wall, light-scattering, temperature, and ORP anomalies were concentrated

between ~1400 and 1600 m, aligned along the trend of wall faults. Another strong area of venting was the dacite cone. Venting on isolated portions of the northwest wall and cone areas was known from previous surface-ship, submersible, and camera studies, but the AUV work found a much broader distribution of discharge than expected. In addition, newly discovered areas of venting were found on the northeastern wall. The simultaneous collection of high-resolution bathymetry, magnetics, and water column data revealed clear correlations between hydrothermal activity, wall geomorphology, and structural lineations that are unobtainable with other survey tools. Moreover, the research vessel was free to conduct other, off-site, operations during each ~12 hr dive. AUV tools thus fill an important research gap between regional water column surveys conducted by CTD operations and precise seafloor sampling by submersibles or tethered vehicles.

**PRELIMINARY INTERPRETATION OF MULTI-CHANNEL SEISMIC DATA
FROM THE ROSS SEA**

Ibrahim Ilhan, Gwang H. Lee, Deniz Cukur, Jong K. Hong, Young K. Jin

Pukyong National University, Busan 608-737, Korea
ibrahimilhan35@hotmail.com

We interpreted the public-domain multi-channel seismic reflection data from the Ross Sea to map the basement structure and three key unconformity surfaces. The basement structure reveals the main structural features in the area, including the Northern Basin, Central Trough, Central High and Eastern Basin from northwest to southeast. The Central Trough consists of three grabens bounded by distinct normal faults. A steep and narrow N-S trending basement high separates the northernmost trough of the Central Trough and the Northern Basin. The maximum depths of the Central Trough and the Northern Basin reach over 8,000 m and over 6,000 m, respectively. The Central High, separating the Central Trough and the Eastern Basin, consists of three structural highs that are shallower than 1000 m. The sedimentary strata in the Central High are locally uplifted, suggesting recent tectonic movement. The Eastern Basin is bounded to the west by a steep normal fault and deepens gradually to the east and northeast. The maximum depth of the East Basin is over 9,000 m. The deep unconformity (UNC-1) is seen only in the Central Trough and southern part of the Eastern Basin. The middle unconformity (UNC-2) is seen over much of the area. UNC-2 onlaps onto the Central High. The shallow unconformity (UNC-1) appears to have been eroded by the recent advance of grounded ice. The erosion of UNC-1 is prominent over the Central High.

**REGIONAL COMPARISONS OF DEEP-OCEAN SOUND FROM THE
BRANSFIELD STRAIT AND SCOTIA SEA**

J.H. Haxel, R.P. Dziak, M. Park, H. Matsumoto, W.S. Lee, T.K. Lau, and M. Fowler

NOAA, Newport, OR, U.S.A
Joe.Haxel@noaa.gov

Hydrophone arrays deployed in the Bransfield Strait and Scotia Sea provide continuous deep-ocean acoustic recordings of ice noise, seismicity, marine mammals and ambient sound levels. This collaborative effort by NOAA and KOPRI from 2005 to present provides insight into the overall structure for the deep-water Southern Ocean sound field. The hydrophones are moored in the SOFAR channel, taking advantage of the efficient propagation characteristics that enable the instruments to effectively monitor large regions of ocean. Although not concurrent, the deployment of the hydrophone arrays in the Bransfield Strait (2005-2007) and the Scotia Sea (2007-2009) allows for a regional comparison of ocean sound levels in discrete frequency bands. Intra- and inter-annual time-averaged ambient-sound levels reveal variations between the arrays. Seismic and volcanic activity dominates the lower frequency band (0-10 Hz) recorded in both ocean regions. Of interest is the periodic nature of broad-band ice noise, suggesting a climate link for these signals related to ice breakup during seasonal warming events (Matsumoto et al., 2008). In addition, the multi-species marine-mammal vocalizations dominate sound-energy levels at specific frequencies.

**EVIDENCE FOR OFF-AXIS SEAMOUNTS ON THE FLANKS OF THE
SOUTHEAST INDIAN RIDGE, 128°E-150°E. IMPLICATIONS FOR MANTLE
DYNAMICS EAST OF THE AUSTRALIA-ANTARCTIC DISCORDANCE.**

Anne Briais, Olga Gomez and Raymond Lataste

CNRS UMR5566 and UMR5562, Univ. Toulouse, Observatoire Midi-Pyrénées,
14 av. Edouard Belin, 31400 Toulouse, France
anne.briais@ntp.obs-mip.fr

The intermediate-spreading Southeast Indian Ridge (SEIR) between Australia and Antarctica is mostly known for the presence of the Australia-Antarctic Discordance, an area of low magma budget on the ridge. Here we focus on the area east of the discordance, where we have analyzed gravity highs observed on satellite-derived maps of the flanks of the Southeast Indian Ridge between Tasmania and Antarctica. We show that these gravity highs likely correspond to volcanic seamounts and seamount chains, similar to those observed on the flanks of the East Pacific Rise. This area, in particular the volcanic chains, are associated with residual mantle Bouguer anomaly (RMBA) lows, suggesting thicker crust or hotter mantle or both under the study area. The large number of off-axis seamounts and the RMBA lows suggests an anomalously high magma supply under the southern flank of the SEIR, not only with respect to the magmatically-starved discordance area, but also with respect to regular sections of intermediate-spreading mid-ocean ridges. We suggest that the seamount chains might have formed above small-scale convective upwellings in the asthenospheric mantle close to the ridge axis, and that the obliquity of the ridges reflects a regional westward asthenospheric flow. This hypothesis is also supported by the intermediate-wavelength gravity lineations observed in the southern flank of the SEIR. We infer that the observed off-axis volcanism results from the partial melting of Pacific-type mantle as it flows from the southeast to the northwest, and that this process likely started with the opening of the oceanic spreading center between Tasmania and Antarctica. The mantle flow at the origin of the magmatic anomaly appears to be partly dammed by the large transform faults. It is not clear how this regional flow from Pacific to Indian domains relates to the Balleny hotspot.

POSTER SESSION 2

**CLIMATE CHANGE
AND
POLAR OCEAN SYSTEM**

BACTERIA FROM SEDIMENT OF LAKE BAIKAL CAN BE USED AS EVIDENCE OF PALEOCLIMATE CHANGE

T.S. Ahn, J.Y. Kim, Y.J. Jung, ¹V. Parfenova, ¹N. Belkova

Department of Environmental Science, Kangwon National University, ChunChon 200-701, Korea

ahnts@kangwon.ac.kr

¹DLimnological Institute, Siberian Division, Russian Academy of Sciences, Irkutsk, Russia

Among various kind of paleo-climatological assay method, we were using bacteria from sediment of Lake Baikal. After retrieving sediment from central Lake Baikal, every 1 cm of sediment was boiled at 70°C for 20 min., and then it was spread on nutrient agar for cultivation. Inoculated agar plates were incubated on 16, 25, and 37°C and 7 days after appeared colonies were counted. All of isolated bacteria identified as *Bacillus* by FISH (fluorescence in situ hybridization) method. Bacteria growing at 16, 25 and 37°C had different peaks of 300 cm depth of sediment core. Considering the sedimentation rate of Lake Baikal, 300 cm depth means 30,000 years of sedimentation history. And by the result of *Bacillus* distribution, we may assume that about 30,000 years ago, Lake Baikal area was hot area and then change into colder. By this assessment, bacteria can be powerful method for assessment for paleolimnology and climatology.

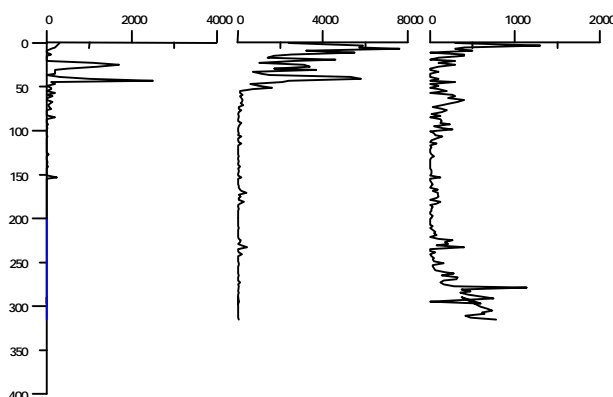


Fig. 1. Distribution of *Bacillus* in sediment of L. Baikal.
(L) cultivation on 16°C, (M) 25°C and (R) 37°C.

**PALEOPRODUCTIVITY VARIATIONS OFF LÜTZOW-HOLM BAY IN THE
INDIAN SECTOR OF THE SOUTHERN OCEAN DURING THE PAST 650
KYRS**

M. Ikehara¹, B.K. Khim², S. Okamoto¹, M. Kobayashi¹, K. Katsuki¹, Y. Suganuma³, M.
Yamane⁴, Y. Yokoyama⁴, Y.H. Kim²

¹Center for Advanced Marine Core Research, Kochi University, B200 Monobe,
Nankoku, 783-8502, Japan
ikehara@cc.kochi-u.ac.jp

²Division of Earth Environmental System, Pusan National University, Busan 609-735,
Korea; ³National Institute of Polar Research, 1-9-10 Kaga, Itabashi-ku, Tokyo 173-8515,
Japan

⁴Department of Earth and Planetary Science, University of Tokyo, 7-3-1 Hongo,
Bunkyo-ku, Tokyo, 113-0033, Japan

The Southern Ocean plays a very important role in the global climate system on the present and geologic past. The Southern Ocean has also become a region of paleoceanographic focus because of its key role in global deep-water circulation and its potential significance for the global carbon. For example, it has been proposed that primary production was higher and utilization of preformed nutrients in surface waters was more efficient in the glacial Southern Ocean than today, effectively lowering the glacial atmospheric CO₂ concentration. To resolve the causes and processes of atmospheric CO₂ change, it is important to understand mechanisms and processes of sub-systems in the Antarctic Cryosphere such as a change of biological productivity, sea surface temperature, surface water frontal system, sea-ice distribution, and East Antarctic ice sheet during the glacial-interglacial climate cycle. We collected a sediment core (LHB-3PC, 66.0°S, 40.0°E, WD4469m) off Lützow-Holm Bay in the Indian Sector of the Southern Ocean during the R/V Hakuho-maru cruise KH07-4 Leg 3. Age model of the core was reconstructed by radiocarbon dating of bulk organic carbon, diatom biostratigraphy and relative paleointensity curve of the geomagnetic field. Biogenic opal contents of core LHB-3PC indicate that the paleoproductivity was significantly enhanced during the interglacials (MIS 1, 5, 7, 9, and 11) in the high-latitude Southern Ocean. However, the paleoproductivity change did not show a clear orbital (glacial-interglacial) cycle before the MIS 12. Thus, the controlling factors of marine paleoproductivity might have been changed in the Southern Ocean at the middle Brunhes chron period.

DISTRIBUTIONS OF PHYTOPLANKTON COMMUNITIES AT DIFFERENT REGIONS IN THE ARCTIC OCEAN

Hyoungh Min Joo^{1,2}, Sang Heon Lee¹, Kyung Ho Chung¹, Sung-Ho Kang¹, Yu Na Shin³,
Sung Soo Hong¹, Oh Youn Kwon⁴, Jin Hwan Lee²

¹Korea Polar Research Institute, Incheon 406-840, Korea
hmjoo77@gmail.com

²National Institute of Environmental Human Resources Development, Incheon 404-708,
Korea

³Department of Biology, Sangmyung University, Seoul 110-743, Korea

⁴South Sea Institute, Geoje 656-830, Korea

In order to investigate the structure of phytoplankton community at surface in the Arctic Ocean, this study was carried out at various study areas on board ice-breaker and ice-strengthened vessels in the Barents Sea, Kara Sea, Okhotsk Sea, Bering Sea, Chukchi Sea and Canadian Basin from 2003 to 2008.

We collected samples at Barents Sea and Kara Sea by Russian Research vessel 'Ivan Petrov' from 2003 to 2005. The data, from the Okhotsk Sea were collected on board the Russian academic research vessel 'Lavrentiev' and in the Bering Sea, Chukchi Sea and Canadian Basin, more data from 2006 to 2008 were obtained on the Japanese training ship 'Oshoro Maru' and Chinese ice breaker 'Xuelong'.

Phytoplankton communities were composed of 53 and 23 taxa in the Barents Sea in 2003 and 2004, respectively. 24 taxa were found in the Kara Sea in 2005 and 25 taxa were appeared in the Okhotsk Sea as a subarctic ocean in 2005. Bering Sea (2006, 2007, and 2008), Chukchi Sea (2007 and 2008) and Canadian Basin (2008) had 43, 56, 57, 57, 42 and 26 taxa, respectively. There were high species diversity and low abundance of phytoplankton in the Barents Sea, Bering Sea and Chukchi Sea, whereas in the Kara Sea and Okhotsk Sea low species diversity and high abundance were distinct.

The most abundant species were nano-pico size phytoplankton at most of the study areas, but the second abundant species were variable such as *Dinobryon belgica* in the Barents and Kara seas whereas *Thalassiosira* sp. in the Okhotsk Sea. Overall, the small size phytoplankton 0-20 μ m had higher species diversity and abundance in the Arctic Ocean.

REGULATING FACTORS ON CONTINUOUS WINTER CO₂ FLUX IN BLACK SPRUCE FOREST SOILS, INTERIOR ALASKA

Yongwon Kim, Yuji Kodama² Mamoru Ishikawa³

¹International Arctic Research Center, University of Alaska Fairbanks, USA
[kimyw@iarc.uaf.edu]

²Institute of Low Temperature Science, Hokkaido University, Japan

³Graduate School of Environmental Earth Science, Hokkaido University, Japan

INTRODUCTION

The environmental factors influencing winter CO₂ flux are atmospheric pressure and wind speed [Takagi *et al.*, 2005; Massman and Frank, 2006], atmospheric temperature [Takagi *et al.*, 2005], soil temperature [Zimov *et al.*, 1993, 1996; Oechel *et al.*, 1997; Winston *et al.*, 1997; Hirano, 2005; Monson *et al.*, 2006], soil moisture [Hirano, 2005], and snow depth [Fahnestock *et al.*, 1998; Takagi *et al.*, 2005]. These environmental factors play important roles in determining and fluctuating winter CO₂ fluxes in snow-covered terrain of the Northern Hemisphere. Moreover, atmospheric pressure affects wind speed and atmospheric temperature, and subsequent wind speed influences the CO₂ fluctuation within the snowpack, and the ambient temperature modulates snow/soil temperatures. The soil temperature, depending on snow depth and atmospheric temperature, also governs the strength of microbial activity that terminally determines the magnitude of CO₂ production in soils. Thus, we investigated the regulating environmental factors on continuous winter CO₂ flux-measurement through the snowpack in this study.

MATERIALS AND METHODS

Black spruce (*Picea mariana*) is the dominant overstory tree species, with ages from 75 to 120 years [Vogel *et al.*, 2005]. The black spruce canopy is sparse. The averaged canopy height is about 3.5 m, but there are taller trees of up to 6 m, sporadically.

The sensor system was built on sphagnum and feather moss layers from October 6, 2006 (DOY 280) to April 30, 2007 (DOY 485) for the monitoring of continuous CO₂ concentration in snowpack during winter of 2006/7. The set-up sensor is non-dispersive infrared (NDIR; Vaisala GMD 20; Helsinki, Finland), which is set on a length of wooden stick (3 cm diameter; 100 cm long) at four levels (10, 20, 30 and 50 cm above the moss surface) with for prevention of disturbance. The sensor is the same type as used for soil CO₂ flux estimation [Hirano *et al.*, 2003; Takagi *et al.*, 2005]. The installed sensor is covered with a PVC pipe (48 mm OD; 40 mm ID; 170 mm long) for water and sensor-window protection. The NDIR sensor window is 50 mm long with 4 mm wide slit on the head, which measures soil CO₂ concentration through the snowpack. The cable from each sensor connected to a 24V-DC/AC converter for AC

electric power supply, and then to logger (CR 1000, Campbell Scientific Inc., USA) within an ice cooler. A commercial heating pad was used within the ice cooler for operation of the datalogger during winter. CO₂ concentration measured at the 50 cm level above the surface was not discussed due to the shallow snow depth (< 40 cm) and the unexpected failure of the sensor. Winter CO₂ flux was estimated between DOY 357 (December 23, 2006) to 466 (April 11, 2007), when the snow depth was greater than 25 cm. While the snow depth was less than 20 cm before DOY 257, the winter flux could not be estimated. The accumulated snowpack began to melt on DOY 446 (March 21, 2007). The snow survey was also conducted at a two-week interval. Two to five snow samples were collected using a snow density sampler (4 cm H x 5 cm W x 5 cm D) and a snow cutter for the estimation of snow porosity [Kim et al., 2007].

We correlated winter CO₂ flux with the non-conductive heat flux component of the active layer. The non-conductive heat component, r_h , is expressed in terms of volumetric heat production in W/m², and is estimated by considering the one-dimensional energy conservation as formulated:

$$r_h = c_h \frac{\partial T}{\partial t} - k_h \frac{\partial^2 T}{\partial z^2} \quad (1)$$

where k_h is bulk thermal conductivity, c_h is the volumetric bulk heat capacity, t is the time, T is temperature and z is depth. Neglecting energy exchange below the lowest measurement, the total amount of non-conductive heat components, R_h , is the summation of r_h multiplied by the thickness of the soil layer, d :

$$R_h = \sum_i r_h^i d^i \quad (2)$$

where the subscript i represents the i -th layer from surface to bottom. We set the mid-depth of the i -th layer to be at the i -th measurement depth from the surface. Accordingly, the soil column was divided into three layers, the thicknesses of which were 5, 7.5, and 10 cm from the surface to bottom (25 cm). Finite element formulations to solve equations (1) and (2) are described in *Ishikawa et al.* [2006].

We assumed k_h to range from 5.5×10^{-7} to 8.0×10^{-7} J kg⁻¹ K⁻¹, referring to the thermal diffusivity for frozen silty clay loess shown by *Yershov* [1998], ($d_h = 5.5 \times 10^{-7}$ - 8×10^{-7} m² s⁻¹) and the heat capacity shown by *Roth and Boike* [2001], ($c_h = 2.2 \pm 0.2 \times 10^6$ J m⁻³ K⁻¹). These calculations neglected the contribution of soil air because of its very low mass density.

RESULTS AND DISCUSSION

1. Environment Factors

The atmospheric pressure seemed to govern ambient temperature at 80 cm above the ground, which showed intense change due to daily variations. Ambient pressure and temperature ranged from 943 to 1020 hPa and -45 to 17 °C during the period of DOY 350 to 466, respectively. The temporal variation of pressure showed an inverse tendency for change in temperature. Thus, in order to quantify the effect of pressure and temperature for winter CO₂ flux, the magnitude of pressure was divided into four phases, which were high pressure (HP: >1000 hPa), intermediate (IP: 985 hPa < P < 1000 hPa), low pressure (LP: <985 hPa), and snow-melting period (MP, after DOY 466) during the snow-covered period, shown in Figure 2. Atmospheric temperature was -31.9 ± 11.0 °C (Coefficient of Variance (CV): 35%) for HP, -22.1 ± 8.6 °C (CV: 39%) for IP, -21.5 ± 6.8 °C for LP, and -8.4 ± 12.4 °C (CV: 146%) for MP, respectively. Thus, the four pressure phases might have influenced the magnitude

of air temperature.

2. Estimation of Winter CO₂ Flux

The winter CO₂ flux varied from 0.19 to 0.26 gCO₂-C/m²/d for HP (>1000 hPa), 0.19 to 0.27 gCO₂-C/m²/d for IP (985<P<1000), 0.20 to 0.32 gCO₂-C/m²/d for LP (<985 hPa), and 0.14 to 0.24 gCO₂-C/m²/d for snow melting period (MP), respectively. During the snow-covered period of 109-day, the averaged CO₂ flux was 0.22±0.02 gCO₂-C/m²/d (CV: 10%), indicating that the value corresponds to those measured by concentration profile (0.21±0.06 gCO₂-C/m² /d) and chamber (0.26±0.06 gCO₂-C/m²/d) methods during winter of 2004/5 in the same black spruce forest soils, interior Alaska [Kim *et al.*, 2007]. Furthermore, the snow depth in winter of 2004/5 was much deeper (> 20 cm) than 2006/7 [Kim *et al.*, 2007]. Although the snow depth was deeper, the minimum of soil temperature 5 cm below the surface was -17°C due to an extreme cold ambient temperature of -55°C (January 12, 2005). This suggests that the thicker snow depth (68 cm) plays little role in insulating the soil below -50°C.

3. Environmental Factors Influencing Winter CO₂ Flux

Winter CO₂ fluxes have a relationship to atmospheric pressures for HP (>1000 hPa), LP (<985 hPa) and snow-melting days (MP) of the snow-covered period (Figure 1a), indicating the inverse correlation for each pressure phase. The data for IP (985<P<1000) was virtually excluded in Figure 1a. The correlation coefficients (R²) were 0.25 for HP, 0.31 for LP, and 0.18 for MP, respectively. The ambient pressure has a lesser effect in determining on winter CO₂ flux through the snowpack to the atmosphere during the snow-covered period.

Winter CO₂ fluxes have a good exponential relationship to ambient temperature for three pressure phases: the coefficients were 0.80 in low temperature for HP, 0.26 in high temperature for LP, and 0.58 for MP, respectively (Figure 1b). Figure 1c showed the relationship between the CO₂ fluxes and ambient temperature for IP (985<P<1000), which has good correlation, suggesting that the air temperature accounted for 58% of the variability of winter CO₂ emission for IP. The winter CO₂ fluxes showed an exponential relation to the soil temperature at 5 cm (Figure 9a and 9b), where the correlation coefficients were 0.40 for HP, 0.14 for LP, 0.33 for MP, and 0.35 for IP, respectively.

The Q₁₀ is the temperature coefficient of the reaction and is defined as the ratio of reaction rate at an interval of 10°C. The Q₁₀ values were 1.22 for HP, 1.25 for LP, 1.26 for MP, and 1.37 for IP, respectively. These values are much lower than the previous studies during the winter

Estimated soil non-conductive heat flux evolved negatively through the period from DOY 357 to 460 for both upper and lower d_h and c_h (Figure 2a). Assuming that this heat arises from single phase transition of water, we compared soil moisture observed with R_h divided by the enthalpy of the transition from phases α to β , $L^{\alpha\beta}$ ($\{L^{sl}, L^{lv}\} = \{0.333, 2.45\}$ MJ/kg, where the subscript s , l and v represents solid, liquid and vapor, respectively), and found that the origin of this heat was mostly from vaporization.

Looking at Figure 10a, winter CO₂ flux showed a decreasing trend until the end of the snow-covered period, while latent heat flux showed an increasing trend. Also, both fluxes showed significant correlations (R² = 0.49 and 0.52, with $p < 0.001$ in both) before the onset of snow melting (Figure 3). These findings suggest that the higher upward vapor movement in the soil column occurred in accordance with the smaller soil-originated CO₂ flux. We postulate that winter soil-originated CO₂ is hampered by

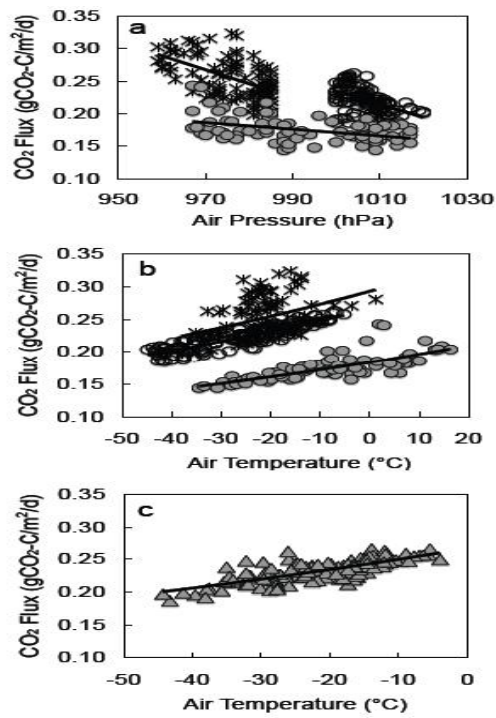


Fig. 1. Relationships between winter CO₂ fluxes and a) air pressure for HP, LP and MP, b) air temperature for HP, LP and MP, and c) air temperature for IP.

the reduction of snow pores linked to the atmosphere, due to compaction of snowpack, vapor condensation in the snow column, and subsequent snow metamorphism. This consideration is supported by the comparison between CO₂ flux and snow temperature gradient (Figure 10b). Winter CO₂ flux is occasionally greater when the snow temperature profile approached the isotherm and the condensation rate was reduced (e.g. DOY 364, 368, 392-399, 406, 411, 423, 434, Figure 2a and b). The temperature gradients govern vapor pressure gradient through snow and soil column, modulating evaporation, condensation and vapor movements. This modifies the passage of winter CO₂.

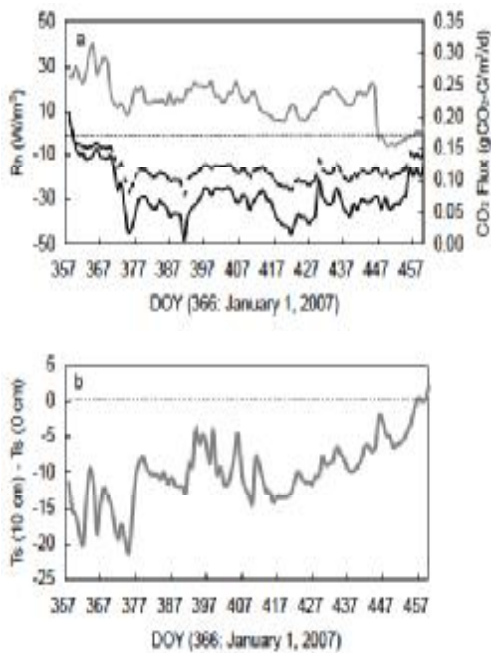


Fig. 2. a) Temporal variations of winter CO₂ flux and soil non-conductive heat flux, R_n , estimated from equation (1), as written in the text. b) Snow temperature gradients between soil surface and 10 cm from DOY 357 to 460. T_s (0 cm) and T_s (10 cm) denote temperatures at soil surface and at 10 cm above the surface.

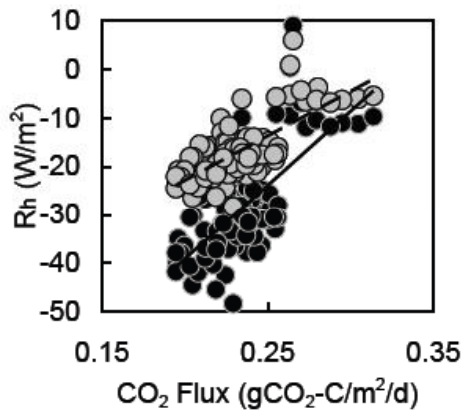


Fig. 3. Correlations between non-conductive heat and winter CO₂ flux until DOY 445.

REFERENCES

- Kim, Y., M. Ueyama, F. Nakagawa, U. Tsunogai, N. Tanaka, and Y. Harazono, 2007: Assessment of winter fluxes of CO₂ and CH₄ in boreal forest soils of central Alaska estimated by the profile method and the chamber method: a diagnosis of methane emission and implications for the regional carbon budget. *Tellus* **59B**, 223-233.

**FLUORESCENCE CHARACTERISTICS OF CDOM IN
DIFFERENT WATER MASSES OF SCOTIA SEA, ANTARCTICA**

M.O. Park, S.W Kang¹ and B. G. Mitchell²

¹Pukyong national university, ²Scripps Institution of Oceanography
[mopark@pknu.ac.kr]

Fluorescence characteristics of Chromophoric Dissolved Organic Matter (CDOM) in seawater collected at the Southern Scotia Sea were investigated by high resolution fluorescence spectroscopy. Various types of water masses - shelf, mixed and Antarctic Circumpolar Current (ACC) water were analyzed to find differences fluorescence characteristics of CDOM. Both fluorescence intensities and excitation and emission maxima showed distinct properties depending on types of water masses, which implies the possibility of distinguishing different water masses based on the fluorescence properties. Interestingly, fluorescence intensity of protein-like peaks from oligotrophic ACC water was about 4-6 times higher compared to the shelf and mixed water, and the abundance of bacteria showed similar pattern. Vertical profiles of fluorescence of CDOM also examined by discrete sea water samples from the surface to 3,000m depth. The fluorescence of protein-like peaks showed maximum at 50-70m depth and was significantly low at the surface layer (0-30m), which reflects the photo-decomposition at the surface layer. The depth of maximum chl α and of the highest fluorescence of DOM was not matched at all stations, and it suggests that direct source for CDOM in the study area is not phytoplankton. From Excitation-Emission spectroscopy (EEMS), 5 different peaks were identified. Among them, fluorescence of protein-like peaks (Ex=300nm, Em=340nm) was relatively significant at the surface layer, while humic-like peaks (Ex=345nm, Em=430nm) become predominant with depth. Effects of temperature and acid on the fluorescence of CDOM were also examined.

**OBSERVATION OF TRACE GASES IN THE AIR AND SURFACE WATER
ALONG ATLANTIC MERIDIONAL TRANSECT**

Tae Siek Rhee¹, A. Jamie Kettle², and Meinrat O. Andreae³

¹Korea Polar Research Institute, Incheon, Korea [rhee@kopri.re.kr]

²State University of New York – Oswego, Oswego, U.S.A

³Max Planck Institute for Chemistry, Mainz, Germany

The ocean plays an important role in the budget of important greenhouse gases in the atmosphere. A well-known example is carbon dioxide. About 30% of the emitted CO₂ by human activities is absorbed by the ocean. In addition to CO₂, it is well known that important non-CO₂ greenhouse gases are emitted from the ocean associated with marine biological activity. However, their oceanic source strengths are largely uncertain or sometimes overestimated in the literature. The ocean also emits sulfur compounds which appear to be negatively effective to the global warming. To estimate the emission rates of these climatologically sensitive trace gases from the ocean, we measured N₂O, CH₄, CO, COS, CS₂, CH₃SH, and DMS in the surface waters of the Atlantic Ocean from England to the Falkland Islands during the 1998 Atlantic Meridional Transect expedition. Based on this observation, we estimate the emission rate of CH₄ as 0.6 – 1.2 Tg yr⁻¹, of N₂O as 0.9 – 1.7 Tg N yr⁻¹, and of CO as 10 – 20 Tg yr⁻¹. We will discuss in the presentation the impact of oceanic emissions of these gases and of the volatile sulfur compounds measured during this expedition.

CARBON AND NITROGEN UPTAKE RATES OF PHYTOPLANKTON IN THE CHUKCHI SEA AND CENTRAL ARCTIC OCEAN

Sang Heon Lee¹, Hyung-Min Joo¹, Mi Sun Yun¹, Kyung Ho Chung¹

¹Korea Polar Research Institute, Incheon 406-840, Korea
[misunyun@kopri.re.kr]

ABSTRACT

As a Chinese IPY event, the 3rd Chinese National Arctic Research Expedition (CHINARE) was conducted from the Chukchi Sea to the central Arctic Ocean from late July to early September in 2008. Using a ¹³C-¹⁵N dual isotope tracer, the primary productivity experiments were measured at 24 stations for total, but 12 stations in the Chukchi Sea and 12 stations in the central Arctic Ocean during the period. In general, the temperature and salinity at surface were 4 to 6°C and 30 in the Chukchi Sea and -1 to 3°C and 25-27 in the central Arctic Ocean, respectively. The lower temperature and salinity in the central Arctic Ocean is believed to mainly due to the melting water from sea ice. The primary productivity of phytoplankton was higher in the Chukchi Sea than in Canada Basin during the cruise period. Especially in the station R03, the productivity was 199.6 mg C m⁻² h⁻¹ which was twice higher than the previous result in 2007. However, the average nitrogen uptake rate in the Chukchi Sea was lower in 2008 than in 2007. Based on high f-ratios in the study areas, nitrate uptake rates compared to ammonium uptake rates were relatively higher than those from other studies.

INTRODUCTION

Recently, higher temperatures have decreased the sea ice extent and thickness in the Arctic Ocean, especially in the western part of the Arctic Ocean, over the past 40 years and have produced more open water. Although the production and biomass of phytoplankton are mainly controlled by available light and nutrients (Smith and Sakshaug 1990), the recent studies show the carbon production of phytoplankton in the surface water under the sea ice are limited by light in the Canada Basin and Barrow regions (Lee and Whitledge 2005). Therefore, the ongoing decrease in sea ice thickness might be favorable to an increase in primary production in the Arctic Ocean. However, we still do not know if the predicted climate change will provide less or more food

because little is known about primary production responding to the changes in these remote regions.

Chukchi Sea is the important connection of the water masses and hence organic matters between the Arctic and North Pacific Oceans. The inflows through Bering Strait convey three different water masses, which are Anadyr Current water (AW), Bering Shelf water (BSW), and Alaskan Coastal water (ACW), into the Chukchi Sea (Lee et al. 2007). These three different water masses through Bering Strait largely affect the primary production in the Chukchi Sea and consequently Canada Basin.

MATERIALS AND METHODS

As a Chinese IPY event, the 3rd Chinese National Arctic Research Expedition (CHINARE) was conducted from the Chukchi Sea to the central Arctic Ocean from late July to early September in 2008. In-situ carbon and nitrogen uptake rates of phytoplankton were measured at 12 stations in the Chukchi Sea and 12 stations in the Canada Basin, using both ^{13}C - ^{15}N dual tracer techniques (Fig. 1). Particulate organic carbon and nitrogen and abundance of ^{13}C and ^{15}N were determined in the Finnigan Delta+XL mass spectrometer at University of Alaska Fairbanks after HCl fuming overnight to remove carbonate.

RESULTS AND DISCUSSION

In general, the temperature and salinity at surface were 4 to 6°C and 30 in the Chukchi Sea and -1 to 3°C and 25-27 in the central Arctic Ocean, respectively (Fig. 1). The lower temperature and salinity in the central Arctic Ocean is believed to mainly due to the melting water from sea ice.

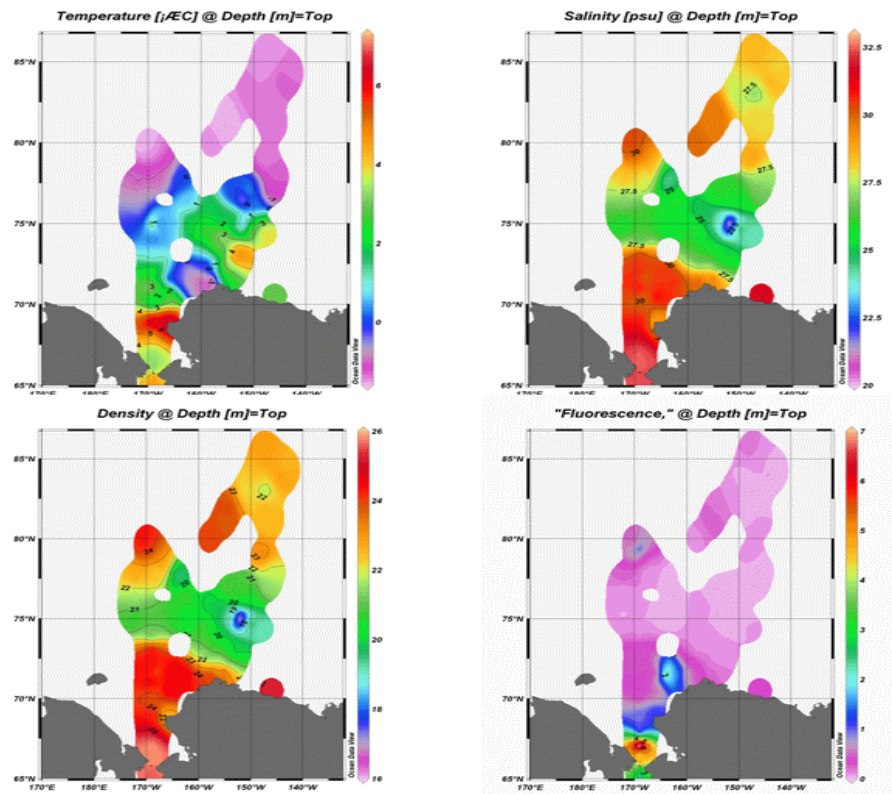


Fig. 1. Temperature, Salinity, Density and Fluorescence at surface in the Chukchi Sea and Central Arctic Ocean in 2008.

The hourly carbon production rate of phytoplankton during the cruise period ranged from 0.43 mg C m⁻² h⁻¹ to 196.6 mg C m⁻² h⁻¹, with a mean of 18.2 mg C m⁻² s⁻¹ (Fig. 2). The primary productivity of phytoplankton was higher in the Chukchi Sea than in Canada Basin during the cruise period. Especially in the station R03, the productivity was 199.6 mg C m⁻² h⁻¹ which was twice higher than the previous result in 2007.

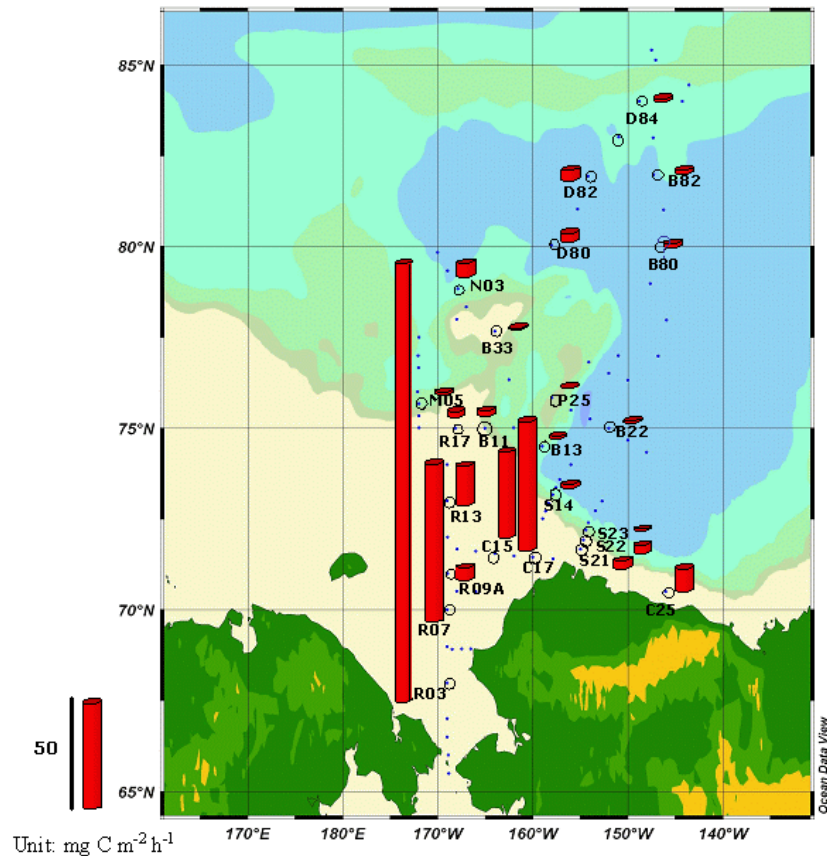


Fig. 2: Carbon uptake rates of phytoplankton in the Chukchi Sea and Canada Basin in 2008.

REFERENCES

- Lee, S.H., Whitledge, T.E., 2005. Primary production in the deep Canada Basin during summer 2002. *Polar Biology* 28:190-197.
- Lee, S.H., Whitledge, T.E., Kang, S.H., 2007. Recent carbon and nitrogen uptake rates of phytoplankton in Bering Strait and the Chukchi Sea. *Cont. Shelf Res.* 27. 2231-2249.
- Smith, W.O., Sakshaug, E., 1990. Polar phytoplankton. In: Smith, W.O. (Ed.) *Polar Oceanography, Part B*. Academic, San Diego, Calif. pp. 475-525.